TORLON® AND SILICALITE MIXED MATRIX MEMBRANES FOR XYLENE ISOMER PURIFICATION

A Thesis
Presented to
The Academic Faculty

By

Raymond W. Chafin II

In Partial Fulfillment
Of the Requirements for the Degree
Doctor of Philosophy in the
School of Chemical & Biomolecular Engineering

Georgia Institute of Technology
May 2007

TORLON® AND SILICALITE MIXED MATRIX MEMBRANES FOR XYLENE ISOMER PURIFICATION

Approved By:

Dr. William J. Koros, Advisor
School of Chemical & Biomolecular Engineering
Georgia Institute of Technology

Dr. Christopher W. Jones
School of Chemical & Biomolecular Engineering
Georgia Institute of Technology

Dr. Carson Meredith
School of Chemical & Biomolecular Engineering
Georgia Institute of Technology

Dr. Jeff Miller
Senior Scientist
BP

Dr. Andrew Lyon
School of Chemistry
Georgia Institute of Technology

Date Approved December 15, 2006

Montani Semper Liberi

To Mom, Dad, Ashley, and Gelareh

ACKNOWLEDGEMENTS

There are so many people who have shaped my life to this point. This thesis represents not only the last few years, but the culmination of maturing and developing over 26 years. There have been so many wonderful and positive influences in my life that have motivated me in my life goals. First, I cannot say enough for the role my family has played in helping me in my endeavors. My parents have always kept me grounded and have established themselves as not only role models, but also as my two very best friends. Second, I would like to thank Dr. Koros for the unbelievable mentoring he has provided as leader of our research group. His positive spirit, persistent work ethic, and never-give-up attitude is the contagious motivation that drives our entire group.

I would like to thank the members of the Koros research group for all the friendships, discussions, and guidance. I would like to especially thank Dr. Ted Moore, Dr. Shilpa Damle, Dr. Jason Williams, Dr. Bill Madden, Dr. Shabbir Husain, Dr. Preet Chandra and future Dr.'s John Perry, Adam Kratochvil, and Shu Shu. As much a dissertation is an individual effort, it would not be possible without the constant daily support of these people. I am truly blessed to have so many intelligent and motivated people as my colleagues.

I would like to thank my committee members, Dr. Andrew Lyon, Dr. Carson Meredith, Dr. Jeff Miller, and Dr. Chris Jones for providing thoughtful guidance on my ideas. Their support is greatly appreciated. Special thanks to the Jones Research group, as they provide invaluable support in zeolite engineering.

Lastly, I would like to thank my friends and family who have given me laughs, insight, and purpose over the past several years. My family (Ashley Chafin, Virgie Chafin, Cynthia Phillips, Ronnie Phillips, Amy Fondo, Todd Chafin, etc.) is a constant source of enjoyment and comfort. My West Virginia University friends (Matt Cooper, Chad Kanick, Jarod McCormick, Chris Taylor, Jerrod Houser, Jared Vance, and Roger Hanshaw) are my brothers and I am truly lucky to have such dependable friends. I would like to thank Shep, Freckles, Cody, Katy, Duchess, Chap, and Sadie as you have been a constant source of fun over 26 years. And finally I would like to thank my fiancé, Gelareh Shakourian. Her unconditional support and love has provided absolute inspiration in my life, and I look forward to a lifetime of the same.

TABLE OF CONTENTS

LIST OF TABLES

Page

LIST OF FIGURES

Page

SUMMARY

Organic/inorganic materials have a high potential to enable major advances in membrane performance. It has previously been impossible to develop polymeric systems with adequate transport properties for xylene purification. Zeolite membranes have been created with the appropriate selectivities; however low productivity, low mechanical durability, and high capital costs have kept these materials from being utilized. So-called mixed matrix hybrid organic/inorganic membranes combine the mechanical durability and cost effectiveness of polymeric membranes with the enhanced performance of zeolitic structures. This project will focus on investigating polymeric and molecular sieve materials for mixed matrix membrane use in xylene isomer separation as a *model system*. Torlon® polyamide-imide has unique properties that should be potentially useful in a mixed matrix composite. Silicalite will be investigated as the dispersed phased given its proven applicability with xylene isomers.

The overarching goal is to establish an approach for creation of mixed matrix materials that can be broadly applied to challenging organic separations. This project has three specific goals: (1) characterization of Torlon®'s inherent properties, processing ability, and important transport potential, (2) characterization of zeolite matching properties and the effect of interfacial engineering on these properties, and (3) development of appropriate approaches to combine the sieve and polymer to obtain a hybrid material with properties that match theoretically predicted separation property enhancements relative to

the neat polymer. High temperature pervaporation will be used to evaluate material transport properties, as this experimental setup closely mimics the high activity vapor streams found in many industrial xylene processes. The results of this research will be used to develop a protocol for development of future mixed matrix membranes that may be applied to a variety of organic liquid systems.

CHAPTER 1

INTRODUCTION AND MOTIVATION

Xylene isomers are important chemical intermediates. For example, phthalic anhydride is made from the oxidation of *o*-xylene and is mainly used to make phthalate plasticizers [1]. Also, isophthalic acid in made from the oxidation of *m*-xylene and is used in manufacturing unsaturated polyester resins [1]. However, *p*-xylene is the most industrially used isomer, as it is consumed almost exclusively in the production of teraphthalic acid (TPA) and dimethyl terephthalate (DMT). TPA and DMT are used to produce polyethylene terephthalate (PET) melt for polyester fibers, films, and solid-state packaging resins. In the next five years, global demand for *p*-xylene is projected to increase by an average of 6% annually, driven mainly by TPA and PET expansions in China, other Asian countries, and the Middle East [2].

Xylene isomers are particularly difficult to manufacture, and isolating the three isomers is energy intensive due to their similarity in physical properties [3-7]. Industry currently relies upon energy intensive crystallization and adsorption techniques to separate these isomers. The total production value of mixed xylenes in 1999 was estimated at $5 billion, second only to benzene in aromatic production [6]. World consumption was about 24 million tons in 1999, and is expected to exceed 33 million tons in 2006 at the current growth rate. With the increase in world production of xylenes and the current expensive industrial processes, many researchers are looking for a way to decrease energy demands and increase the economic return of the separation.

1.1 Industrial Motivation and Economics

The United States consumed approximately one fourth of the world's energy in 2004 at nearly 100 quadrillion BTU [1]. The petroleum and chemical industries accounted for 13 quadrillion BTUs in 1998 with approximately 35% being used in manufacturing and separating organic chemicals [1-2]. The high energy demands in the refining and chemicals industry have led economic forecasters to suggest that advanced energy efficient chemical separation techniques will grow by ~10%/year to reach nearly a $1.2 billion dollar industry in 2006 [3]. Separating organic liquids poses an opportunity for such techniques since the mixtures are often azeotropic, close boiling, isomeric, or heat sensitive. Traditionally organic liquids have required energy intensive methods such as complex distillation, cryogenic crystallization, or adsorption to obtain the desired component [6]. For example, aromatic processes (benzene, toluene, and xylene related processes) accounted for approximately 1 quad of energy consumption in 1997, and therefore could greatly benefit from a less energy intensive approach [7]. This thesis will concentrate on developing an efficient alternative to the energy intensive methods listed above.

1.2 Polymeric Gas Separation Membranes

The majority of previous work involving polymeric membranes has focused on developing solutions for the separation of various gas and aqueous mixtures. The separation of gases using polymers involves diffusion and sorption phenomena, an

characterization by corresponding sorption and diffusion coefficients that will be discussed in Chapter 2. The product of the above two parameters results in the *permeability*, which is an intrinsic property of the membrane material that effectively describes its productivity. This result was first proposed by Graham in 1866 [13], later quantified by von Wroblewski in 1879 [14], and can be described by the "solution-diffusion" model for permeation. Different gases permeate through polymer films at different rates, and therefore a *permselectivity* can be achieved for one gas over another. Since the permeability is a product of diffusion and sorption coefficients, the observed differences in permeability of a particular gas pair is actually a combined function of the ratio of diffusion and sorption of each gas in the polymer. The Fickian diffusion coefficient is described as the proportionality constant between the flux and the concentration gradient [15], although the chemical potential gradient is a more fundamental driving force. Sorption in glassy polymers has been described as the sum of uptake into Henry's law and Langmuir regions, using the popular "dual-mode" sorption model. These concepts are defined in more detail in Chapter 2, however they are introduced here as the basic concepts for quantifying membrane performance, and are used to establish the foundation for liquid membrane separation.

Polymeric membranes have been studied as a means to improve many industrial separations ranging from natural gas purification to organic liquids, including xylene isomers. In 1991 Robeson observed that a trade-off exists between the permeability (productivity) and selectivity (efficiency) of solution-processed polymers for essentially any penetrant pair of interest [11]. Robeson developed an "upper-bound trade off line"

that shows the existing limits for transport properties for solution processed polymers. For illustration purposes, and since xylene or organic liquids were not considered, Robeson's results for oxygen/nitrogen and carbon dioxide/methane are useful to discuss, and are shown in Figure 1.1. This figure indicates that as polymers are tailored to have a higher selectivity, there is a corresponding drop in permeability. Although many polymers have been developed close to the upper-bound, there have been few reports of processable polymers with properties above the upper-bound. In contrast, Figure 1.1 also shows how the transport property of a popular molecular sieve, Zeolite 4A, compares with the upper-bound curve. Zeolite membranes have been developed with superb selectivities, but have limited applications on a large scale due to low productivity, low mechanical durability, and high capital cost [6-8]. In the specific case of xylene isomers, reported polymeric permeabilities and selectivities are both extremely low, therefore chemical tailoring a polymer for high selectivity for permeability may be extremely challenging. In fact, a similar situation is likely to be encountered for many other

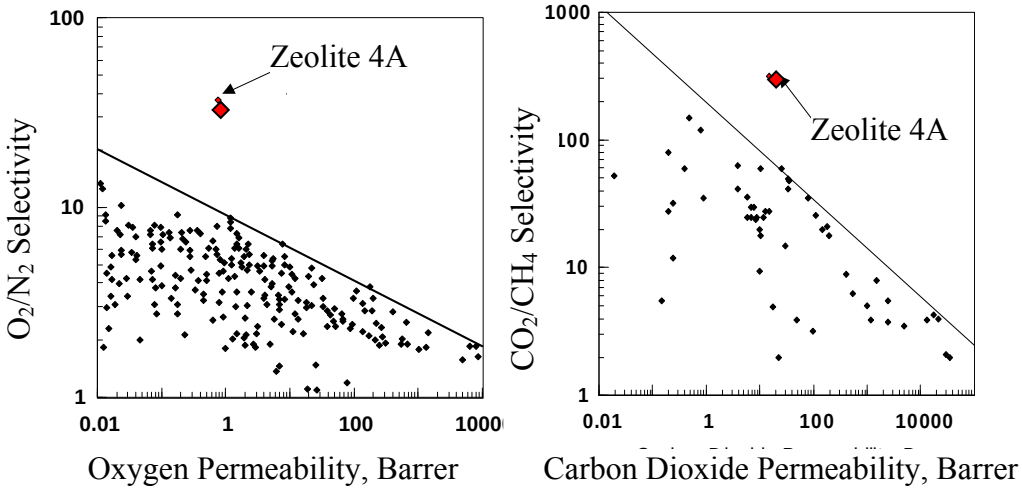

Figure 1.1: Upper-bound trade-off curves (1991) for the (a) oxygen-nitrogen and (b) carbon dioxide –methane gas pairs. Adapted from [11] and [16]. Also shown are the properties for the zeolite 4A, a commercially attractive molecular sieve.

Table 1.1: Potential pervaporation based processes for various applications. List adapted from [18]

Process	Application	Hybrid Process	Membrane
Acetic acid dehydration	Removal of low concentrations of water from acetic acid	Pervaporation-reverse osmosis	Hydrophilic
Benzene-cyclohexane separation	Separation of benzene-cyclohexane azeotrope	Pervaporation-distillation	Organophilic
Butyl acetate production	Removal of water from reactor to overcome equilibrium	Pervaporation-esterification reactor	Hydrophilic
n-Butyl oleate production	Removal of water from reactor to overcome equilibrium	Pervaporation-esterification reactor	Hydrophilic
Carboxylic-acid-ester production	Separation of carboxylic-acid-ester-methanol azeotrope	Pervaporation-distillation	Organophilic
Diethyltartrate production	Removal of water from reactor to overcome equilibrium	Pervaporation-esterification reactor	Hydrophilic
Dimethyl carbonate production	Separation of dimethyl carbonate-methanol azeotrope	Pervaporation-distillation	Organophilic
Dimethyl acetal production	Separation of dimethyl acetal-water azeotrope	Pervaporation-distillation	Hydrophilic
Dimethy urea production	Removal of water from reactor to overcome equilibrium	Pervaporation-reactor	Hydrophilic
Ethanol production	Separation of water-ethanol azeotrope	Pervaporation-distillation	Hydrophilic
Ethyl acetate production	Removal of water from reactor to overcome equilibrium	Pervaporation-esterification reactor	Hydrophilic
Ethyl carboxylate production	Removal of water from reactor to overcome equilibrium	Pervaporation-esterification reactor	Hydrophilic
Ethyl oleate production	Removal of water from reactor to overcome equilibrium	Pervaporation-esterification reactor	Hydrophilic
Ethyl valerate	Removal of water from reactor to overcome equilibrium	Pervaporation-esterification reactor	Hydrophilic
Ethyl tert-butyl ether production	Separation of ethyl tert-butyl ether-methanol-C4's azeotrope Removal of water to shift distillation equilibrium	Pervaporation-distillation	Organophilic
Fusel oil separation	Separation of fusel oil-water azeotropes	Pervaporation-distillation	Hydrophilic
Isopropanol production	Separation of water-isopropanol azeotrope	Pervaporation-distillation	Hydrophilic
Isopropyl propionate production	Removal of water from reactor to overcome equilibrium	Pervaporation-esterification reactor	Hydrophilic
Methylisobutyketone production	Separation of water-methylisobutylketone azeotrope Removal of water from reactor to overcome equilibrium	Pervaporation-distillation	Hydrophilic
Xylene isomers	Separation of p-xylene from o-xylene, m-xylene, and other C8 aromatics	Pervaporation-Crystallization/Adsorption	Organophilic

important organic penetrant systems, which have been stated as very energy intensive. Therefore the overarching goal of this project will be to use the xylene system as a "model" to define principles to extend the membrane paradigm to the high impact applications of separating organic liquids.

1.3 Pervaporation

Membranes for pervaporation separation operate in a different manner as compared to gas separation membranes. In this case the membrane is in direct contact with a liquid phase on the upstream side of the membrane, and the penetrant must leave the liquid phase, and then diffuse into the membrane. The membrane yields a vapor permeate, and the downstream side of the membrane is maintained either under vacuum or with a sweep gas that maintains the chemical potential driving force across the membrane. These systems are commonly operated at temperatures very close to the boiling point of the upstream liquid, to facilitate the transport through the membrane. Most industrial applications for separating organic liquids will operate at a high temperature under vapor feed conditions. Although pervaporation will not mimic the industrial conditions exactly, it should provide excellent insight to how membrane candidates will respond to actual saturated vapor candidates.

The applications of pervaporation can be basically classified into three categories: (1) dehydration of organic solvents, (2) removal of organics from aqueous solution, and (3) separation of organic mixtures [17]. These potential applications can apply to various liquid mixtures, and over a range of different concentrations. The two major limitations

associated with utilizing membranes are achieving (1) the necessary flux and (2) the needed purity to replace current industrial unit operations. Consequently, pervaporation will be used rarely as a stand-alone unit. The current optimum configuration is most likely the use of pervaporation as a concentration step or to overcome process restrictions such as chemical equilibrium or inhibition [18]. Potential applications of pervaporation process are given in Table 1.1. The required membrane type for each process is given as either hydrophilic (desired water permeate) or organophilic (desired organic permeate). This thesis focuses on what is perceived to be the most difficult of the organic separations; the purification of xylene isomers.

1.4 Membrane Technology

Many different polymer types have been investigated as membranes for various industrial and academic separations. These include, but are not limited to, polycarbonates, polyesters, polysulfones, polyimides, polypyrrolones, etc. [16]. The most common industrial scale membrane materials for gas separation are cellulose acetate, polysulfone, and polyamide [16]. These polymers are popular because they can be spun into asymmetric hollow fiber membranes, which is one of the two most common geometries for employing polymeric membranes [19]. Asymmetric hollow fiber membranes can contain up to 10,000 m^2 per m^3 of module, which is desirable to provide the needed volumetric productivity to maintain compact system sizes for large scale applications [19]. Hollow fiber membranes are comprised of a thin selective skin on the outside of a porous support layer as shown in Figure 1.2 [20]. This thin layer allows for high fluxes

in addition to the high surface area to volume ratio, and makes asymmetric hollow fiber economics competitive with more traditional techniques.

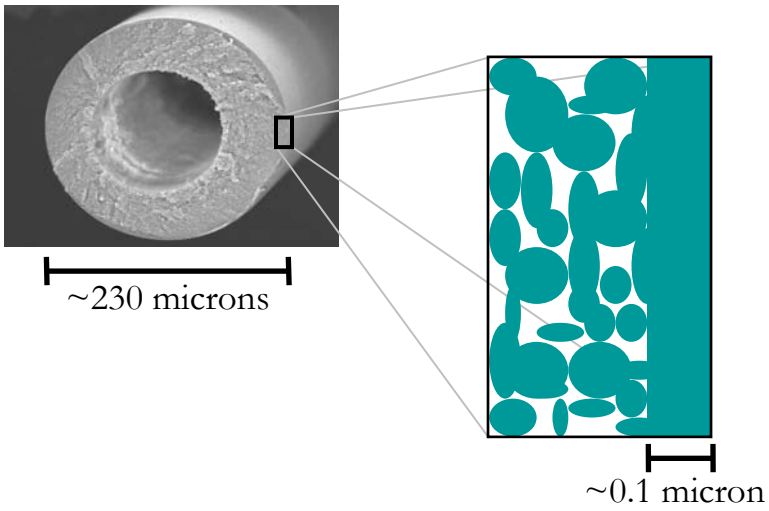

Figure 1.2 SEM picture of typical asymmetric hollow fiber and schematic of the thin separating skin layer

Other competitive technologies for aqueous-organic and organic-organic separation include absorption, adsorption, and distillation. In general, membranes are economical when either low purity or low flowrates of product materials are acceptable [16]. Advances in membrane materials which offer better permeability or selectivity will improve the economics and applicability of membrane based separations, and it is envisioned that this can be accomplished by formulating membrane materials that exceed the polymer upper bound shown in Figure 1.1. While efforts are ongoing to achieve these goals within gas separations, little is being done to propel organic liquid separations in the same direction.

1.5 Mixed Matrix Technology

Mixed matrix membranes are currently being studied as a class of composite membranes that can exceed the polymeric upper-bound curve and approach the attractive properties of pure zeolite membranes [8-10]. Mixed matrix membranes are under development for several commercial gas separations including carbon dioxide/methane, oxygen/nitrogen, propane/propylene, and various others [16]. However, extensive work has yet to be completed for various industrially applicable organic liquid systems.

Mixed matrix materials consist of a dispersed molecular sieving phase in a continuous polymer matrix. The most common dispersed phase materials are zeolites and carbon molecular sieves that have attractive separation properties for a desired separation. This type of composite should yield transport properties between the pure polymer and molecular sieve, while still maintaining the processability associated with many polymer techniques. Ideally, these materials would ultimately be commercialized in an asymmetric hollow fiber, with the dispersed sieving phase in the thin dense skin layer. This thesis will focus on formation and testing of dense films to approximate transport in the skin layer of hollow fibers.

Although the feasibility of the mixed matrix concept has been developed for gas separations, there are several challenges before this technology can be successfully applied to organic liquids. Two of the key challenges are selecting the ideal polymer-sieve combination to separate the desired components, and overcoming interfacial adhesion problems at the organic-inorganic interface. Selecting the polymer sieve

combination is complicated due to the fact that the interfacial bonding and the presence of the penetrants most likely affects the properties of each phase. The interface is a complicated issue in most composites, but is especially important in mixed matrix materials because small changes in interfacial properties will affect the transport properties of the composite. Both challenges will be addressed in this thesis.

1.6 Research Objectives

Although mixed matrix materials have been developed for gas separations, little has been done to develop similar composites for organic liquid separation. The major challenge is to develop reliable membranes with desirable properties from "off the shelf" polymers and molecular sieves. The overall objective of this thesis is to *use the xylene isomer separation as a "model" system to develop the principles for organic liquid separation using mixed matrix composite materials*. These principles will be investigated in the following objectives:

1. **Polymer Characterization**—Torlon® polyamide-imide has unique properties that should be potentially useful in a mixed matrix composite. Therefore the first part of this thesis will characterize Torlon®'s inherent properties, processing ability, and important transport potential. Torlon® will also be investigated to ensure the polymer satisfies various mixed matrix polymer constraints, thus enabling the polymer as a candidate for future composites.

2. **Characterization of the Zeolite Sieves**—The zeolite sieves are key components in the mixed matrix membranes and ultimately determine the required polymer

matrix properties. Better characterization of their intrinsic zeolite transport properties will therefore be pursued. Moreover, characterization of the effects of processing on properties of the sieves will also be key goals to ensure no loss in "matching" of properties occur during the procedures. Sorption/desorption kinetics of the sieves following exposure to different processing steps will be used to probe these issues.

3. **Polymer/Sieve Engineering**—Unlike mixed matrix materials for gas separation, for pervaporation and high activity organic vapor feeds, interfacial stresses between the sieve and matrix may possibly be mitigated by matrix swelling during operation. This situation may change the requirements for chemical tethering between the polymer and sieve surface to prevent de-lamination. Probing the requirements for surface tethering using silane type linkers and newly developed Grignard reagent techniques will also be an important part of the work. This will also be coordinated with objective (2) to ensure that any such processing to improve adhesion does not degrade intrinsic sieve or polymer properties.

1.7 Dissertation Overview

Chapter two provides background and fundamental theories for this thesis. All materials used and experimental procedures used throughout this work are summarized in chapter three. Chapter four presents an understanding of the unique properties of Torlon® polyamide-imide as a membrane for organic liquid separation. Chapter five examines the properties of the molecular sieve selected for this work, MFI. The principles investigated

in Chapters four and five are used in Chapter six to provide an understanding of bonding at the organic-inorganic interface, as well as the understanding of practical use of these materials as mixed matrix composite membranes. Chapter seven provides additional information on the interfacial morphologies of the composites developed in chapter six. Finally chapter eight gives conclusions and recommendations.

1.8 References

1. Xylenes, Publication Details. Nexant Chem Systems. 01-May-02. http://nexant.ecnext.com/coms2/summary_0255-114_ITM .

2. Advances in p-Xylene Technologies. Process Economics Program, SRI Consulting. 2006. http://www.sriconsulting.com/PEP/PEP/reports.upcoming.htm#3 .

3. Petroleum Industry Analysis Brief 20 August 2004. Department of Energy, 02 February 2004. http://www.eia.doe.gov/emeu/mexs/iab98/petroleum.sector.html .

4. Chemical Industry Analysis Brief 20 August 2004. Department of Energy 7 Jan 2004. http://www.eia.doe.gov/emeu/mecs/iab98/chemicals/feul_consumption.html .

5. Moore, Samuel K., Sorting out the prospects for novel separations. Chemical Week, 1991. 161(44): p 53.

6. Smitha, B., Suhanya, D., Sridhar, S., Ramakrishna, M., Separation of organic-organic mixtures by pervaporation—a review. Journal of Membrane Science, 2004. 241: p 1-21.

7. Energy and Environmental Profile of the U.S. Chemical Industry May 2000. U.S. Department of Energy Office of Industrial Technologies. Energetic Inc., Columbia Maryland, 2000.

8. Matsufuji, T., Norikazu, N., Matsukata, M., Ueyama, K., Separation of butane and xylene isomers with MFI-type zeolitic membrane synthesized by a vapor-phase transport method. Journal of Membrane Science, 2000. 178: p 25-34.

9. Wegner, K., Dong, J, Lin, Y.S., Polycrystalline MFI zeolite membranes: xylene pervaporation and its implication on membrane microstructure. Journal of Membrane Science, 1999. 158: p 17-27.

10. Sakai, H., Tomita, T., Takahashi, T., p-Xylene separation with MFI-type zeolite membrane. Separtion and Purification Technology 2001. 25: p 297-306.

11. Robeson, Lloyd M., Correlation of Separation factor versus permeability for polymeric membranes. Journal of Membrane Science, 1991. 62: p 165-185.

12. Mahajan, R., Vu, De Q., Koros, William J., Mixed Matrix Membrane Materials: An Answer to the Challenges Faced by Membrane Based Gas Separation Today? Journal Chin. Institute of Chemical Engineers, 2002. 33(1): p 77-86.

13. Graham, T. The London, Edinburgh, and Dublin Philosophical Magazine and Journal of Science 1866, XXXII, 401-20.

14. von Wroblewski, S. Wied. Annalen der Physik 1879, 8, 29.

15. Fick, A. Poggendorff's Annalen der Physic and Chemie 1855, 94, 59-86.

16. Moore, T. Effects of Materials, Processing Conditions, and Usage Conditions on the Morphology and Gas Transport Properties of Mixed Matrix Membranes. PhD dissertation, The University of Texas at Austin, 2004. Austin, Texas.

17. Feng, Xianshe and Huang, Robert Y. Liquid Separation by Membrane Pervaporation: A Review. Ind. Eng. Chem. Res. 1997, 36, 1048-1066.

18. Lipinzki, Frank; Field, Robert W.; Ten, Po-Kiong. Pervaporation-based hybrid process: a review of process design, applications and economics. Jounal of Membrane Science. 1999, 153, 183-210.

19. Koros, William J. Evolving Beyond the Thermal Age of Separation Processes: Membranes Can Lead the Way. AICHE Journal. 2004, 50, 2326-2334.

20. Wallace, David. Crosslinked Hollow Fiber Membranes for Natural Gas Purification and Their Manufacture from Novel Polymers. PhD dissertation, The University of Texas at Austin, 2004. Austin, Texas.

CHAPTER 2

BACKGROUND AND THEORY

This chapter introduces the fundamental theory that is essential to developing an understanding of membrane separations. The fundamentals will include an in depth look at the theory of liquid separation by membrane pervaporation. Next, the modeling of these systems are discussed, including modeling of composite membrane solutions. Finally this chapter will review xylene separations utilizing membrane techniques, as well as the development of mixed matrix materials for various gas separations.

2.1 Transport Property Theory

2.1.1 Permeation

Polymer membrane materials are typically characterized by two basic parameters: permeability, (P_i) for component *i*, and selectivity, (α_{ij}) for component *i* vs. *j*. Permeability characterizes intrinsic productivity of different membrane materials. The permeability in a ***gas*** or ***vapor*** separation is calculated by normalizing penetrant flux by the thickness, *l*, and partial pressure drop across a particular membrane sample, Δp_i; as shown below:

$$P_i = \frac{Flux_i \cdot l}{\Delta p_i} \tag{2.1}$$

The units of permeability are usually given in Barrers, defined as:

$$Barrer = 1 \times 10^{-10} \frac{cc(STP) \cdot cm}{cm^2 \cdot s \cdot cmHg} \tag{2.2}$$

Permeability may also be reported in scientific units, whereas:

$$1 \quad Barrer = 0.033485 \frac{\mu mol \cdot \mu m}{m^2 \cdot \sec \cdot Pa} \tag{2.3}$$

Permeation through a polymeric membrane occurs via a coupled diffusion and sorption mechanism [1], therefore permeability also equals the product of an effective diffusion coefficient, D_i, and effective sorption coefficient, S_i; as shown below:

$$P_i = \overline{D}_i \cdot \overline{S}_i \tag{2.4}$$

Diffusion and sorption are discussed separately in the following two subsections.

Selectivity provides a measure of a particular membrane's efficiency at separating one penetrant from another. For ***gas*** separations, where the condition of negligible downstream pressure exisits, for an A, B penetrant pair the ideal selectivity, $\alpha_{A/B}$, is given as:

$$\alpha_{A/B} = \frac{P_A}{P_B} \tag{2.5}$$

Equation (2.5) is used when the ideal permeabilities of each species are known in the material. Typically the permeability of the slower gas is used as the denominator, so selectivity is greater than or equal to one. Permeabilities and permselectivities are intrinsic properties of homogeneous materials. Like other intrinsic properties of homogenous materials, permeabilities and permselectivities are functions of temperature and pressure. A more general definition of mixed gas selectivity is given by the ratio of the mole fraction or partial pressures of the components in the permeate stream, *p"*, and feed stream, *p'*:

$$\alpha_{A/B} = \frac{p''_A / p''_B}{p'_A / p'_B} \tag{2.6}$$

In Chapter 1, Robeson's upper bound curve and corresponding trade-off between permeability and selectivity was introduced. The curve was originally developed as an empirical relationship [2], and had been given a theoretical basis by Freeman [3]. Robeson gives curves of the following form in terms of the empirical parameters k and n:

$$P_A = k\alpha_{AB}^n \tag{2.7}$$

Both Robeson and Freeman predicted that the exponential parameter, n, is related to the size difference between the two penetrants, A and B. The other parameter, k, depends on the relative condensabilities of the two gases and polymer properties such as interchain spacing (fractional free volume) and polymer chain rigidity. For a particular penetrant pair, the relative condensabilities are fixed, and therefore the polymer structure is the main factor affecting transport properties. Roughly, increasing interchain spacing will increase permeability and increasing chain rigidity will increase selectivity. However, once interchain spacing is increased beyond the point where diffusion is controlled by thermally induced motions, no additional increases in permeability can be obtained and the selectivity will decrease.

2.1.2 Diffusion

The transport of gas molecules in polymers and molecular sieves both undergo solution-diffusion based permeation, however diffusion in each material proceeds via different mechanisms. Each mechanism is discussed below.

2.1.2.1 Diffusion in Polymers

Diffusion in polymers takes place via locally occurring transient "gaps" that arise because of thermal fluctuations that cause "segment" scale random displacements within the dense polymer matrix [4]. Because both the frequency and size of these fluctuations increase with temperature, the diffusion coefficient increases with temperature following an Arrhenius expression. This usually favors the larger molecule, so the diffusion selectivity typically decreases with temperature.

2.1.2.2 Diffusion in Molecular Sieving Materials

Molecular sieves used in this thesis are crystalline aluminosilicates having a three-dimensional interconnecting network of silica and alumina tetrahedra. These sieves have microporous structures with dimensions similar to the dynamic sizes of the penetrant molecules. Diffusion in this type of media occurs by a pore "window" moderated mechanism [5]. In this case negligible motion of the sieve is involved in the diffusion process. The penetrant basically jumps from "cage" to "cage" via a "window" that is similar in size to the penetrant molecule. In a zeolite, the transition state occurs when the molecule occupies the window between cages. There can be a substantial entropic selectivity when there is a size or shape difference between two penetrants, because the number of allowed configurations in the transition state will be greater for the smaller penetrant [6]. Like polymers, the diffusion coefficient in molecular sieves increases with temperatures, as diffusion selectivity decreases. This can be explained by an Arrhenius expression as well.

2.1.3 Sorption

The sorption coefficient is defined as:

$$\bar{S}_i = \frac{C_i}{p_i} \tag{2.8}$$

Equation (2.8) indicates the thermodynamic affinity of the penetrant by the matrix, where C_i represents the sorbed concentration of a gas molecule in the membrane, and p_i is the upstream partial pressure when the downstream partial pressure is negligible in comparison with the upstream pressure.

2.1.3.1 Sorption in Polymers

Polymer sorption is classically described by the so called "dual-mode" model. According to this model, molecules may sorb into one of two "modes" comprising of Henry's Law regions, and Langmuir Regions [7]. The dual-mode model for penetrant "A" is expressed in terms of the Henry's law coefficient, k_D, and the Langmuir sorption parameters: the affinity, b, and hole saturation, C_H', constants. This is given by:

$$C_A = k_{D,A} p_A + \frac{C'_{H,A} b_A p_A}{1 + b_A p_A} \tag{2.9}$$

Sorption is roughly correlated to the fractional free volume of a polymer [8,9]. The Langmuir mode occurs only in polymers below their respective glass transition temperature, which have entrapped nonequilibrium "excess" free volume. The quantity of Langmuir sites depends on how far below the glass transition temperature the polymers current thermodynamic state is, as shown in Figure 2.1. The Henry's law coefficient and Langmuir affinity constants both increase with penetrant condensability [10].

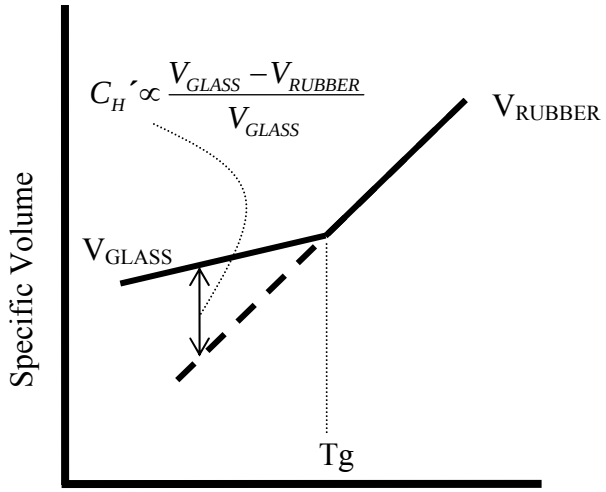

Figure 2.1: Sketch demonstrating the nature of polymer free volume about the glass transition temperature of the material. Adapted from [10].

Plasticization and Antiplasticization are two phenomena that can occur via penetrant sorption. Swelling of a polymer occurs due to excessive uptake in the Henry's Law region, after the Langmuir sites are full. This excessive swelling allows increased polymer chain mobility, and therefore increases the diffusion coefficient and respective permeability. This concept is described as plasticization, and commonly leads to decreased selectivities as well. This phenomena commonly occurs with carbon dioxide at high pressures, but can also be caused by condensable species at more moderate conditions including organics such as aromatics. Antiplasticization, as its name suggests, is the opposite effect, where sorbed penetrants induce a stiffening of the polymer matrix due to molecular interaction between the penetrant and monomer molecules. As expected, this phenomenon is characterized by reduced permeability and enhanced selectivity. This phenomenon can be observed when a small quantity of solvent remains in polymers after drying steps.

2.1.3.2 Sorption in Molecular Sieving Materials

Sorption in molecular sieves can be described by equation (2.9) as well, with the modification of setting k_d equal to zero, since there are no Henry's Law regions within the molecular sieve. The Langmuir sites for molecular sieve sorption commonly occur at channel intersection and in zeolitic cages within the framework structure. Most zeolites will behave in a strict Langmuir fashion, although some instances can induce multi-layer sorption, where different sorption sites have different energies of adsorption. In this situation, more complex characterizations are needed such as the BET characterization method [11]. Most of the sorption characterized in this work will follow a Langmuir type methodology.

2.1.4 Pervaporation

Separation using pervaporation membrane operates in a different manner as compared to gas separation membranes. In this case, the membrane is in direct contact with a liquid phase on the upstream face of the membrane and yields a vapor permeate; for this case the selectivity is represented as:

$$\alpha_{A/B} = \frac{p''_A / p''_B}{x_A / x_B} = \frac{ratio\ of\ \ permeate\ vapor\ components}{ratio\ of\ \ feed\ liquid\ components} \quad (2.10)$$

The penetrant must leave the liquid phase, and then diffuse into the membrane. Mathematically this can be expressed by manipulating equation (2.10) and observing that the ratio of the permeate partial pressures is also equal to the ratio of the individual species flux in the downstream receiver:

$$\alpha_{A/B} = \frac{p''_A / p''_B}{x_A / x_B} = \frac{Flux_A / Flux_B}{x_A / x_B} = \frac{\left(\frac{P}{l}\right)_A \Delta p_A}{\left(\frac{P}{l}\right)_B \Delta p_B (x_A / x_B)} = \frac{\left(\frac{P}{l}\right)_A (p_A' - p_A'')}{\left(\frac{P}{l}\right)_B (p_B' - p_B'')(x_A / x_B)} \quad (2.11)$$

Equation (2.11) can be further simplified by assuming negligible downstream pressure (vacuum permeate), constant membrane thickness, and by observing that a generalization of Raoult's law at the feed temperature gives:

$$p_i = \gamma_i x_i p_i^* \quad (2.12)$$

where γ_i represents the activity coefficient of component *i*, and p_i^* represents the saturated vapor pressure of component *i*. Therefore equation (2.11) becomes:

$$\alpha_{A/B} = \frac{p''_A / p''_B}{x_A / x_B} = \frac{(P)_A (\gamma_A x_A p_A^{*\prime})}{(P)_B (\gamma_B x_B p_B^{*\prime})(x_A / x_B)} = \left[\frac{(P)_A}{(P)_B}\right] \cdot \left[\frac{\gamma_A p_A^*}{\gamma_B p_B^*}\right] \quad (2.13)$$

This result shows that the observed pervaporative selectivity is comprised of two distinct factors, one due to the relative volatility of the two species, α_{evap}, and the other due to the different permeabilities of A and B in the membrane material, α_{mem}. Therefore we can express equation 2.13 as:

$$\alpha_{A/B} = \alpha_{evap} \cdot \alpha_{mem} \quad (2.14)$$

where α_{evap} is given by:

$$\alpha_{evap} = \left[\frac{\gamma_A p_A^*}{\gamma_B p_B^*}\right] \quad (2.15)$$

And α_{mem} is given by the same type expression as for simple gas separation:

$$\alpha_{mem} = \left[\frac{(P)_A}{(P)_B}\right] = \left[\frac{\overline{D}_A}{\overline{D}_B}\right] \cdot \left[\frac{\overline{S}_A}{\overline{S}_B}\right] \quad (2.16)$$

Clearly, the observed membrane selectivity gets a "boost" from the evaporative selectivity when the faster penetrating species is also the more volatile component in the feed mixture (therefore $\alpha_{evap} > 1$). For our model xylene isomer systems, this calculation will be simplified in the way that the xylene isomers in the xylene solution are similar enough that $\gamma_{p\text{-xylene}} \approx \gamma_{m\text{-xylene}} \approx \gamma_{o\text{-xylene}}$. Another key point in choosing to study pervaporation is that in our study the system operates at saturation pressure for the feed mixture, whereas an industrial process would typically operate with a "near-saturation" vapor feed, and require slightly more complex calculations. Our system will not mimic the industrial conditions completely; however it will provide an excellent starting point for identifying usable materials under these conditions.

2.2 Modeling Mixed Matrix Materials

While developing mixed matrix materials it is important to predict and evaluate the transport properties of composite materials against an appropriate model. This enables better understanding of the morphologies and adds a predictive component for development of future composites. Over the course of mixed matrix development, the Maxwell Model has been utilized as a reliable tool to accomplish these developmental needs. This section will explain this model and its application in composite membrane studies, multi-component separation, and non-ideal morphological effects.

2.2.1 The Maxwell Model

This work will use a model adapted from James C. Maxwell's 1873 work to predict the permittivity of a dielectric [12]. Maxwell's work has been applied to mixed matrix membranes [13, 14], by use of the two-phase equation:

$$P_{MM} = P_M \left(\frac{P_D + 2P_M - 2\Phi_D (P_M - P_D)}{P_D + 2P_M + \Phi_D (P_M - P_D)} \right) \tag{2.17}$$

In this equation, P is the permeability, and Φ_D is the volume fraction of the dispersed phase. The M subscript refers to the polymer matrix, the D subscript refers to the dispersed phase, and the MM subscript refers to the overall mixed matrix material. Other models have been studied and give reasonable results [15, 16], however these models are more complicated, and show no significant improvements over the Maxwell Model within experimental uncertainty. Therefore the Maxwell Model will be used as the theoretical framework of this study.

Further work has been completed for instances where model systems are more complex than the basic two-phase model. In the non-ideal instances, polymeric material forms "void" areas or "rigidified" areas surrounding the molecular sieves within the mixed matrix material, and will be discussed later in section 2.2.2. It will be useful to have a model that predicts such behavior, and this can be accomplished by use of the "three-phase Maxwell Model" [17]. This model treats the interfacial region around the sieve as a third phase and calculates an effective permeability for the sieve and the interfacial region, as shown:

$$P_{eff} = P_I \left(\frac{P_D + 2P_I - 2\Phi_S (P_I - P_D)}{P_D + 2P_I + \Phi_S (P_I - P_D)} \right) \tag{2.18}$$

In this equation, I is the interfacial subscript, and Φ_S is the volume fraction of the sieve in the sieve and interface region; this can be expressed:

$$\Phi_S = \frac{\Phi_D}{\Phi_D + \Phi_I} \tag{2.19}$$

The three-phase Maxwell Model (subscript 3MM) combines the above effective permeability with the permeability of the bulk polymer to yield a permeability for the composite system.

$$P_{3MM} = P_M \left(\frac{P_{eff} + 2P_M - 2(\Phi_D + \Phi_I)(P_M - P_{eff})}{P_{eff} + 2P_M + (\Phi_D + \Phi_I)(P_M - P_{eff})} \right) \tag{2.20}$$

Therefore, if the volume fraction and permeability of the interfacial region can be estimated, the Maxwell model can be extended to more complicated systems.

2.2.2 *Non-Ideal Effects*

As mixed matrix materials have been developed, several common non-ideal morphologies have been identified and characterized [10]. These non-ideal cases lead to composite materials that show little or no enhancement in separating potential. These cases are characterized by modifications to the Maxwell models discussed above, and each non-ideal case will be described in the subsequent sections.

2.2.1.1 Plugged Molecular Sieves

Many molecular sieving materials were developed to act as efficient adsorbents in a variety of chemical processes. By their vary nature they are highly prone to "clogging" with penetrants that they were originally designed to scavenge from the surrounding atmosphere. Great care must be taken when processing such materials to ensure clean sieving materials that are free of sorbed contamination and able to achieve desirable transport properties. When molecular sieving materials are clogged and used in a mixed matrix membrane the sieves act only as dispersed impermeable regions throughout the composite. The effect of such materials on transport properties can be predicted by the Maxwell Model. The permeability for the dispersed phase is essentially zero, and therefore equation (2.17) reduces to:

$$P_{MM} = 2P_M\left(\frac{1-\phi_d}{2+\phi_d}\right) \qquad (2.18)$$

For the case of a composite membrane containing 15 vol% molecular sieves, the effective permeability is reduced to ~80% of the neat polymer value. This reduction in permeability leads to no enhancement in selectivity, and therefore only reduces the productivity of the membrane composite. Several different contaminants can cause this type of effect. In the case of zeolite 4A which are highly water sorbing, the pores can be completely clogged if left exposed to the atmosphere for short periods of time [10]. ZSM-5 materials are highly organophilic which do not readily de-sorb at low temperatures [18]; therefore if left exposed at room temperature, the sieves will be clogged.

2.2.1.2 Matrix Rigidification

One of the key challenges in the study of many composite materials is the quality of interface between the two composite materials. This holds true for mixed matrix membranes, where good quality of the organic (polymer) and inorganic (molecular sieve) interface is essential for achieving the optimum separating performance. One of the non-ideal effects that can occur due to interfacial complications is matrix rigidification. When a polymer material is anchored to the inorganic dispersed phase, it is possible for the polymer chains to have a reduced mobility in the sieve region. Reduced mobility near such inserts has been reported in several systems, and shown to reduce the overall permeability of the membrane (although an enhancement in selectivity can still be observed) [10,19]. This phenomenon becomes more pronounced as the sieve loading increases, due to increased interfacial areas in the membrane, and it can lead to films to become to mechanically unstable or "brittle" for practical use [10]. If the permeability

and the size of the rigidified region is known, then the three phase Maxwell Model (equation 2.20) can be used to predict the transport properties of the composite material.

2.2.1.3 "Sieve-in-a-Cage"

The phrase "Sieve-in-a-Cage" has been utilized by mixed matrix material developers to describe composite materials with voids at the organic/inorganic interface. This non-ideality is probably the most widely studied effect, and is most often caused by de-lamination of the polymer from the sieve material during solvent removal. Figure 2.2 shows an example of such behavior. The depicted composite is silicalite dispersed randomly throughout Torlon ® polyamide-imide. It is apparent that the two native surfaces are not attracted to each other, and have de-laminated leaving void space (or a "cage") surrounding each individual zeolite crystal. This morphology is undesirable

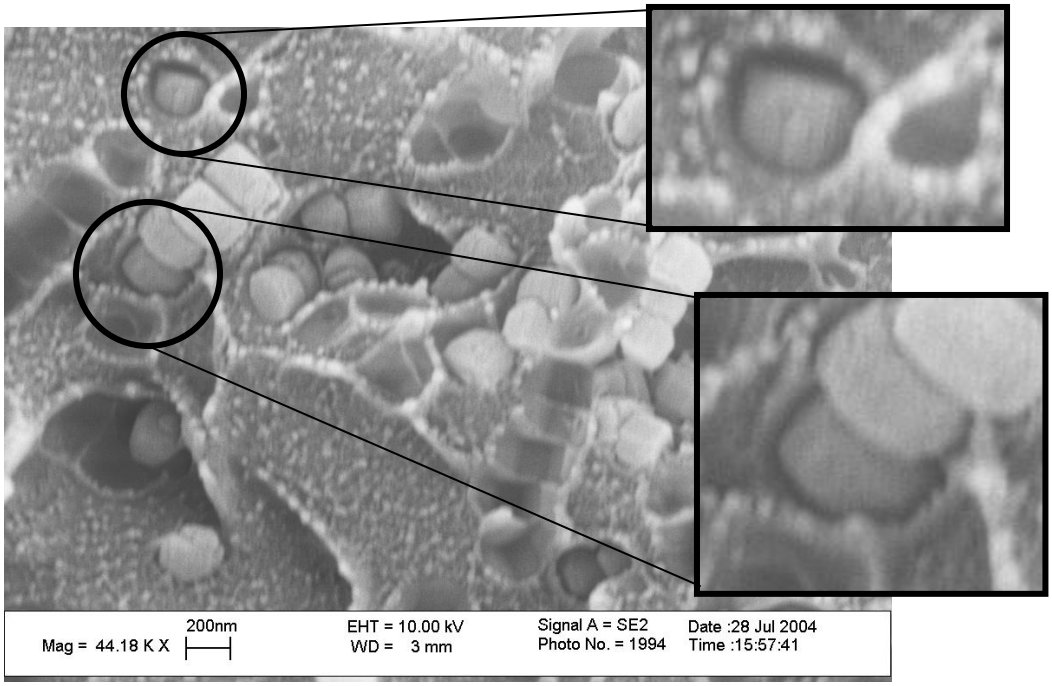

Figure 2.2: Silicalite dispersed in Torlon® PAI showing "sieve-in-a-cage" morphology."

since the void is much more permeable than the zeolite and penetrants will bypass the zeolite. In mixed matrix materials, this leads to composite membranes with permeabilities greater than and selectivities equal to or lower than the neat polymer. If the void is similar in size to the gas molecules, then the penetrants can have Knudson type diffusion values within the void space [20]. Again, this effect can be modeled by the three phase Maxwell model by inserting reasonable estimations for the void size and permeability. This work has been completed by utilizing Knudson transport regimes [10], and accordingly will favor the lighter penetrant. Although Figure 2.2 easily identifies "Sieve-in-a-Cage" morphology, more subtle, molecular sized voids are generally below the resolution of SEM. TEM has been used to characterize the void space with difficulty [10], and in practice it is very difficult to get an accurate representation of the void thickness. Surface modifications and chemical tethering are commonly used and developed to overcome such non-idealities, and will be explored in this thesis.

2.3 Polymer-Sieve Selection Criteria

Previous mixed matrix material development has shown that several factors should be considered when choosing polymers and molecular sieves for mixed matrix composite materials [10]. For the molecular sieve phase, the most obvious property that should be considered is the pore size. Table 2.1 shows a list of molecular sieves [18], and gives example molecules that can be accepted at that size. From the table it can be seen that for many industrial applicable separations a highly crystalline microporous zeolite (< 20 Å) is well suited. For our model system of xylene isomers, it can be seen that p-xylene can

Table 2.1: Examples of Molecules Accepted by Various Zeolites. Adapted from [18].

Zeolite	Approx. Window Size (Å)	Molecules accepted
KA (3A)	2.8	He, H_2O, NH_3
Ca and Ba Mordenite	3.8	Ne, Ar, CO, CO_2, H_2O_2, N_2, O_2, and above
NaA (4A)	4.0	Kr, Ch_4, C_2H_6, CH_3OH, CH_3CI, C_2H_2, CS_2, CH_3NH_2, and above
CaA (5A)	4.9	C_3H_8, n-C_4H_{10}, C_2H_5Cl, C_2H_5OH, $C_2H_5NH_2$, CHF_2Cl, CHF_3, CH_3,I, B_2H_6, and above.
MFI (ZSM-5, Silicalite)	5.6	Benzene, p-xylene, ethylbenzene, isobutane, and above.
NaX (13X)	7.8	SF6, isobutane, isopentane, $CHCl_3$, C_3F_8, CCl_4, toluene, naphthalene, o-xylene, m-xylene, and above
CaX (10A)	10.0	1,3,5-Triethylbenzene and above.

fit into MFI structures, whereas the ortho and meta isomers can not (there are exceptions [21-23].)

Pore structure is another property to be considered. A one dimensional structure can only allow single file diffusion, where the diffusion is limited by the slowest penetrant. Zeolites with two dimensional structures such as MFI structures can display anisotropic effects. Three dimensional structures are ideally suited to mixed matrix membranes because they require no orientation of the pores, and therefore allow random orientation of zeolite crystals to achieve transport property enhancement.

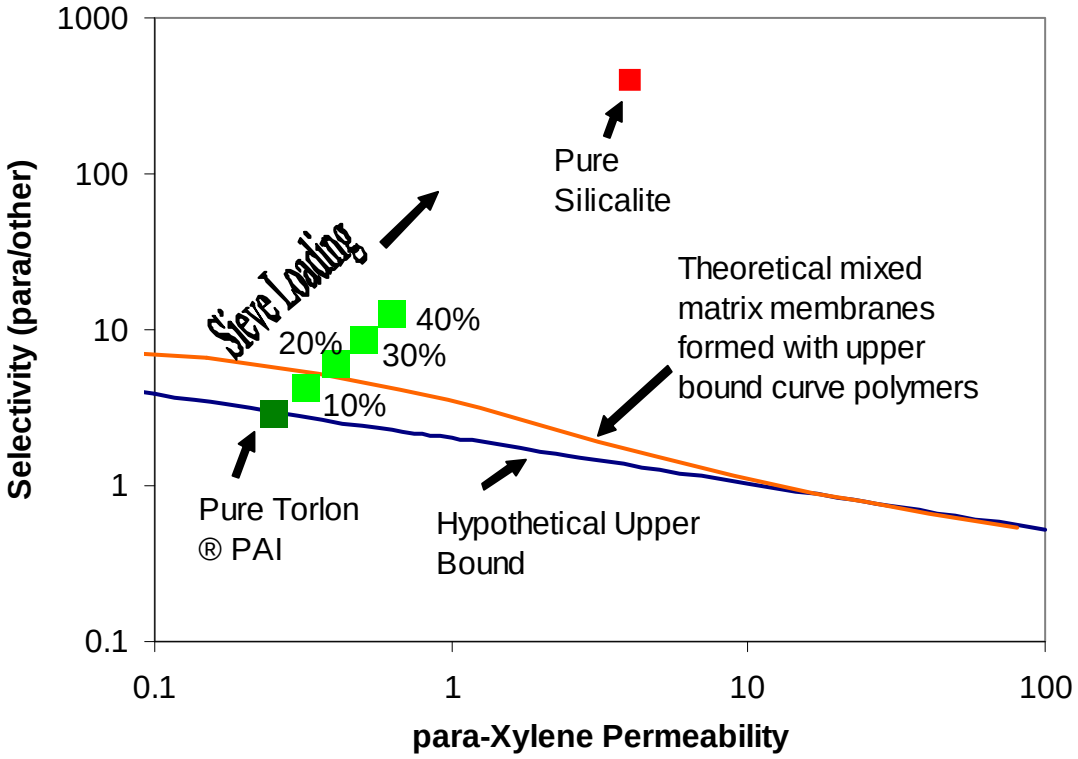

Figure 2.3: The use of the Maxwell model for the selection of optimal polymer-sieve combinations. The blue line represents an upper-bound for the purification of para-xylene from other c8 isomers. The orange line represents the calculated performance of composite mixed matrix membranes made with polymers along the upper bound. The most advanced polymer to date, Torlon ® is shown as the dark green square, with the predicted performance of mixed matrix materials with Torlon ® and silicalite shown in light green with increased zeolite loading.

The Maxwell Model described above provides a useful framework for matching desirable sieve and polymer properties. Figure 2.3 illustrates the use of the Maxwell Model to calculate the properties of potential mixed matrix membranes. An upper bound line has been estimated based on the work of Burns [69] and Freeman [70], and assuming Torlon® lies on this upper bound, as will later be shown to be an advanced candidate for xylene separation. For a zeolite with an intrinsic permeability of 4 Barrer, and an intrinsic selectivity of 400, it can be seen that a maximum selectivity exists in the potential mixed matrix membrane curve. This maximum corresponds to selecting a

polymer that is slightly less permeable than the molecular sieve. This allows the fast diffusing penetrant to pass through the membrane without difficulty, while the slower diffusing penetrant takes a more tortuous path around the molecular sieve. In light of this, it is unwise to select a polymer that is much more permeable than the sieve, which corresponds to the right side of Figure 2.3, and this combination results in very little enhancement of selectivity properties. Once a proper zeolite is selected for a particular separation, this matching process is the most important step to obtain well engineered composite membranes with desirable overall transport properties and this approach has been developed by various researchers for this purpose [24-25].

2.4 Literature Review on Pertinent Topics

This thesis seeks to establish protocols for developing composite mixed matrix membrane for use in organic liquid separation. It is important to understand prior work that has been completed related to this study, and how previous work can be applied to the present research. This work will apply mixed matrix theory to xylene separation as a model system to identify the key issues in liquid membrane separation. In the first subsection, a high performance polyamide-imide polymer will be introduced and relative literature on its use in separation will be reviewed. The second section will review previous work on separating xylene isomers via membranes. The third subsection will review the basic knowledge of the zeolite selected for this work, MFI, otherwise known as ZSM-5 or silicalite. Lastly, the development of composite mixed matrix membranes will be reviewed.

2.4.1 Torlon® Polyamide-imide

This thesis will focus on an established polyamide-imide family that is sold under the tradename, Torlon® from Solvay Advanced Polymers©. The chemical structure of Torlon 4000T® is shown in Figure 2.4, as provided by [26]. Torlon® appears interesting due to its commercial use as a polymer coating material, in which it was specifically designed to be chemically resistant, thermally stable, and mechanically durable. Also, polyamide-imides have been shown to allow higher inorganic loadings and the ability to disperse inorganics more homogeneously in a mixed matrix type material [27].

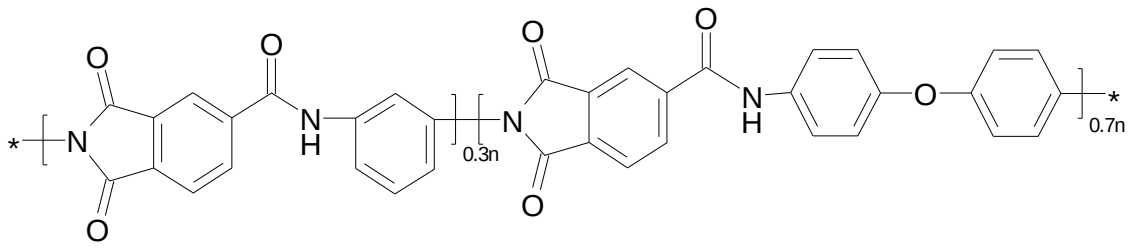

Figure 2.4: Structure of Torlon ® 4000T polyamide-imide proposed by [26].

Torlon ® is mainly marketed as a candidate for injection molding for use in hydraulic parts, seal rings, washers, bushings, etc. Recently Torlon ® has also found use in the electrical industry as a delicate device shield, given its resilient properties when properly cured [28]. Very little academic literature has been published on Torlon ®, with most of the activity being within the last 5 years. A small selection of literature has focused on Torlon®'s use in electronics and optics [29, 30]. A larger, but still small, subset, of literature has utilized Torlon® as a membrane material for vapor permeation of 2-propanol [31-33], however no literature could be found with regard to Torlon® as a candidate for C8 aromatic separation or mixed matrix composite technology.

2.4.2 *p*-Xylene Membrane Separation

Separation of organic-organic mixtures has been investigated extensively due to their importance to the chemical and petrochemical industries, including the separation of xylene isomers. Membrane techniques for this separation can be classified into two areas; polymeric membranes without additives and polymeric membranes with additives. Xylene separation has been studied with polyurethane [34, 35], polyvinyl alcohol (PVA) [34, 36], and polyimides [34, 37, 38], but none have produced substantial selectivities (most report α~1) at reasonable permeabilities. For this reason researchers began exploring the notion of blending bulk polymer with additives, (similar to mixed matrix materials but comprising a molecular level blend) and most of this work has focused on organic materials such as cyclodextrin (CD). In this class of polymeric membrane materials, there has been some limited success. Chen et. Al. [36] reported an increase in PVA selectivity from 1.35 to 2.96 (para/ortho at 25°C) after adding CD to form a 33-wt % blend. Although this is a significant increase, it still is too low for an industrially competitive process. Also this experiment took place at low temperature (25°C), and with a bulk polymer (PVA) that has a low glass transition temperature (~77°C), thus not meeting the high temperature requirement of many industrial processes. Further, with CD being comprised of several adjoined sugar rings, it is unclear as to the attainable thermal stability of the additive itself, and is unlikely to withstand more aggressive feed streams at higher temperature while maintaining membrane integrity. Other researchers have shown cyclodextrin additives can also be reversely selective for the ortho isomer

depending on the particular type of CD added to the bulk polymer. For these reasons, and the concern of thermal stability, CD was not considered as an alternative for this research.

Some early studies with "mixed matrix-like" materials have also been completed. Vankelecom et. al. [39-41] worked on mixed matrix materials from poly-dimethylsiloxane (PDMS) and polyimides. Molecular zeolite sieves were initially added to PDMS and studied for sorption of water and chlorinated hydrocarbons. Later work investigated the separation of xylene isomers, but found void formation and organic-inorganic interface detachment in the case of polyimides. The use of silane coupling agents was also investigated, but significant work on transport properties was neglected; only the possibility of coupling agent used to improve the interface was identified.

2.4.3 MFI for *p*-Xylene Purification

For some time now, MFI type zeolites have been used for organic applications, mainly centered on catalysis. ZSM-5 and its pure silica analog, "silicalite," are among the most important examples. These are widely used in the petroleum and petrochemical industries as catalysts for xylene isomerization, catalytic dewaxing, and selective

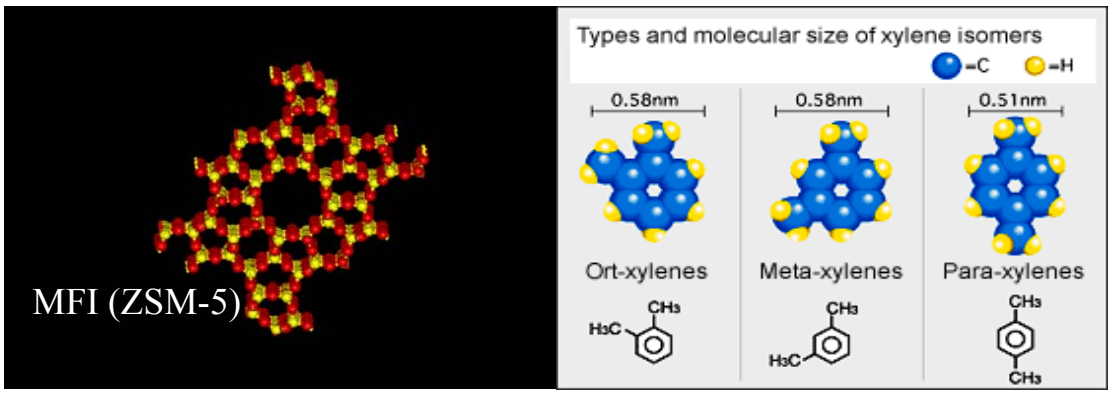

Figure 2.5: An example of the pore structure of MFI type zeolites (left) and models of xylene isomer configurations (right).

adsorbents. Their distinctive features include high thermal/hydrothermal stability, hydrophobic/organophillic adsorptive properties, and an intermediate pore size of 5.5 Å, which offers molecular size selectivity [42]. The Si/Al ratio ranges from 20-30 in a typical ZSM-5 to over 1000 in "silicalite." It is the low aluminum content which is responsible for the hydrophobic nature of these materials. Previous researchers have attempted to manufacture zeolite membranes for large scale industrial use; however, these materials have shown to be as much as 3 orders of magnitude more expensive to produce, and are much more fragile than commercial polymers [43]. As a result, there are virtually no large commercial membrane products based on molecular sieves.

Molecular sieve membranes have very regular pore structures that preferentially allow the smaller molecules to penetrate through the membrane faster, while mainly restricting the larger gas molecule from penetrating. In the case of MFI, this methodology applies well to our xylene isomer model system. In Figure 2.5 an example can be seen of the MFI pore, which is approximately 5.6Å. *p*-Xylene can preferentially transport through this pore due to its minimum cross-section of ~5.1Å. The larger cross-section (~5.8Å) o-xylene and m-xylene are restricted.

Several authors have reported using MFI type membranes to separate xylene isomer systems, however their results are inconsistent [23, 44, 45]. These researchers have shown xylene separation factors ranging from unity to as high as several hundred. It is believed that these inconsistent results are due to defect formation during the growth of the zeolite membrane. Recent reports of MFI type membranes grown in "self-

supporting" structures have obtained reasonably high selectivities at high temperature (>200°C ~100 para/ortho) [46]. However, it is extremely difficult to assure defect free membrane formation, and also difficult to quantify the effective thickness of the selective layer in these membranes. These uncertainties make it difficult to obtain fundamental properties, such as MFI's inherent selectivities and permeabilities. Fortunately, an MFI/xylene separation research group developed a method to create thin zeolitic membranes [21]. These new ultra thin membranes have very high selectivities (~400 para/ortho) while the total thickness of the membrane is maintained at nearly 1μ. The integrity of the crystal structure was probed by fluorescence microscopy, and shows little, if any, defects. Using these data, a permeability range of 25-100 Barrers, and a selectivity of at least 400 (para/ortho) can be estimated at 200°C. This data will be used to match the zeolite to a polymer matrix with a similar permeability. These values will ultimately be checked for consistency using models of mixed matrix materials using matrices of known permeabilities.

The synthetic history of the MFI structure has also been shown to have an effect on the transport properties of the crystals. Systematic studies have been completed on the calcination rate [48] and the Si/Al ratio [47]. Surface reactivity has also been investigated with emphasis on reducing surface reactivity by synthesizing inert silicalite shells on the acidic ZSM-5 [49, 50]. MFI containing higher concentrations of aluminum are more reactive due to the increased number of Bronsted acid sites at aluminum surface atoms [18]. However it is this low amount of aluminum and acidity that makes MFI silicalite type structures hydrophobic, and therefore preferential for organic separation. It

may be advantageous to have a pure silica core particle with a slightly alumina containing surface to enhance surface reactivity (i.e. tethering to the bulk polymer in mixed matrix material). All literature available in creating such "zoned" particles have synthesized completely the opposite: a hydrophilic, high aluminum containing core, with a silicalite shell to remove surface reactivity [49-50].

2.4.4 Mixed Matrix Materials

The majority of mixed matrix development has taken place over the past 10-15 years, however the first membrane application was introduced in 1960 by Barrer and James [51, 52]. These membranes showed reduced performance apparently due to voids at the inorganic-organic interface. Further development occurred in 1973 when Paul and Kemp prepared zeolite 5A and silicone rubber composite materials, but again showed poor performance due to poor sieve selection for the attempted gas pair [53]. Several authors have attempted organic separations such as alcohol water mixtures from Poly(dimethyl siloxane) PDMS and zeolite composites [54-57]. Others have tried similar composite combinations in gas separations, again with moderate success [58, 59]. This technique has shown moderate success due to better interfacial adhesion of the more flexible PDMS backbone to the zeolitic surface; however, all of these composites lie well below the polymeric upper bound, due to the low intrinsic performance of the neat PDMS polymer membranes.

Glassy materials offer more attractive intrinsic properties that lie closer to the upper-bound, but are often more difficult to form successful composites. Silicalite has been dispersed in cellulose acetate to achieve enhanced gas selectivity; however, poor results

were obtained, which was attributed to interfacial voids [60-61]. Further work has been done to increase the selectivity of polyethersulfone filled with zeolites 13X and 4A for various gas pairs and shown modest improvements [62]. Vankelecom has reported polyimide based mixed matrix membranes filled with borosilicate, silicalite, or zeolite Y, which exhibited voids at the polymer-sieve interface [40]. To resolve the void issue, several research groups have studied silanation as a means to tether the polymeric matrix to the inorganic surface [10, 39].

The development of models for predicting the transport properties of heterogeneous systems for mixed matrix membranes was a significant development for membrane evaluation [25]. Zimmerman et al [63] published criteria for selecting a suitable polymer-sieve pair for a given separation to achieve a specific mixed matrix effect. Thereafter, a number of techniques have been applied to create mixed matrix materials that achieve predicted composite properties [64-67]. Most recently, Husain has demonstrated a novel procedure to overcome interfacial voids via a Grignard treatment process [68]. This process has had success in thin dense films, as well as polymeric hollow fibers which are traditionally used in industrial separations. All of these tools will be applied to develop mixed matrix materials for xylene isomeric separations.

2.5 References

1. Wijmans, J.G. and R.W. Baker. J. Membr. Sci. 1995, 107, 1-21.
2. Robeson, L.M. J. Membr. Sci. 1991, 62, 165-85.
3. Freeman, B.D. Macromolecules 1999, 32, 375-380.
4. Koros, W.J. and G.K. Fleming. J. Membr. Sci. 1993, 83, 1-80.

5. Breck, D.W. Zeolite molecular sieves: Structure, chemistry, and use. 1974, Malabar, FL: Robert E. Krieger Publishing Co, Inc.

6. Singh, A. and W.J. Koros. Ind. Eng. Chem. Res. 1996, 35, 1231-4.

7. Paul, D.R. and W.J. Koros. J. Polym. Sci., Polym. Phys. Ed. 1976, 14, 675-85.

8. Ganesh, K.; R. Nagarajan; and J.L. Duda. Ind. Eng. Chem. Res. 1992, 31, 746-55.

9. Jordan, S.S. and W.J. Koros. Macromolecules 1995, 28, 2228-35.

10. M oore, T. Effects of Materials, Processing Conditions, and Usage Conditions on the Morphology and Gas Transport Properties of Mixed Matrix Membranes. PhD dissertation, The University of Texas at Austin, 2004. Austin, Texas.

11. Brunauer, S., Emmett, P.H., and Teller, E.; J. Am. Chem. Soc., 1938, **60**, 309.

12. Maxwell, J.C., A treatise on electricity and magnetism. Vol. 1. 1873, Oxford: Clarendon press.

13. Petropoulos, J.H. Journal of Polymer Science, Polymer Physics, 1985. **23**(7): p. 1309-24.

14. Bouma, R.H.B., et al. Journal of Membrane Science, 1997. **128**(2): p. 141-149.

15. Davis, H.T. Journal of the American Chemical Society, 1977. **60**(11-12): p. 499-501.

16. Bruggemann, D.A.G. Annalen der Physik V, 1935. **24**: p. 636

17. Mahajan, R. and Koros, W.J. Polymer Engineering and Science, 2002. **42**(7): p. 1420-1431.

18. Auerback, S., Carrado, A., Dutta, P., Handbook of Zeolite Science and Technology. Marcel Dekker, Inc. New York. 2003.

19. Manson, J.A. and E.H. Chiu. J. Polym. Sci., Polym. Symp. 1973, No. 41, 95-108.

20. Knudsen, M. Annalen der Physik 1909, 28, 75-130.

21. Lai, Z., Tsapatisis, M. Science. 2003, 300, 456.

22. Nair, S., Tsapatsis, M. J. Phys. Chem. B 2000, 104, 8982-8988.

23. Xomeritakis, G., Nair, S., Tsapatsis, M. Microporous and Mesoporous Materials. 2000, 38, 61-73.

24. Kulprathipanja, S.; R.W. Neuzil; and N.N. Li, Separation of fluids by means of mixed matrix membranes. US Patent No. 697,990. 1988.

25. Zimmerman, C.M.; A. Singh; and W.J. Koros. J. Membr. Sci. 1997, 137, 145-154.

26. Robertson, G.P., Guiver, M.D., Yoshikaws, M., Brownstein, S. Polymer, 2004. 45: p 1111-1117.

27. Fritsch, D., Peinemann, K.V. Journal of Membrane Science, 1995. 99: p 29-38.

28. Torlon® Polyamide-imide. Solvay Advance Polymers. August, 01, 2006. http://www.solvayadvancedpolymers.com/products/bybrand/torlon/0,6647,329-2-0,00.htm

29. Yoshikawa, M., Guiver, M.D., Robertson, G.P.. Journal of Molecular Structure. 2005, 739, p. 41-46.

30. Barucci, M.; Olivieri, E.; Pasca, E.; Risegari, L.; Ventura, G.; Cryogenics, 2005, 45, p. 295.

31. Higuchi, Ako. Separation Science and Technology, 2005, 40, p. 3419.

32. Higuchi, Ako; Yoshikawa, Masakazu; Guiver, Michael D.; Robertson, Gilles P. Separation Science and Technology, 2005, 40, p. 2697-270.

33. Yoshikawa, Masakazu ;Higuchi, Ako; Ishikawa, Masaaki; Guiver, Michael D.; Robertson, Gilles P. Journal of Membrane Science, 2004, 243, p 89-95.

34. Wegner, K., Dong, J, Lin, Y.S. Journal of Membrane Science, 1999. 158: p 17-27.

35. Cunha, V.S., Paredes, M.L.L., Borges, C.P., Habert, A.C., Nobrega, R.. Journal of Membrane Science 2002. 206: p 277-290.

36. Chen, H.L., Wu, L.G., Tan, J., Lhu, C.L. Chemical Engineering Journal, 2000. 78: p 159-164.

37. Hao, J., Tanaka, K., Kita, H., Okamoto, K. Journal of Membrane Science, 1997. 132: p 97-108.

38. Schleiffelder, M. Staudt-Cickel, C. Reactive & Functional Polymers, 2001. 49: p 205-213.

39. Vankelecom, I.F.J., Van den broeck, S., Mercks, E., Geerts, H., Grobet, P., Uytterhoeve, J. Journal of Physical Chemistry, 1996. 100 : p 3753-3758.

40. Vankelecom, I.F.J., Merckx, E., Luts, M., Uytterhoeven, J. Journal of Physical Chemistry, 1995. 99: p 13187-13192.

41. Vankelecom, I.F.K., Scheppers, E., Heus, R., Uytterhoeven, J. Journal of Physical Chemistry, 1994. 98: 12390-12396.

42. Karger, J., and Ruthven, D.M., Diffusion in Zeolites and Other Microporous Solids. 1991, John Wiley & Sons, Inc. p 467-508.

43. Mahajan, R., Vu, De Q., Koros, William J. Journal Chin. Institute of Chemical Engineers, 2002. 33(1): p 77-86.

44. Nair, S., Lai, Z, Nikolakis, V., Xomeritakix, G., Bonilla, G., Tsapatsis, M. Microporous and Mesoporous Materials 2001. 48: p 219-228.

45. Xomeritakis, G., Lai, Z., Tsapatsis, M. Industrial Engineering Chemical Resources, 2001. 40: p 544-552.

46. Sakai, H., Tomita, T., Takahashi, T. Separation and Purification Technology, 2002. 25: p 297-306.

47. Noack, M., et. Al. Microporous and Mesoporous Materials 2005, 79, p. 329-337.

48. Jareman, F.; Andersson, C.; Hedlund, J. Microporous and Mesoporous Materials, 2005, 79, p. 1-5.

49. Qinghua, Li; Wang, Z.; et al. Microporous and Mesoporous Materials. 2005. 78, p 1-10.

50. Lee, W.Y.; Park, T.J.; Lee, C.S. Applied Catalysis A. 1993, 96, p 151-161.

51. Barrer, R.M. and S.D. James. J. Phys. Chem. 1960, 64, 421-7.

52. Barrer, R.M. and S.D. James. J. Phys. Chem. 1960, 64, 417-21.

53. Paul, D.R. and D.R. Kemp. J. Polym. Sci., Polym. Symp. 1973, No. 41, 79-93.

54. Vankelecom, I.F.J.; S. De Beukelaer; and J.B. Uytterhoeven. J. Phys. Chem. B 1997, 101, 5186-5190.

55. Te Hennepe, H.J.C.; C.A. Smolders; D. Bargeman; and M.H.V. Mulder. Sep. Sci. Tech. 1991, 26, 585-96.

56. Bartels-Caspers, C.; E. Tusel-Langer; and R.N. Lichtenthaler. J. Membr. Sci. 1992, 70, 75-83.

57. Dotremont, C.; I.F.J. Vankelecom; M. Morobe; J.B. Uytterhoeven; and C. Vandecasteele. J. Phys. Chem. B 1997, 101, 2160-2163.

58. Duval, J.M.; B. Folkers; M.H.V. Mulder; G. Desgrandchamps; and C.A. Smolders. J. Membr. Sci. 1993, 80, 189-98.

59. Duval, J.M.; A.J.B. Kemperman; B. Folkers; M.H.V. Mulder; G. Desgrandchamps; and C.A. Smolders. J. Appl. Polym. Sci. 1994, 54, 409-18.

60. Kazarian, S.G.; M.F. Vincent; F.V. Bright; C.L. Liotta; and C.A. Eckert. J. Am. Chem. Soc. 1996, 118, 1729-36.

61. Duval, J.M.; A.J.B. Kemperman; B. Folkers; M.H.V. Mulder; G. Desgrandchamps; and C.A. Smolders. J. Appl. Polym. Sci. 1994, 54, 409-18.

62. Süer, M.G.; N. Ba; and L. Yilmaz. J. Membr. Sci. 1994, 91, 77-86.

63. Zimmerman, C.M.; R. Mahajan; and W.J. Koros. Polym. Mater. Sci. Engr. 1997, 77, 328-329.

64. Mahajan, R.; R. Burns; M. Schaeffer; and W.J. Koros. J. Appl. Polym. Sci. 2002, 86, 881-890.

65. Mahajan, R. and W.J. Koros. Polym. Engr. and Sci. 2002, 42, 1432-1441.

66. Vu, D.Q.; W.J. Koros; and S.J. Miller. J. Membr. Sci. 2003, 211, 335-348.

67. Vu, D.Q.; W.J. Koros; and S.J. Miller. J. Membr. Sci. 2003, 211, 311-334.

68. Hussain, S. Mixed Matrix Dual Layer Hollow Fiber Membranes for Natural Gas Separation. PhD dissertation, Georgia Institute of Technology, 2006. Atlanta, Georgia.

69. Burns, R.L.; Koros, W.J. Journal of Membrane Science. 2003, 211, 299-309.

70. Freeman, B.D. Macromolecules. 1999, 32, 375-380.

CHAPTER 3

MATERIALS AND METHODS

This thesis focuses on mixed matrix membranes with MFI zeolite inserts for use as a potential *p*-xylene purification membrane. This chapter introduces materials utilized to form membrane composites, as well as the methods to characterize their properties. The first section will discuss polymers, zeolites, and zeolite surface modification methods used in the formation of composite membranes. Secondly, the basic procedures and processes used in membrane formation will be detailed. Lastly, the equipment used for measuring permeability, selectivity, and complimentary material techniques will be discussed.

3.1 Materials

This research builds on previous techniques for developing mixed matrix membranes for gas separation, and expands the existing knowledge for use in organic liquid separation. Most materials were used "as- received" with little processing. The main solvent used for this work was N-methyl pyrrolidinone (NMP), and unless otherwise specified, all polymer materials were cast from this solvent. Dimethylacetamide (DMAc), and Dimethylformamide (DMF) were also used in rare occasions. All solvents were supplied from Sigma-Aldrich (Milwaukee, WI) in anhydrous form. Regardless of their end use, all solvents were transferred from "Sure-Seal" bottles to prevent contamination from water.

3.1.1 Polymers

Given the numerous commercial polymer candidates readily available, this research focuses on one high performance polymer as a "proof of concept." A slightly different polymer may be required to achieve optimum properties of the mixed matrix membrane. This research will focus on an established polyamide-imide, Torlon ® from Solvay Advanced Polymers © in Alpharetta, Georgia. The chemical structure is shown in Figure 3.1, as provided by Robertson et. al. [1]. Torlon® appears interesting due to

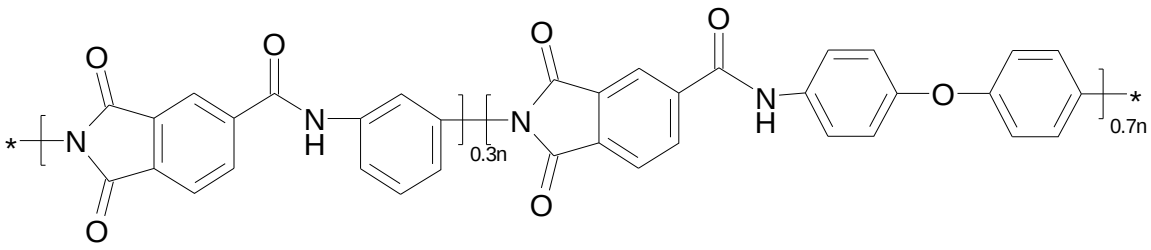

Figure 3.1: Structure of Torlon ® 4000T polyamide-imide proposed by [1].

its commercial use as a polymer coating material, in which the material was specifically designed to be chemically resistant, thermally stable, and mechanically durable. Polyamide-imides are derived from trimellitic anhydride and aromatic diamines. Polyamide-imides have not been investigated as extensively as polyimides in membrane applications, primarily because of lower permeability due to the presence of amide group. However, the amide group is also responsible for better mechanical properties and improved chemical resistance when compared to polyimides.

Given these properties, if the basic amorphous polymer could be configured into useful films for organic liquid separation, it is likely to expect that Torlon ® could be spun as a hollow fiber. Also, it is believed that a "densely packed" polymer structure (one with a lower free volume) is likely to be useful for this particular separation since the small

relative size difference among xylene isomers demand a more discriminating polymer like Torlon®. Torlon® has a rigid chemical backbone that will allow efficient packing, and is resistant to organic solvents due to the amide group that provides hydrogen bonding between neighboring segments (Figure 3). Moreover, Torlon® is an attractive candidate because Solvay© manufactures several "variants" on the original backbone. If desired, these variants (Appendix A) can be used to probe the effects of small differences in the polymer structures and how they affect transport properties. This may help in ultimate selection of a particular polyamide-imide structure that would be best suited for this particular separation. Table 3.1 shows the basic properties of Torlon 4000T® as published by Solvay Advanced Polymers © [2]. For the remainder of this thesis, all references to Torlon® refer to the 4000T variant. Internal testing determined that the Torlon 4000T® glass transition temperature is ~280°C, and has a molecular weight of ~20,000 M_w determined by inherent viscosity.

Table 3.1. Torlon ® 4000T Powder Properties [2]

Possible Solvents	NMP, DMAc, DMF, DMSO
Particle Size Range	0-150 □m
Percent Solids	99%
Solution Viscosity, 25% NMP, 40°C	7,000 cp

3.1.2 Molecular Sieves

This work focuses on zeolite molecular sieves as the dispersed phase in mixed matrix materials. MFI is the structure of choice due to its previously stated success in adsorbing xylene isomers (p-xylene permeability ~25 Barrers, p-xylene/other isomer selectivity ~400) and wealth of available literature resources. MFI is a two dimensional structure with a generalized pore structure shown in Figure 3.2. The pore structure contains

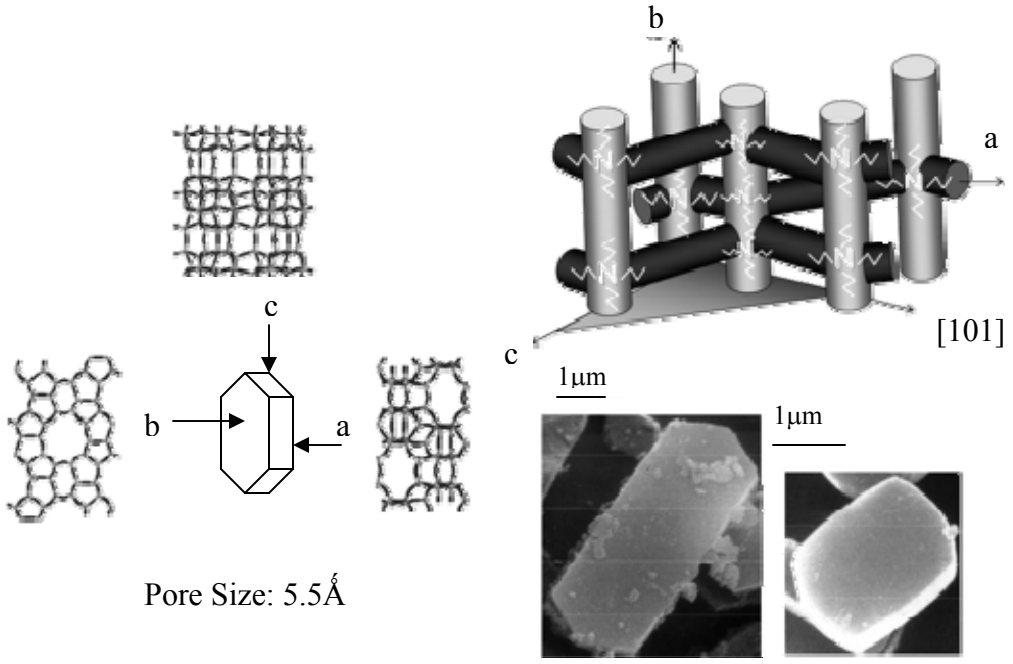

Figure 3.2: Schematic of the pore structure of TPA-MFI with the TPA located at channel intersections. Typical SEM images of coffin-shaped crystals are shown. A schematic identifying the crystal faces and directions along with the corresponding framework projections are also shown. Figure modified from [3].

straight channels in the "b" axis, and sinusoidal channels in the "a" axis, and no channels in the "c" axis. High silica containing MFI, or silicalite, that has been grown with tetrapropylammonium (TPA) cations as the structure directing agent, generally takes the shape of the "coffin" like crystals shown by SEM in Figure 3.2 These crystals generally have the "c" axis in the shortest dimension. This is convenient for mixed matrix formation, as the shearing process that accompanies all film and fiber formations will most likely align the crystal so that the "b" or "a" axis will be perpendicular to the plane of the film/fiber, and thus in the direction of transport. Smaller crystals (<500nm) may not have developed the coffin like structure, and therefore may not benefit from this phenomenon.

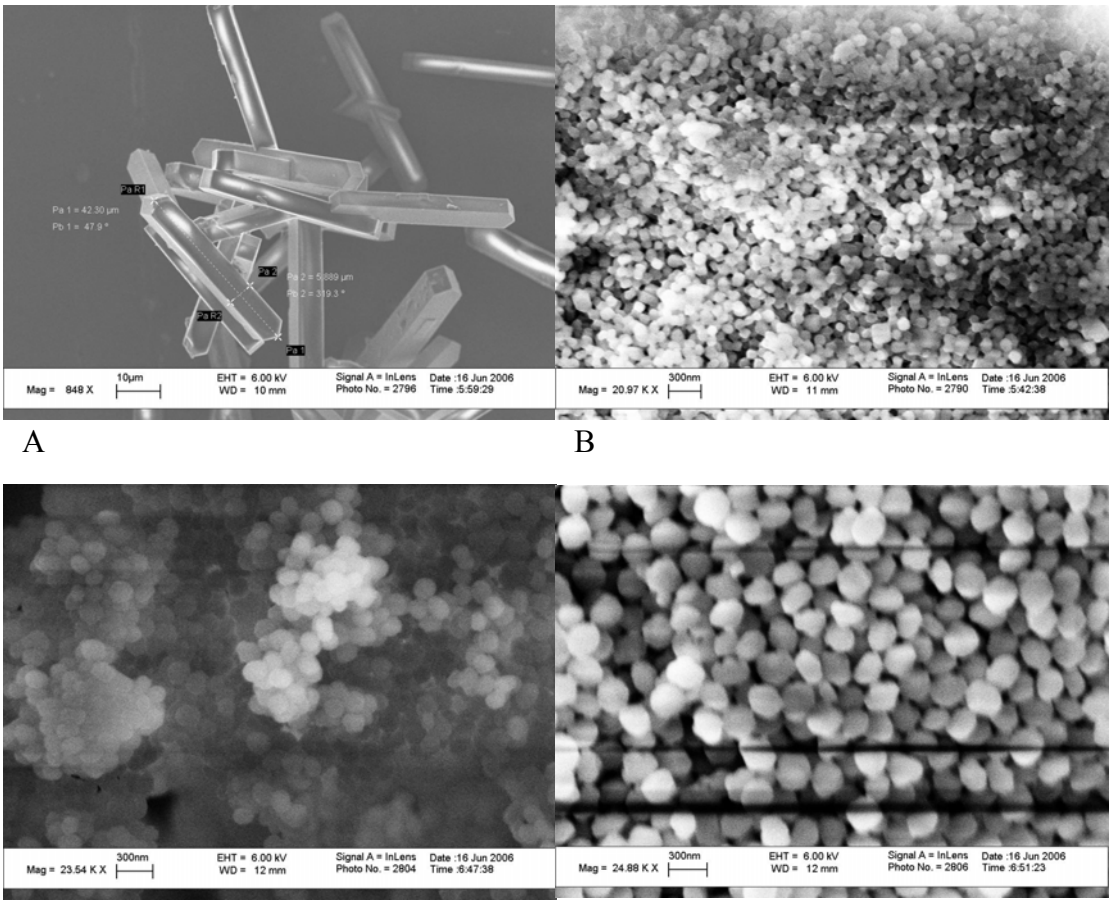

A B

C D

Figure 3.3: Silicalite samples used for p-xylene mixed matrix materials. A.) BP provided large silicalite samples (~43µm). B.) BP provided small silicalite samples (~75nm). C.) RWC003 synthesized silicalite sample (250nm). D.) RWC004 zoned silicalite sample with thin aluminum containing shell (275nm.)

For this specific work, silicalite was either provided by research collaborators (British Petroleum), or was synthesized using School of Chemical & Biomolecular Engineering facilities. All of these materials have the basic cage structure shown in Figure 3.2, with differences being in particle size, and synthesis procedures. Figure 3.3 shows SEMs of all zeolites used in this work.

3.1.2.1 Synthesis of RWC003 Silicalite Sample

A pure silicalite sample was synthesized for use in mixed matrix films and for morphology comparison. The sieves were hydrothermally synthesized in teflon lined reactor vessels with constant agitation by a teflon stirrer. The reactants used were 1M tetrapropylammonium hydroxide (TPAOH) (Aldrich), tetraethoxy silane (TEOS) 98% (Aldrich), 1N sodium hydroxide NaOH (Alrich), and de-ionized water. The total molar concentration of the reactant mixture was: 5 TPAOH : 25 SiO_2 : 480 H_2O : 100 EtOH. The mixture was hydrothermally reacted at 100°C for 24 hours. This synthesis produced crystals approximately 250 nm in diameter, as shown in Figure 3.3(C).

3.1.2.2 Synthesis of RWC004 Zoned Silicalite Sample

A second silicalite sample was synthesized with an effort to increase surface reactivity. The second sample was designed to have a core very much like the previous RWC003 sample, but also have a thin crystalline layer that contained a larger amount of aluminum tetrahedra. This sample was synthesized in two parts. First the exact same synthesis as RWC003 was carried out. Upon cooling of the reaction mixture, an amount of aluminum isopropylate (Sigma-Aldrich) and sodium hydroxide (Sigma-Aldrich 1N) was added to the vessel, and allowed to react at 100°C for 12 hours. The amount was such that the total concentration inside the vessel would be: 5 TPAOH : 0.25 Al_2O_3 : 25 SiO_2 : 480 H_2O : 100 EtOH : 0.1 Na_2O. This yielded ~275nm particles as shown in Figure 3.3(D). Development and further analysis of this zeolite sample will be discussed in Chapter 5.

3.1.3 Surface Modifying Agents

Previous work has commonly treated zeolites with silane coupling agents such as γ-aminopropyldimethylethoxysilane (Gelest; Morrisville, PA) [4,5]. This modification attempts to enhance adhesion of the zeolitic surface to the polymer matrix. The ethoxy group hydrolyzes in solution and then reacts with surface hydroxyls groups on the zeolite. Amino silanes are used to allow the free amine groups to react with the imide rings on the polymer backbone. Several different aminosilanes (Gelest) were investigated for this work, and will be discussed later in Chapter 6.

Another technique recently developed by Husain [6] was also used to enhance interfacial bonding. This procedure involves Grignard Chemistry to "roughen" the surface and increase the likelihood of surface adhesion. Thionyl Chloride (99.5% Sigma-Aldrich) was used in the first reaction step with the zeolite followed by methylmagnesium bromide (3.0M in diethyl ether, Sigma-Aldrich). This technique will be discussed in more detail in Chapter 6.

3.1.4 Chemicals

For all pervaporation experiments, the feed mixture was prepared before hand to the desired composition. All xylene pervaporation experiments were carried out with a feed composition of 30% p-xylene (99% Sigma-Aldrich), 30% m-xylene (99% Sigma-Aldrich), 30% o-xylene (97% Sigma-Aldrich), and 10% ethyl benzene (99% Sigma-Aldrich). This is an approximate composition for an actual industrial feed composition entering a p-xylene recovery unit. All compositions were made by weighing each

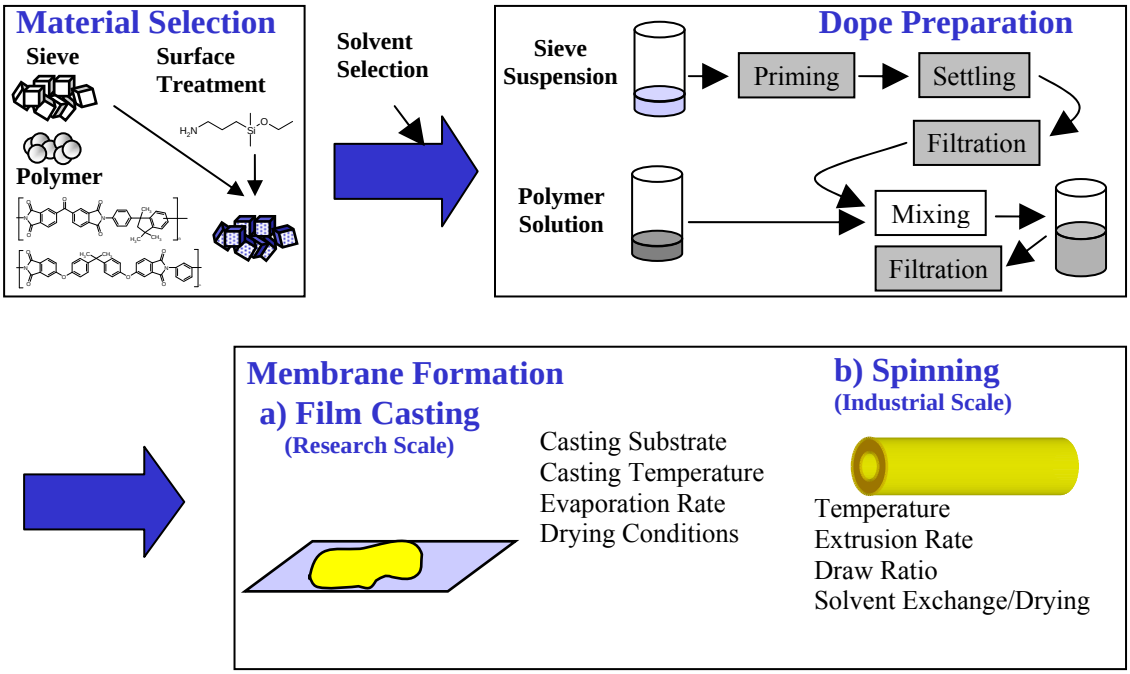

Figure 3.4: A typical preparation flow chart of mixed matrix composite membranes. Adapted from [5].

individual component to the tenth of a gram, and the total batch sizes were 400 grams of solution.

3.2 Membrane Preparation

The procedure for preparing a mixed matrix composite membrane is outlined in Figure 3.4. The first major step is material selection as discussed in section 2.3. In addition to issues outlined in previous sections, there are two additional issues that should be considered. First, the polymer-zeolite combination should form a favorable morphology that is conducive to a homogeneous material with few defects. Secondly, a solvent for the composite solution should be selected that dissolves the components and will not clog the pores of the sieving phase, or in any other way negatively affect membrane performance. Once these conditions have been addressed, dope preparation can begin by

mixing the solvent, polymer, and sieve in the correct proportions. Once the dope is formed, the membrane can be created in a variety of different geometries. In this research, thin dense films of approximately 1 mil thickness were prepared to simplify experimentation. For industrially applicable membranes, the hollow fiber morphology is preferred due to its high surface area to volume ratio. The following subsections detail this process.

3.2.1 Materials Selection

For this research Torlon ® PAI and MFI zeolite will be used to generate and test mixed matrix materials. Once this selection has been made, the materials should be examined to decide the necessity of modifying the zeolite surface to enhance the quality of the organic-inorganic interface. As mentioned in section 3.1.3, two options are available in either short silane coupling agents or Grignard reagents. After either procedure is completed on the zeolites, the resulting treated sieves and the Torlon® polymer can be used to form mixed matrix dope solutions. This procedure will remain constant regardless of the polymer or sieve used, and is independent of the particular organic liquid separation desired.

3.2.2 Dope Preparation

All films used in the research are cast via the draw casting method. It is also possible to cast via dropping a dilute solution (3-7 wt% solids) into a predefined space; however, this technique is not used in this work, and will therefore not be discussed. Draw casting requires highly viscous solutions which prevent sieve particles from settling. This method can easily form film morphologies with a draw knife. Torlon ® is dried at 110°C

under vacuum to remove any residual water remaining in the "as-received" powder. Zeolites, both treated and un-treated, are dried at 180°C for 18 hours to remove any sorbed water. Each component is prepared in two separate solutions: a sieve suspension and a polymer solution, which are subsequently mixed together. The sieve suspension is of low viscosity (~5-10 wt% solids), and the polymer solution is concentrated (~30 wt% solids). The actual amounts of each component are adjusted to yield a final solution concentration of typically 20-25 wt% total solids. This solution will yield approximately a 1 mil film with a casting knife of ~12 mil clearance. To prepare a sieve solution, dried sieves are placed in a vial with a predetermined amount of the casting solvent (typically 0.3g sieve in 3ml solvent). The amount of sieves is determined by the final sieve loading in the membrane, which is 10-15 wt% for this work. This mixture is sonicated in 30 second bursts to break agglomerates and create a well-dispersed suspension. At this time, the suspension is "primed" (as developed by Moore [5]) with a small amount of the viscous polymer. If the zeolites have been surface modified with silane coupling agents, the solution is heated in an oil bath for ~4 hours at 150°C to allow tethering to the surface. Lastly, the remaining viscous polymer solution and the sieve suspension are mixed, in a vial by hand, and then placed on a roller overnight. A homogenous mixed matrix dope is then formed, and can be used for film formation.

3.2.3 Film Preparation

Once the dope has been prepared and is free of agglomeration and vapor bubbles, composite films can be prepared. Casting is performed inside a fume hood due to the hazards created by the evaporation of solvents. A tempered glass substrate is thoroughly cleaned with soap and water, rinsed with de-ionized water, and finnaly rinsed with

acetone. Once dry, the plate is heated on a hotplate to ~140°C inside the fume hood. The casting knife is placed at the far end of the glass plate, to enable the drawing motion toward the person. The dope is poured slowly into an oblong "puddle" directly in front of the casting knife. The knife is then drawn in a smooth, even motion across the length of the plate and removed without hesitation. The remaining film is immediately covered with an inverted square glass "baking" dish that allows visual inspection of the film, and keeps the atmosphere above the film saturated with solvent, thus reducing the rate of evaporation. A vitrified film is formed in ~1 hour using a 20 wt% viscous solution in NMP. The casting knife is manufactured by Paul N. Gardner & Co., Pampano Beach, Fl.

Once the film is formed, it must be completely free of solvent to provide reliable experimental results (See Chapter 4.) The film is easily removed from the glass substrate using a sharp razor blade and peeling up a corner. The film will "release" from the surface with little effort. The film is then suspended on a wire hanger, attached at top and bottom to maintain the film geometry as a flat plane. The suspended film is placed in a special vacuum oven capable of ramping to the glass transition temperature of the polymer (~280°C), and holding overnight, before cooling back to room temperature over 25 hours. This process was developed to remove essentially all the solvent, and is discussed in Chapter 4. The resulting film is flat in geometry, contains less than 0.5% solvent, and is ready for characterization.

3.3 Membrane Testing Methods

All membranes for this work are tested for performance by pervaporation experiments. The permeability and selectivity are obtained from this measurement. Due to the

flammable nature of the xylene feed mixture, a special apparatus was designed to safely and efficiently perform the desired experiments. The apparatus and procedure are described in the following sections.

3.3.1 Pervaporation Measurements

The permeability and selectivity of gas pairs were determined using the standard isochoric (constant-volume, variable pressure) technique [7-9]. In this technique, the steady state pressure increase in the permeate pressure, [dp/dt (torr/s)], is directly proportional to the permeability by the following equation:

$$Permeability\left(Barrer\right)_i = \left[X_i\right]\times\left[\frac{dp}{dt}\left(\frac{Torr}{s}\right)\right]\times\frac{\left(\frac{101325Pa}{760Torr}\right)\left[V_D(m^3)\right]}{\left(8.314\frac{Pa\cdot m^3}{mol\cdot K}\right)\left[T(K)\right]}\times$$
$$\left\{\frac{\left(8.314\times10^6\,\frac{Pa\cdot cm^3 STP}{mol\cdot K}\right)(273.15K)}{(1atm)\left(\frac{101325Pa}{atm}\right)}\right\}\times \qquad (3.1)$$
$$\frac{\left[\ell(cm)\right]\left(\frac{14.696\,psia}{76cmHg}\right)}{\left[A(cm^2)\right]\left[p_F(psia)\right]}\times\frac{1\times10^{10}\,Barrer}{\frac{cm^3 STP\cdot cm}{cm^2\cdot s\cdot cmHg}}$$

The terms in brackets are known, with the respective units given in parentheses: permeate reservoir volume, V_D *(m^3)*; temperature, *T (K)*; membrane thickness, *l (cm)*; membrane area, *A (cm^2)*; and feed pressure, p_F *(psia).* To determine the permeability of component *i*, the mol fraction of the downstream permeate as determined by gas chromatography, is multiplied by the steady state pressure increase. The feed pressure for component *i* is

determined by the vapor pressure of the feed solution at the feed temperature. These values are determined via Antoine's Equation [10].

3.3.2 Experimental Apparatus

A process flow diagram (PFD) of the experimental apparatus is shown in Figure 3.5. The system is contained within a large micro-processor controlled vacuum oven (VWR model number 1430M), and can be heated from room temperature to over 210°C. The atmosphere surrounding the apparatus can be evacuated to ensure the removal of a flammable atmosphere, thus greatly reducing any chance of ignition in the case of a xylene leak at elevated temperatures. All fittings for the apparatus are stainless steel Swagelok® (Solon, OH) welds, tube fittings, or Swagelok® VCR® fittings.

The temperature of the system is measured via a thermocouple, and an internal mercury thermometer to ensure accuracy. The temperature is maintained within 0.5°C of the set-point, thus adequately maintaining the upstream vapor pressure or membrane feed pressure. The downstream transducer is a 10 torr Baratron® 615A bake-able pressure transducer supplied by MKS instruments (Andover, MA). The transducer signal is passed through a Baratron® (MKS) 270D signal conditioner before being recorded with a Keithly KCPI-3107 data acquisition board installed on a computer running Labview® software (National Instruments, Austin , TX) for data acquisition.

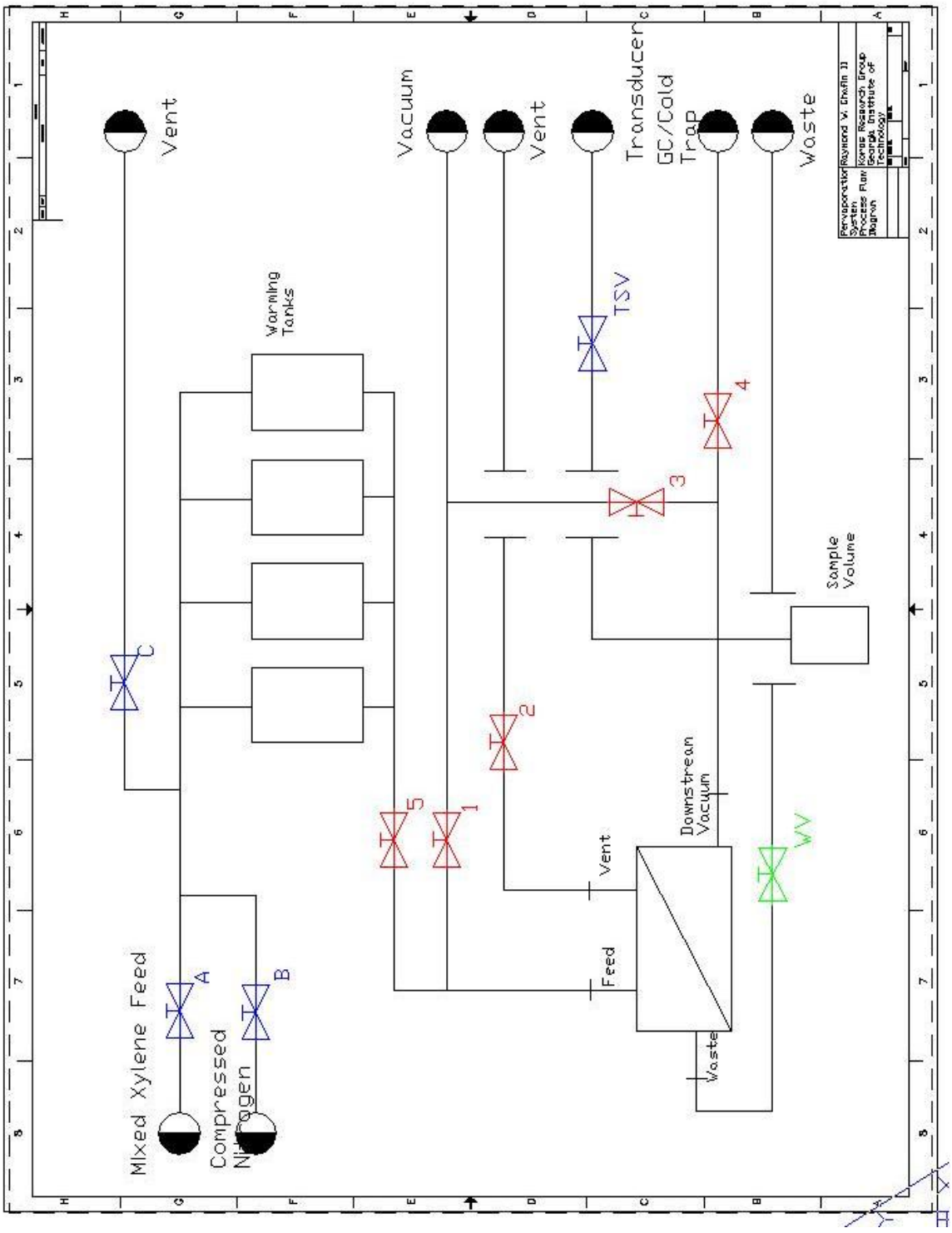

Figure 3.5: Process Flow Diagram of Pervaporation System. Valves A, B, and C are used to load and transfer feed mixture to pervaporation cell. Valves 1-5 are used to control pervaporation experiments for permeation and selectivity. The waste valve (WV) is used to remove the feed mixture from the apparatus via an external cold trap.

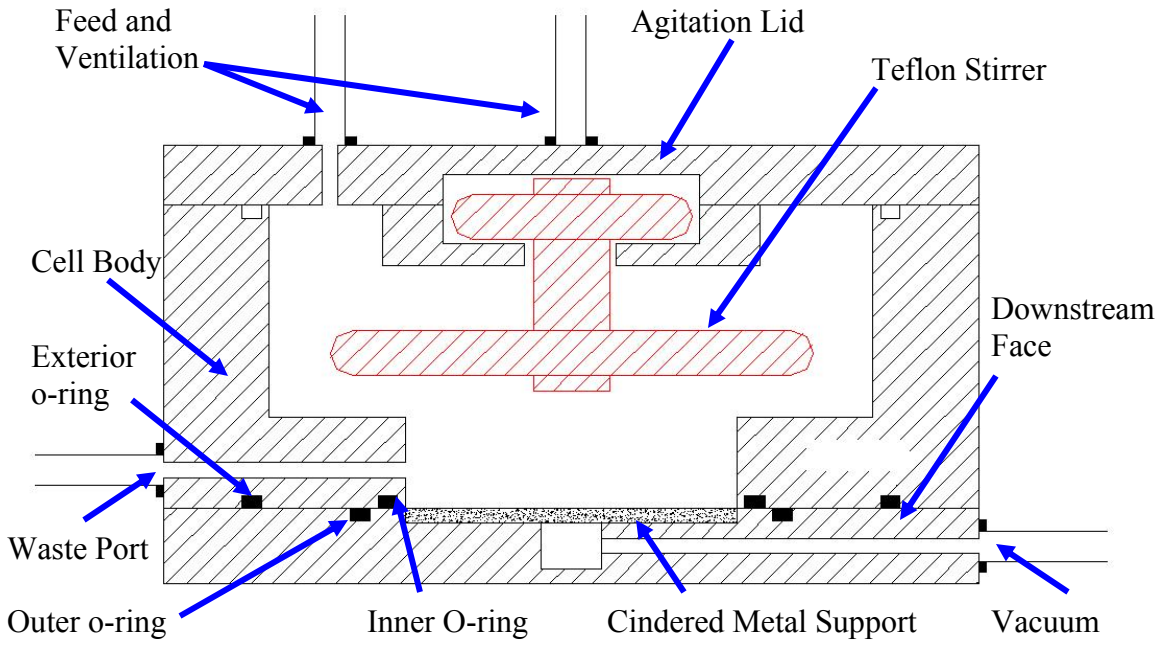

Figure 3.6: A cross-section of the stainless steel pervaporation cell. The agitation lid holds a teflon stir bar controlled by a magnet spinning on top of the cell. The lid also contains a feed inlet, and ventilation opening. The cell body can contain ~450ml of solution, and includes a waste port for draining of the feed mixture at experimental completion. The downstream face seals the membranes on the imbedded o-rings, and supports the membrane with cindered metal. Vacuum is established on the downstream face to maintain the chemical potential difference which is the driving force for separation.

The pervaporation cell was designed to be contained inside the vacuum oven, and to operate consistently at high temperatures. The cell is constructed of stainless steel components with the exception of a stir-bar. The cell consists of three components: the downstream face, the body, and the agitation lid. The downstream is flat with the exception of o-ring grooves for Viton® o-rings (supplied by McMaster Carr) for sealing. A piece of porous grade D sintered metal (Metron Technology; Austin, TX) is inserted in the downstream face, which is connected to the permeate reservoir. The body of the pervaporation cell provides a space where approximately 450 ml of feed solution can be

agitated while in direct contact with the membrane. The agitation lid covers the body, and contains a magnetic stirring apparatus that is controlled by a magnet spinning above the cell. This keeps the solution well mixed, and prevents concentration polarization close to the membrane surface. The cell contains inlets to allow the feed to be added, and contains outlets for venting, liquid removal, and permeate removal. A general drawing is shown in Figure 3.6, while more detailed AutoCAD® representations can be found in Appendix B.

The entire apparatus is designed for safe operation while at temperatures in excess of 200°C. This is accomplished by the removal of all valve control to the exterior of the oven. All valve handles are on top of the oven, while the valve stems extend within to control the process in the high temperature environment. Agitation also passes through the oven wall, with a large powerful stirring magnet residing approximately 0.25" above the cell, and is controlled via a variable speed motor mounted on top the oven. The feed solution is weighed and measured in a graduated 1000 ml addition funnel, and is connected to the system on top of the oven. The liquid is then fed to four 150 ml holding tanks inside the oven via gravity. Once inside, the liquid can be moved to the body of the pervaporation cell with 20psi nitrogen head. At the conclusion of the experiment, the liquid can be removed via a "waste" vent connected to a 1000ml vacuum dewar that leaves the pervaporation body essential empty. This entire process can be completed without exposing the operator to excessive temperatures.

3.3.3 Membrane Sealing Procedures

Due to the low membrane fluxes experienced with many PAI type materials, it is desirable to test the largest membrane areas possible. Given the mechanical durability of Torlon® at high temperatures, membranes are sealed directly on the pervaporation cell o-rings, thus maximizing the area for testing. Figure 3.6 depicts the cell cross-section at the membrane seal. The seal is in three parts: an upstream o-ring, a down stream o-ring, and an exterior o-ring. The upstream o-ring is slightly larger than the sintered metal opening in the downstream face, and defines the area for permeation. The downstream o-ring is slightly larger than the upstream o-ring, and ensures proper sealing at low pressure. The exterior o-ring is outside the upstream o-ring, downstream o-ring, and the enclosed film to ensure no external atmosphere leaks into the cell, and is the last measure to prevent internal liquids from diffusion into the pervaporation system. Blank aluminum disks of varying thickness (0.7-3 mils) were sealed in this manner as a surrogate for films to verify seal, and all exhibited essentially no permeability overnight. All membranes for this thesis are sealed in this manner.

3.3.4 Pervaporation Procedure

This section outlines the basic procedure for testing membranes via pervaporation, and generally refers to Figure 3.5. After the cell is inserted into the system, the main vacuum valve is opened to expose the downstream of the membrane to vacuum. The downstream pressure is monitored, and the rate of evacuation is indicative of seal quality, and judged by previous experience. Once the downstream is evacuated, the feed solution is gravity fed from a graduated addition funnel into four 150 ml holding tanks by opening the feed valve (A) and opening the holding tank ventilation valves (C) to relieve any pressure.

Upon completion, the feed valve (A) and ventilation valve (C) are closed, and the compressed nitrogen valve is opened along with pervaporation cell valves (5) and (2) to allow the compressed nitrogen to move the liquid from the holding tanks to the pervaporation cell. This step can either be completed before or after the temperature set-point has been reached. Once the liquid is in contact with the membrane, the system is allowed to maintain temperature overnight, while the downstream is under active vacuum, to ensure steady state transport is achieved. To measure permeability, the vacuum valve (3) and the GC/cold trap valve (4) are closed, to isolate the downstream. The pressure rise data are collected as discussed above, and then the vacuum valves (3 or 4) are re-opened. For selectivity measurements, the permeate is allowed to collect in a cold trap via valve (4). In this case the vacuum valve (3) is closed, and the vacuum is maintained through the cold trap, and condenses permeate in the liquid nitrogen trap. After collection, valve (4) is closed, the permeate is analyzed with an Agilent 6890 Gas Chromatograph for composition ratio. Upon completion of the experiment, the liquid is removed from the cell via a 1000 ml liquid nitrogen trap through the "waste valve" (WV). The feed solution is collected and analyzed via GC to ensure stable composition. The system is allowed to cool to room temperature before removal of the pervaporation cell and film.

3.4 Complimentary Characterization Methods

Several complementary techniques were used to examine materials for this thesis. Frequently used complementary techniques are discussed here in no particular order. Other techniques that were used infrequently are discussed at the appropriate place in the

text. More detailed discussion of each of these techniques can be found in open literature.

3.4.1 Scanning Electron Microscopy (SEM)

For many films and zeolites, SEM is a useful tool to directly observe material morphology. Although the SEM cannot resolve Ångstrom sized entities, larger entities can be clearly discerned with this technique. Film cross-sections are prepared by fracturing film samples in liquid nitrogen after submersion for 1 minute. The samples are sputter coated with gold in argon plasma, and observed using a high resolution Field Emission Scanning Electron Microscope, Leo 1530 (Leo Electron Microscopy, Cambridge, UK). Zeolite samples are prepared by evaporating a very dilute dispersion of particles in water on a flat sample stage. The samples are then viewed with the instrument.

3.4.2 Thermogravimetric Analysis (TGA)

Thermogravimetric analysis can be used to determine solvent content, degradation temperatures of membranes, and zeolite loadings. TGA was performed in a Netzch STA 409 PC TGA (Burlington, MA). Samples can be heated to a maximum of 1600°C in nitrogen or 1500°C in air at rates of 1°C to 20°C per minute. Infrared analysis can also be performed on the evolved gas, however this option was not used in this work.

3.4.3 Nitrogen Adsorption

Nitrogen adsorption was used in this work to monitor porosity of zeolite samples after a particular modification or a new synthesis. The data was collected using a Micromeritics ASAP 2020 surface area analyzer (Micromeritics, Norcross, GA). The samples were

degassed for 18 hours at 180°C under vacuum prior to being analyzed. The samples were probed for micro-pore and mesopore volumes, surface area reports, and pore size distributions.

The pore volume and distributions were determined using the Horvath-Kawazoe (H-K) method for cylindrical pores of aluminosilicates [11]. All pores less than approximately 60 Å were included. Comparisons with Density Function Theory (DFT) [12] using models for oxide surfaces were also made for similar pore sizes. Above this range, standard Langmuir sorption methods were used to characterize the porosity.

3.5 References

1. Robertson, G.P., Guiver, M.D., Yoshikaws, M., Brownstein, S. Polymer, 2004. 45: p 1111-1117.

2. Torlon® Polyamide-imide. Solvay Advance Polymers. August, 01, 2006. http://www.solvayadvancedpolymers.com/products/bybrand/torlon/0,6647,329-2-0,00.htm

3. Bonilla, G.; Diaz, I.; Tsapatsis, M; Jeong, H.; Lee, Y; Vlachos, D. Chem. Mater. 2004, 16, 5697-5705.

4. Plueddemann, E.P., Silane coupling agents. 1982, New York: Plenum Press

5. Moore, T. Effects of Materials, Processing Conditions, and Usage Conditions on the Morphology and Gas Transport Properties of Mixed Matrix Membranes. PhD dissertation, The University of Texas at Austin, 2004. Austin, Texas.

6. Hussain, S. Mixed Matrix Dual Layer Hollow Fiber Membranes for Natural Gas Separation. PhD dissertation, Georgia Institute of Technology, 2006. Atlanta, Georgia.

7. O'Brien, K.C.; W.J. Koros; T.A. Barbari; and E.S. Sanders. J. Membr. Sci. 1986, 29, 229-38.

8. Pye, D.G.; H.H. Hoehn; and M. Panar. J. Appl. Polym. Sci. 1976, 20, 1921-31.

9. Moore, T.T.; S. Damle; J. Williams; and W.J. Koros. J. Membr. Sci. 2004, 245, pp227-231.

10. Felder, R.; Rousseau, R. Elementary Processes of Chemical Processes, 2005 Wiley.

11. Horvath, G. and Kawazoe, K., J. Chem. Eng. Japan *16(6)*, 470 (1983).

12. Ross, J. and Olivier, J.P., "On Physical Adsorption," J. Wiley and Sons, New York (1964).

CHAPTER 4

CHARACTERIZATION OF TORLON® POLYAMIDE-IMIDE

This chapter discusses the characterization of Torlon® polyamide-imide for utilization as the bulk polymer phase in mixed matrix membranes for xylene isomer separation. Solvay Advanced Polymers© in Alpharetta, Georgia markets Torlon® as a high performance thermo-resin for use in the space shuttle, automotive transmissions, and also as a barrier coating with excellent heat and chemical resistivity. Since it is marketed as a barrier coating, little work has been done to characterize Torlon® as a commercial membrane candidate. This chapter will introduce Torlon® for xylene isomer separation, develop optimum film processing parameters, and establish a transport property basis for utilization of Torlon® in mixed matrix materials.

4.1 Torlon® Polyamide-imide for Xylene Purification

4.1.1 Previous Polymer Based Xylene Separations

Before exploring Torlon® as a candidate for xylene separations, it is useful to understand previous attempts to purify p-xylene via membranes. Table 4.1 shows a list of common commercial membranes for xylene isomer separation as compiled by BP [1]. All of these polymer structures (See Appendix C) have selectivities that are very close to evaporative values (Chapter 2), and none of the testing exceeds 150°C. Thus none of these cases approach the realistic industrial feed condition of ~200°C, where diffusion selectivity would tend to be further reduced. Kapton, Matrimid, and 6FDA based polymer structures represent "advanced" materials available for commercial applications, so it is clear that

achieving desirable xylene properties with a polymer membrane is difficult; requiring an unique polymer.

Table 4.1. Common Polymers Tested for Xylene Separation

Membrane	Temp, °C	Flux (μmol/m^2-sec)	Selectivity
Kapton	100-150	10^{-5}	(PX/MX) 1.2-1.3
Unannealed Matrimid	50-75	10^{-1}	(PX/MX) 1.3
Polyethylene	100	10^{-3}	(PX/MX) 1.3
6FDA-DAM	100	10^{-1}	(PX/MX) 1.0 (PX/OX) 1.3
Silicone Rubber	75-100	10^{-1}	(PX/MX) 1.0 (PX/OX) 1.5

4.1.2 *Torlon® Polyamide-imide Structures*

The structure of Torlon® polyamide-imide was previously introduced in Chapter 3. In addition to the Torlon® 4000T structure used for this work, several backbone variants are available from Solvay®, which can be tailored for a particular organic separation. These structures are shown in Figure 4.1. As previously discussed, the material used for this work is the 99% imidized Torlon® 4000T, supplied in powder form. It may be desirable to consider other Torlon® family backbones to allow different chain mobility or possible functionalization through the open imide groups in the partially imidized samples. These "tuning" options can be explored to improve polymer transport performance, but will not

be considered in this work. Transport property testing will focus on Torlon® 4000T as a proof of concept.

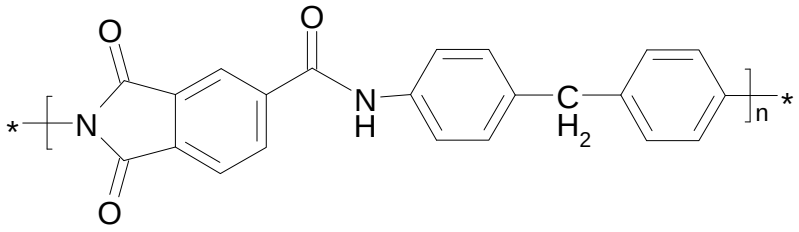

Torlon ® AI-10
Distributed as 95% (AI-10) imidized and 50% imidized (AI-30)

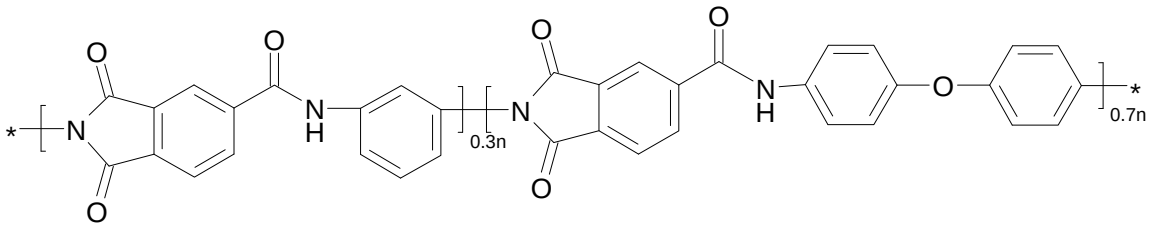

Torlon ® 4000T
Distributed as 99% imidized (4000T) and ~50% imidized in NMP (AI-50)
and 50% Dry (PXM 03028)

Figure 4.1. Various structures of Tolron® polyamide-imide from Solvay Advanced Polymers. This list is not meant to be exhaustive, and Solvay has experimented with and could possibly provide many different backbone variations. AI-10 and 4000T are the two most popular variants, both sold in imidized and partially imidized form, as well as in varying amounts of solvent.

4.1.2 Initial Results

As discussed in Chapter 3, several authors have described methods to form solution processable films for gas separation [2]. Torlon® 4000T was processed in a similar manner to these conventional approaches. It was draw-cast into dense film membrane form, and vacuum dried at 200°C over approximately 18hrs. The results shown in Table 4.2, indicate a significant variance in transport properties, but suggest Torlon® is a more

attractive candidate than commonly available industrial polymers in Table 4.1. Resolving the film property variance and developing procedures for reliable, repeatable membrane formation was, therefore, identified as a high priority.

Table 4.2. Initial Torlon® results indicating poor transport property repeatability.

Film ID ▼	Flux normalized by thickness	Selectivity	Selectivity	Para-Xylene Permeability
Units ►	(cc(STP)*cm)/(cm^2*sec)	Para/Unwanted	Para/Ortho	Barrer
TOR-ANL-007	1.57E-07	2.80	2.45	0.68
TOR-ANL-008	1.31E-07	3.96	7.44	0.73
TOR-ANL-010	1.42E-07	1.81	2.23	0.54

All samples pervaporation tested at 200°C

4.1.3 Methods for Torlon® Membrane Optimization

Solvay Advanced Polymers® published a "Powder Bulletin" [3], for each Torlon® variant that describes a series of processes that take place during proper formation of Torlon® polymer coatings. Solvay® publications recommend a high temperature cure of 250°-300°C for polymer coatings. Solvay® claims that three processes occur during this curing stage. *First*, final imidization should occur from 40°-140°C. *Second*, the majority of the casting solvent is removed from 140°-232°C. *Finally*, removal of the last traces of solvent and the molecular weight increase are suggested to occur from 232°C and up. This thesis will seek to explain each of these three processes in the next section, and use this information to form repeatable Torlon® membranes for xylene separation.

4.2 Optimization of Torlon® 4000T Polyamide-imide

This section discusses causes of poor transport property repeatability by investigating the three different processes suggested in section 4.1.4 to occur during temperature curing of Torlon® membranes. This section will consider imidization, molecular weight enhancement and solvent removal during the temperature curing steps.

4.2.1 Thermally Induced Imidization

A Bruker Tensor 27 FTIR spectrometer outfitted with a Harrick MVP2 ATR minis-sampler was used to obtain infrared spectra (IR) of film and powder samples in order to compare levels of imidization. As-received powder samples were scanned by IR, while films were prepared in similar methods as described in Section 4.1.3. The resulting powder spectrum is shown in Figure 4.2, along with identification of all the major peaks associated with the polyamide-imide backbone structure. In addition, Figure 4.2 also shows a spectrum of a 200°C temperature treated Torlon® membrane film (red line). Clearly, there is very little change in the overall IR spectra, with negligible change in the imide peaks associated with further imidization. As a result, it is fair to conclude that imidization is unlikely to have caused the poor repeatability in Torlon® membrane samples, and the polymer is essentially completely imidized upon receipt from Solvay®.

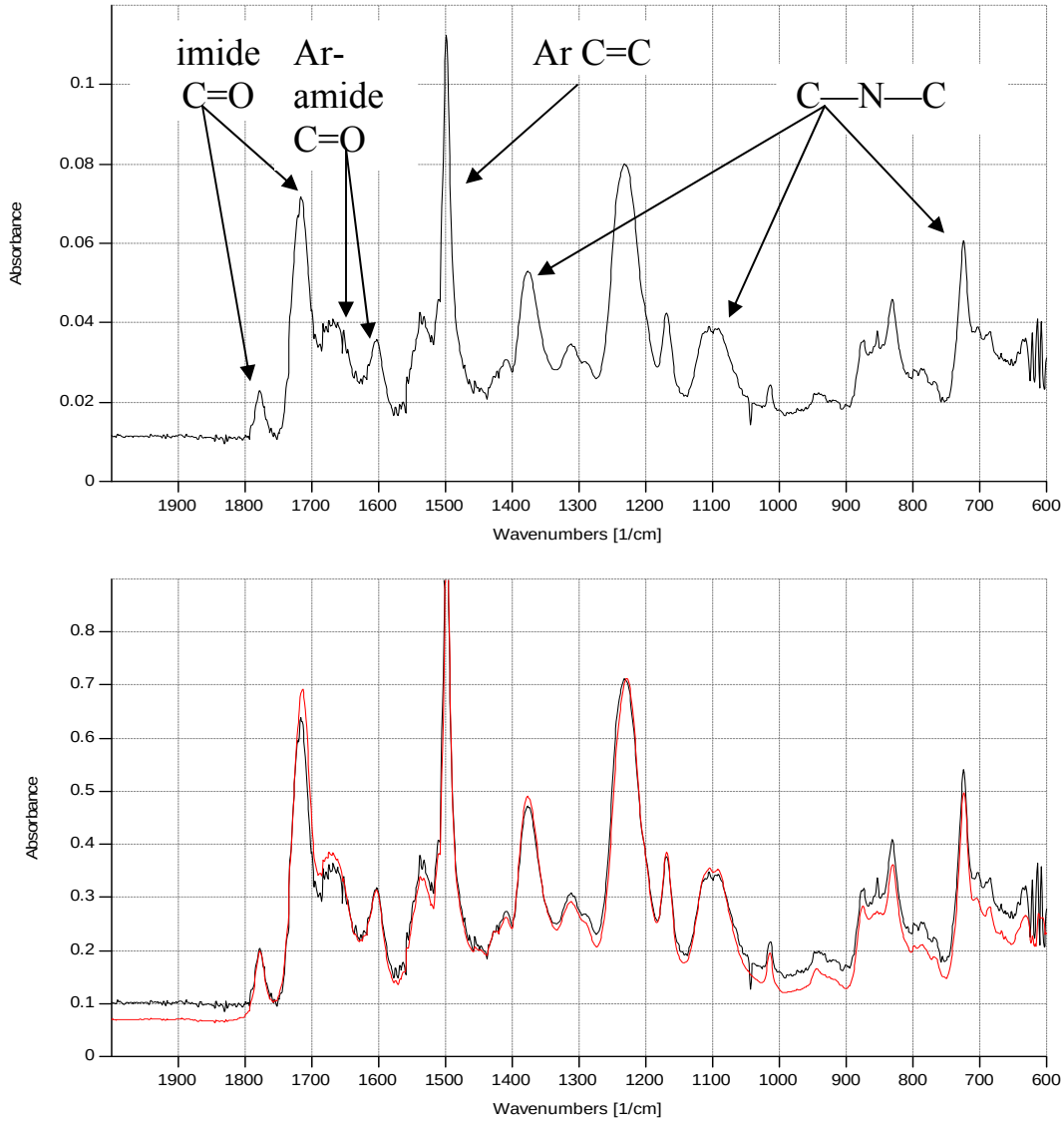

Figure 4.2. Infrared Spectra of Torlon® 4000T powder as received from Solvay Advanced Polymers® (Top) and identification of all major peaks associated with chemical groups in the Torlon® chemical structure. Also shown is a comparison (bottom) of a 200°C temperature treated Torlon® film with the as received powder, showing essentially no change in imidization peaks.

4.2.2 Molecular Weight Enhancement

Polyamide-imide average molecular weights can be estimated by inherent viscosity (η_{inh}) correlations using an Ubbelohde viscometer. Dilute polymer solutions are prepared in NMP and tested at 25°C to determine if there is any change in molecular weight during

high temperature treatments. Actual experimental procedures are described elsewhere [4]. Table 4.3 shows the results of comparing an "as-received" Torlon® powder with films treated at different temperatures. The data in Table 4.3 suggests no significant trends in molecular weight for samples treated at or above 150°C. There may be slight increases, but this increase is most likely not the cause for poor repeatability in transport properties.

Table 4.3. Comparison of inherent viscosities of several Torlon® samples. Molecular weight data take from published literature correlations [5].

Torlon® 4000T Samples	**η_{inv} (dl/g)**	**~ Mw (kg/mol) Amoco/Va Tech**	
"As received" powder	0.53	20.1	23.6
Film cast from NMP, air dried overnight	0.44	17.6	19.9
Film with 8% xylene	0.50	19.3	22.4
Film, dried at 150° C	0.52	19.8	23.2
Film, dried at 260° C / 24 hrs /vac oven)	0.59	21.8	26.1

4.2.3 Solvent Removal

The last process investigated was solvent removal, which occurs at the higher temperature range of 232°C to over 300°C. Initial film preparation procedures require vacuum drying of polymer samples at 200°C, without annealing the film above the glass transition temperature (T_g=280°C). In order to investigate the amount of solvent remaining in the films after membrane formation, thermogravimetric analysis (TGA) was completed on a series of film samples to determine residual solvent content. Figure

4.3(a) shows the results of TGA on three separate polymer samples: Torlon® Powder, an NMP cast film, and a DMAC cast film. In these examples it can be seen that solvent desorbs from the sample over the temperature range of 100°C to approximately 300°C. First, it should be noted that the Torlon® powder contains a residual amount of NMP in the "as-received" form, as evidenced by the mass loss around 270°C. This residual amount of NMP in the powder is reduced with temperature treating to 250°C, although it remains slightly apparent in the analysis. The NMP cast film contains a very high amount (nearly 20 wt%) of residual solvent before temperature treatment overnight at 200°C, after which nearly 6 wt% of NMP still remains. This amount of solvent remaining in films to be used for membrane testing is unacceptable as it may induce an un-expected non-ideal effect. Another film using DMAC as the casting solvent was also tested, and was found to be an improvement over the NMP case, however most commercial fiber spinning operations would prefer to operate with NMP as the casting solvent, and therefore a method to prepare essentially solvent free membranes is needed. Figure 4.3(b) shows the effect of different temperature treatment options as a method to reduce the overall remaining solvent content. It can be seen that once the polymer has been taken above the glass transition temperature of the structure, the polymer appears to more readily de-sorb the solvent molecules. By exposing dense films to 315°C and vacuum overnight, essentially all of the residual NMP can be removed from the system. This should allow testing of the neat polymer's properties for organic liquid separation without interference from the residual solvent.

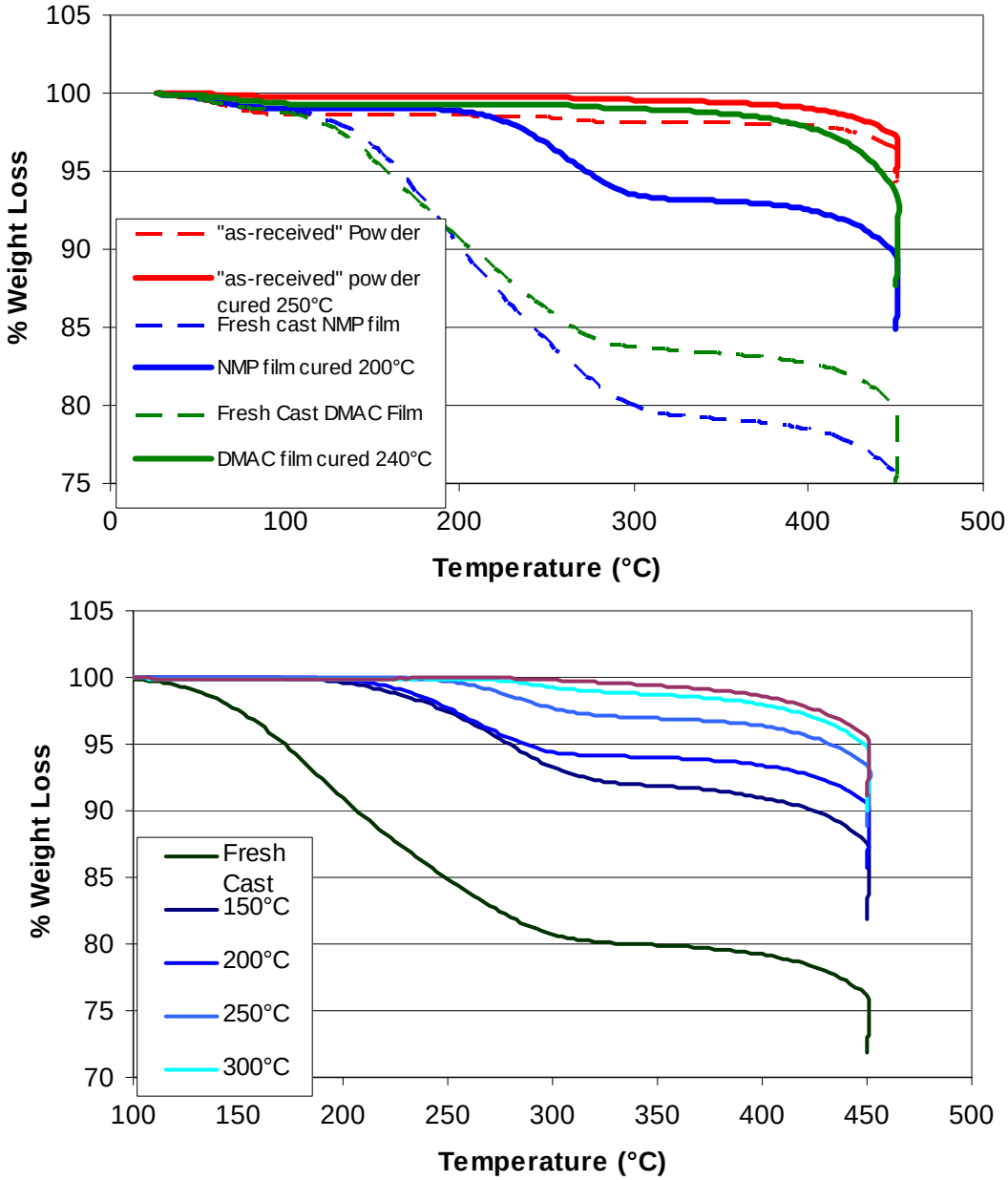

Figure 4.3. (a) (top) TGA of three polymer samples: Torlon® powder, NMP cast film, DMAC cast film. Dashed lines show sample before temperature treatment, solid lines show samples after treatment. (b) (bottom) NMP cast films temperature treated up to 315°C. The high temperature essentially removes all residual solvent.

4.2.4 Final Film Methodology

Based on the previous characterization, a new method was developed in order to provide solvent free, temperature treated films that provide repeatable transport properties. The procedure is as follows:

1. Torlon® powder is dried at 110°C overnight, under vacuum to remove water.
2. Dehydrated Torlon® is mixed with dry NMP solvent, to yield an approximately 23% solution in 20ml vials.
3. Solutions are rolled overnight to allow adequate mixing and dissolution of all polymer powder.
4. Polymer solutions are draw-cast on a heated tempered glass plate at ~115°C, covered with an inverted baking dish, and allowed to vitrify for one hour and twenty minutes.
5. Vitrified films are removed from the casting plate, and placed in a spring holder to maintain thin dense film shape.
6. Film and holder are treated in a vacuum oven at 315°C for 24 hours, and allowed to cool to room temperature over the following 25 hours.
7. Cooled films are immediately tested for transport properties.

This procedure has yielded excellent results and films utilizing this procedure will be characterized in the next section.

4.3 Characterization of Torlon® 4000T PAI for Xylene Purification

4.3.1 Pervaporation of Torlon® 4000T Thermally Treated Films

The film methodology developed in previous sections was used to generate films for xylene purification testing via pervaporation experiments. These films were tested under

a xylene mixture comprised of 30% *para*-xylene, 30% *meta*-xylene, 30% *ortho*-xylene, and 10% ethylbenzene, thus mimicking a possible industrial feed entering a *para*-xylene recovery unit. Membrane flux measurements were taken daily, while permeate was collected over different intervals, depending on the flux, and the collected liquid was analyzed by gas chromatograph for composition and selectivity. Due to the inability to collect permeate composition and flux data simultaneously, exact permeability data are not plotted. Instead, length normalized flux and selectivity in their actual intervals are reported. The author feels this is a more accurate representation of the dynamics of the system, and will provide a more useful basis for comparison later in subsequent chapters. Since the final permeability and selectivity are essentially stable during periods of membrane performance, final membrane permeability will be reported.

The results of three films are shown in Figure 4.4. The first thing that is readily apparent from the data is the obvious decrease in membrane flux over time. This decrease appears to be an intrinsic property of the polymer under these testing conditions, and corresponds to an appropriate increase in the selectivity for the *para* isomer. It should be noted that this selectivity (3.1 p/o, and 2.1 p/m) is the highest reported value to date at 200°C for a polymeric material separating xylene isomers. The permeability appears to reach equilibrium at about 0.25 Barrer, which is questionably low for a commercially feasible membrane. For a para-xylene recovery unit operating at 500 KMTA, and a membrane unit enriching 25% of the feed stream, a hollow fiber unit with approximately 400,000 m^2 of membrane area would be required (See Appendix D).

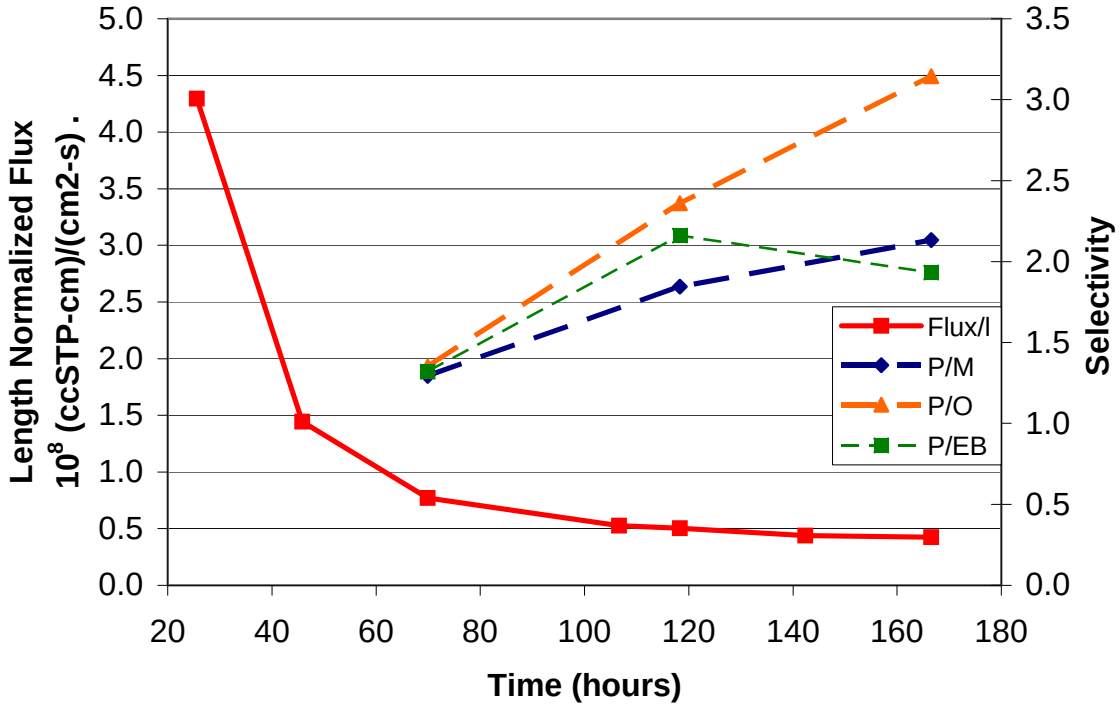

Figure 4.4. Normalized flux and selectivity of thermally treated Torlon 4000T films. Normalized flux is represented by a solid red line, while selectivities for different components are represented by dashed lines.

The "permeability crash" apparent in Figure 4.4 is an unusual phenomenon, not usually seen in typical gas separation applications. There is a large difference between gas applications versus pervaporation operating conditions in which an elevated feed activity and high operating temperature apply. It is possible that during the annealing step, NMP is removed from the system and leaves some free volume remaining in the material; i.e. a sorption site previously occupied by NMP is now presumably empty. It is also believed that the presence of the xylene isomers allows the polymer a certain amount of mobility, not possible without the isomer, which eventually allows this excess free volume to relax and reach a more equilibrium state. The nature of the conditioning effect of the xylene isomers will be discussed over the next two sections.

4.3.2 Thermal Post-treatment of Torlon® 4000T

The decrease in permeability could be due to either testing at elevated temperatures, exposure to high activity xylene, or a combination of both components. In order to decouple the effects of the high temperature atmosphere, a film was prepared in an identical manner as in section 4.3.1. This film was then reheated in a vacuum oven to 200°C and allowed to remain heated for 120hrs, (the length of time needed for a "permeability crash" to occur in section 4.3.1). The film was subsequently cooled slowly, and then tested by pervaporation for xylene isomer permeation. Figure 4.5 compares this film to the average film in section 4.3.1, and an overall decrease in the location of the crash, shifting the entire curve down, and ultimately causing a 40% change in the final membrane flux. The shape of the permeability decline is maintained, along with the overall difference. It appears the long term temperature heating of the sample did slightly reduce the amount of available free volume in the polymer, and hence reduced the permeability. Although there appears to be an effect of the long term thermal treatment, it is obvious that there is some additional effect that occurs due to the presence of xylene at high temperature.

4.3.3 Relaxation Theories

The permeability decline phenomena observed in Figures 4.4 and 4.5 are presumably related to aging phenomena reported in gas permeation literature [6,7,8]. The shorter time scale associated with the higher temperature conditioning study here may be a differentiating factor as compared to previous literature. Another differentiating factor may be the use of a more interacting penetrant vs. the simple penetrant gases. In any case, it is reasonable to presume that the permeability decrease may be caused by aging

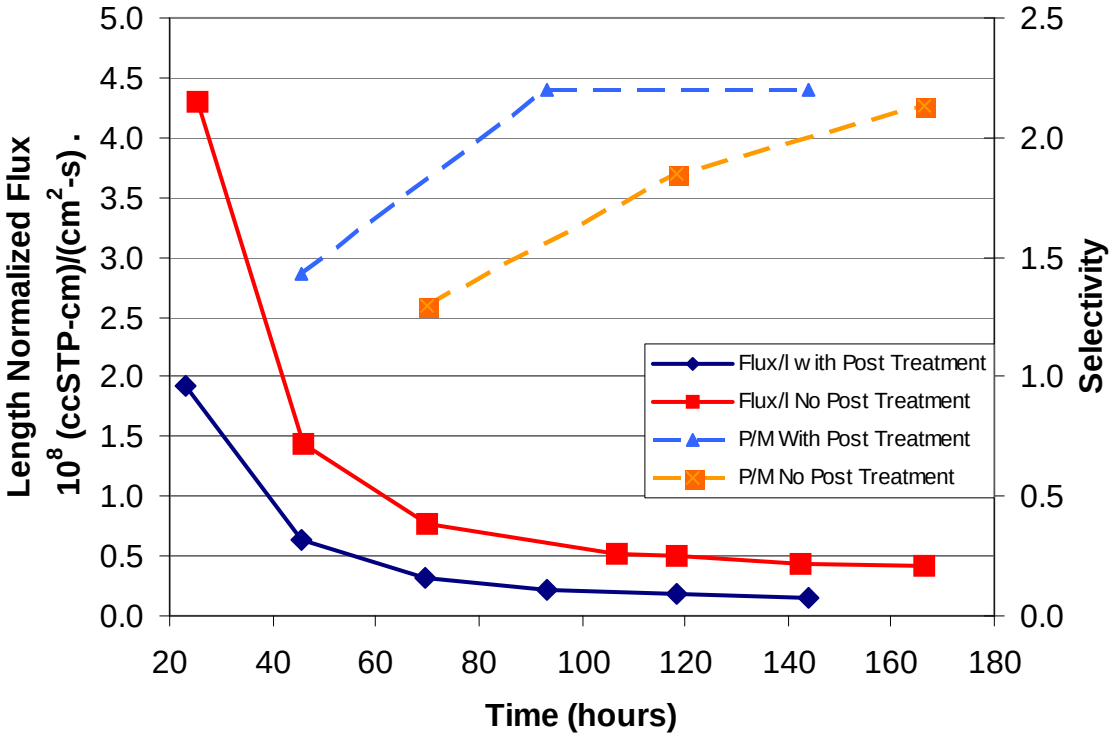

Figure 4.5. A comparison of the average Torlon® film prepared by thermal annealing with a similar film that received a 5 day thermal treatment at 200°C.

mechanisms similar to those reported in those reported in earlier studies. Therefore, lattice contraction and diffusion of free volume, possibly accelerated in this case due to the operating conditions, appear to provide a reasonable framework to interpret the present observation. Both of these aging mechanisms could result in a material with an overall reduced amount and type of free volume available to a particular penetrant for transport. In theory, as a polymer material relaxes, packets of free volume will be removed, and diffusion of free volume will ideally allow the general location and size of the free volume packets to change in a Fickian nature [9]. This could create a more discriminating material with fewer opportunities for transport due to more infrequent adequately large size diffusion gaps to enable diffusion steps. Moreover, this process would be expected to lead to more size discriminating transport due to a reduced relative

number of "large" diffusion gaps [9]. This ultimately describes a more dense structure after exposure to xylene and high temperature. It appears that aging in the presence of the desired feed produces a more favorable amount and distribution of diffusion-enabling free volume packets after the structure settles in to a more-or-less "altered" glassy matrix structure.

In order to corroborate this hypothesis, two separate avenues have been explored, albeit briefly. First, given the swelling nature of the penetrant and the glass transition temperature of the polymer at 280°C, depression of the T_g can yield a system with higher chain mobility, thus rendering the polymer more conducive to free volume relaxation. Chow [10] has developed a theoretical relation (Equation 4.1) for the estimation of T_g depression caused by a diluent.

$$\ln\frac{T_g}{T_{g_o}} = \beta\left[(1-\theta)\ln(1-\theta)+\theta\ln\theta\right] \tag{4.1}$$

where,

$$\theta = \frac{M_P}{zM_d}\frac{\omega}{1-\omega} \tag{4.2}$$

and,

$$\beta = \frac{zR}{M_p\Delta C_P} \tag{4.3}$$

In the above equations, T_{go} is the glass transition temperature for the pure polymer, while T_g is the value when the weight fraction of the diluent is ω. M_d is the molecular weight of

the diluent, M_p is the molecular weight of the polymer repeat unit, and ΔC_P is the change in specific heat of the polymer at its glass transition. The parameter z is the average coordination number in the matrix and R is the gas constant. All of the above parameters are known or can be measured directly, with the exception of the coordination number. For this, Chow has suggested using the coordination number of 1. While the case for choosing a coordination number of 1 is physically not easily justified, it can be used as a base case for calculation.

Thermogravimetric Analysis (TGA) of films after exposure to xylene provides an estimate of the sorption capacity of xylene isomers in Torlon® 4000T films, and consistently point to ~5 wt% xylene that is contained in the polymer during exposure to saturated liquid xylene feeds. Although there are inaccuracies in this technique, it serves as an approximation since more rigorous testing of xylene sorption at 200°C demands many safety concerns. Using this sorption value, and equation (4.1) an approximate reduction in T_g from 280°C to ~265°C can be calculated, which suggests that xylene transport in Torlon® at 200°C is indeed occurring in the glassy regime, with some enhanced mobility over the neat polymer condition at 200°C.

The second avenue to explore in order to understand the results in Figure 4.4 is the idea that reduction in free volume in the plasticized sample leads to a more densified polymer matrix. Directly measuring density changes of Torlon® films is difficult, since sorbed amounts of xylene cannot be desorbed without disturbing the free volume distribution in the matrix, and the density. In light of this challenge, optical methods were utilized,

which measure refractive indices of dense polymer films [11,12]. This measurement can be corrected for the amount of solvent sorbed, to provide inferences about polymer density based on the known proportional relationship between refractive index and density for a given material. This methods use a helium laser, and an optical waveguide to measure refractive index in all three dimensions and yield an average refractive index for the material. Thus an average polymer density can be estimated [11,12]. Three types of films were tested for refractive index and the results are shown in Figure 4.6. Annealed films were first prepared under the same conditions as the 315°C treated samples in section 4.2.3. The annealed films have very similar refractive indices of approximately 1.7040, and are assigned the literature density of Torlon® given at 1.41 g/cc (This may be a source of inaccuracy in later conclusions, and will be addressed later). After one day of xylene testing, (equivalent to the first data point in Figures 4.4) the film shows a significantly lower refractive index of 1.7015, which is associated with a lower density and/or swollen state. However, after 5 days of xylene testing, the film shows a higher refractive index than the originally annealed sample, suggesting a densified film. This observation strongly supports the idea that the membrane is originally swollen upon initial xylene exposure, and then relaxes to a more densified, and more discriminating state.

To further probe the concept of densification, refractive index measurements can be further manipulated directly to free volume measurements within the polymer. Using the Lorentz equation,

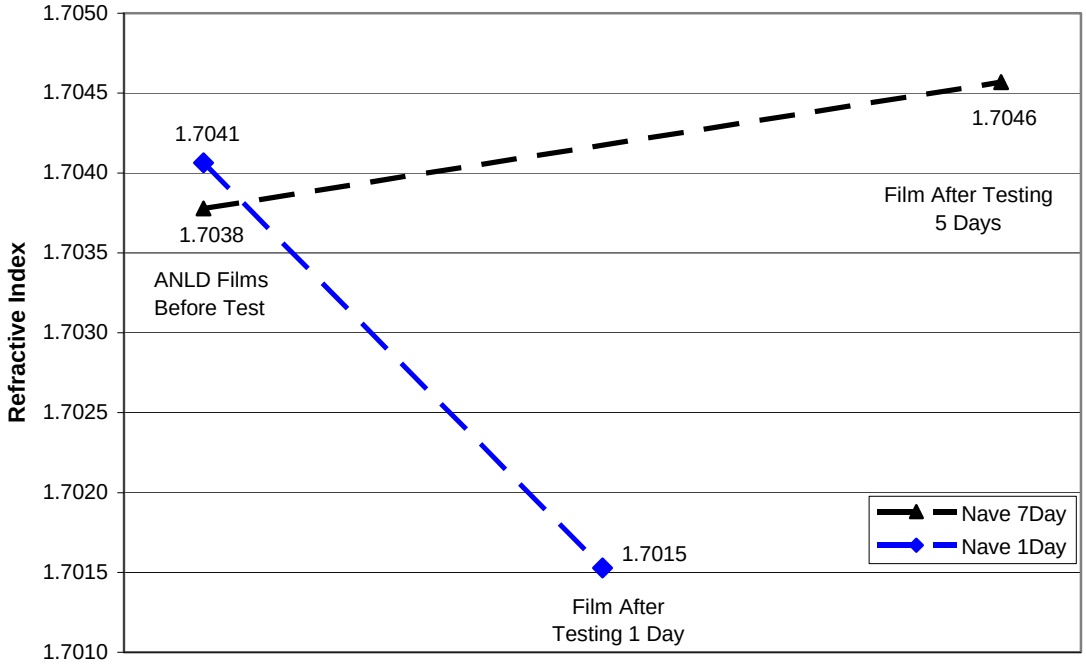

Figure 4.6. Refractive index measurements of separate films at different points during pervaporation testing. The blue line represents a film from the annealed state through 1 day of testing. The black line represents a film from the annealed state through 5 days of testing. The difference in the ending points shows a more dense film after exposure to high temperature and xylene.

$$L = \frac{n^2 - 1}{n^2 + 1} = \rho \cdot C \tag{4.4}$$

Refractive indices, n, can be used to obtain the Lorentz parameter, L, which is directly proportional to the polymer density via a constant, C. By assuming the annealed state has the literature density, the constant can be determined, and thus the density at different values of the refractive index can be determined. As mentioned before it would be preferable to have an accurate measurement of the density of Torlon® in the annealed state, but in the absence of such a measurement, this assumption does not introduce extreme errors and any later inferences made about *changes* in density are still valid. It is

well known that fractional free volume, *f*, can be correlated to density as well as permeability, *P*, to fractional free volume, by the following two relationships:

$$f = 1 - \rho \cdot V_o \tag{4.5}$$

$$P = a \cdot \exp\left(\frac{-b}{f}\right) \tag{4.6}$$

where,

$$V_O = 1.3V_w \tag{4.7}$$

V_w is the van der waals volume of the polymer chains calculated by group contribution methods by van Krevelen [13], and *a* and *b* are fitting parameters that have been shown to depend on the polymer family (*a*) and the penetrants relationship with the available free volume (*b*). Using these equations Table 4.4 can be generalized. These results suggest that even very small changes in fractional free volume can have large effects on large molecule permeability, and also lead to significantly increased permeation discrimination between large molecules with similar sizes and shaped molecules like the xylene isomers and ethylbenzene. If the free volume values are used with the permeabilities from Figures 4.4 and 4.5 values of *a* and *b* can be determined as ~275 and ~30, respectively. These values are shown in Table 4.5 in comparison with other molecule/polymer examples from literature and they compare well considering the size of the xylene molecule.

Table 4.4. Free Volume Calculations of Torlon® Membranes.

State	*n*	L	r (g/cc)	*f*
Annealed	1.7039	0.4876	1.4100	0.1086
1 Day	1.7015	0.4865	1.4069	0.1105
5 Day	1.7046	0.4879	1.4108	0.1080

Table 4.5. Fit parameters for Equation (3.6), various polymers.

Penetrant	Polymer	a (Barrer)	b	Ref
CO2	Polysulfone	1.08×10^{-4}	1.89	14
CH4	Polysulfone	1.14×10^{-5}	2.04	14
N2	Polysulfone	1.16×10^{-5}	2.01	14
Toluene	$6FDA/DAM_i/DABA_i$	81	13.82	15
Iso-Octane	$6FDA/DAM_i/DABA_i$	140	25.3	15
p-xylene	Torlon®	270	29.66	This Study

To further illustrate this possible conditioning scenario, Figure 4.7 shows two hypothesized free volume distributions that could arise from this type of relaxation process. The first free volume distribution (blue line) is typical Gaussian distribution of free volume expected after annealing of a polymer film. In this illustration, molecules on the size order of xylene isomers have very little size discrimination due to the similar availability of free volume of the same size. However, after a hypothesized relaxation (red line) the free volume changes in such a way that it is no longer as accessible to molecules of similar size and shape of xylene isomers, and can in fact become discriminating between such isomers. For this particular illustration, there is very little difference in the area under the two curves, or two total free volumes available. It is difficult, if not impossible, to tell if this is exactly the scenario in the xylene/Torlon® system, however this suggestion is at least consistent with the previous explanation of mobility and fractional free volume. Positron annihilation has recently become an attractive method to probe such changes, and future work could possibly explore this avenue of characterization [16].

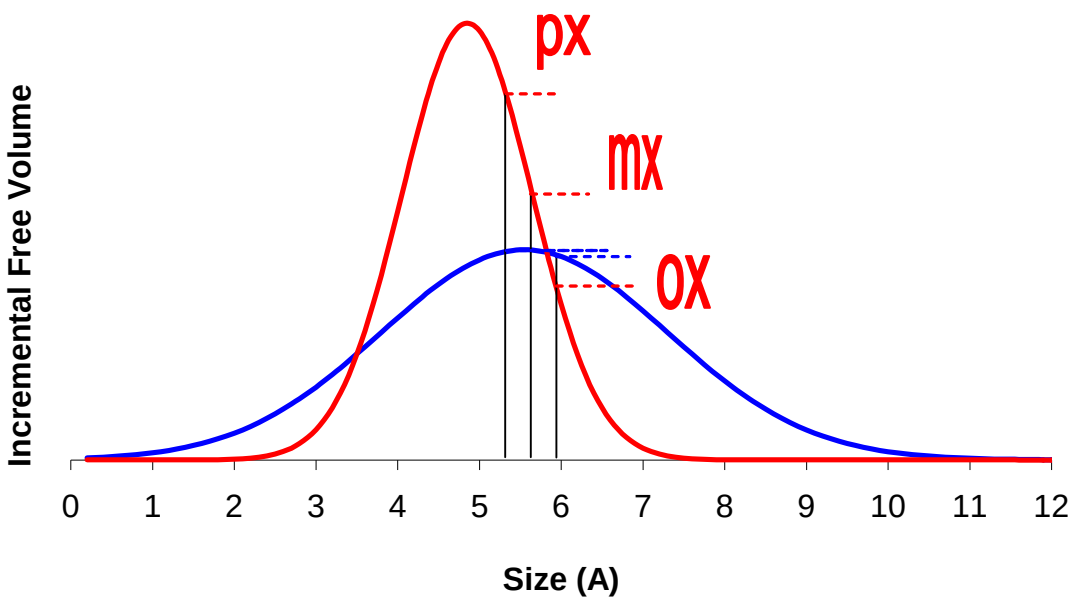

Figure 4.7. An illustration of what a possible free volume relaxation may do. The blue represents a hypothetical annealed polymer sample with a Gaussian distribution around a mean free volume size. Upon relaxing, the size and standard deviation of the distribution could hypothetically change resulting in a more discriminating type of free volume as demonstrated by the red line. The area under the curve in each distribution, or the total free volume remains unchanged.

4.4 References

1. Huff, George; Miller, Jeffrey T. (Spring 2003). *Early Results: Xylene separations with polymer membranes.* Presentation given to describe beginning of graduate project. Atlanta, Ga.

2. Moore, T. Effects of Materials, Processing Conditions, and Usage Conditions on the Morphology and Gas Transport Properties of Mixed Matrix Membranes. PhD dissertation, The University of Texas at Austin, 2004. Austin, Texas.

3. Torlon® Polyamide-imide. Solvay Advance Polymers. August, 01, 2006. http://www.solvayadvancedpolymers.com/static/wma/pdf/3/2/7/AI_10_APP_SAP.pdf.

4. Hoppin, C.R. *Synthesis of Polyamide-imides for Potential Membrane Applications.* Internal Georgia Institute of Technology Communication. June, 4th, 2004.

5. Yokelson, H.B.; Sakellarides, S.L.; Behrends, R.T.; Hackett, M. (Amoco). US 5,124,428. June 23, 1992.

6. Paul, D.R.; Koros, W.J.; Kim, J.H. Journal of Membrane Science. 282 (2006) p. 21-32.

7. Paul, D.R.; Koros, W.J.; Kim, J.H. Polymer. 47 (2006) p. 3104-3111.

8. Paul, D.R.; Wang, X.; Huang, Y.. Journal of Membrane Science. 277 (2006) 219-229.

9. Yampolskii, Yu.P. Alentiev, A Yu. Journal of Membrane Science. 165 (2000). 201-216.

10. Chow, T.S.. Macromolecules, 13 (1980) Iss. 2. p. 362-4.

11. Samuels, R.J.; Cha, C.Y.; Moghazy, S.; Hardaker, S.S. Journal of Polymer Science: Part B: Polymer Physics. 31(1993) p. 1951-1963.

12. Samuels, R.J.; Henderson, C.L.; Liu, T.; Journal of Polymer Science: Part B. Polymer Physics. 41(2003) p. 842-855.

13. Krevelen DWV. Chermin HAG. Ingenieur. 62(1950). P. 65-74.

14. Nagai, K.; Kanehashi, S. Journal of Membrane Science. 235(2005) p. 117-138.

15. Paul, D.R.; Koros, W.J.; Xu, W. Journal of Membrane Science. 219(2003) p. 89-102.

16. Jean, Y.C.; Hong, H. Macromolecules. 29 (1996) p. 7859.

CHAPTER 5

INTRODUCTION TO MIXED MATRIX MATERIALS

This chapter introduces the concept of using previously characterized Torlon® polymer with MFI molecular sieves to form mixed matrix materials. The matching properties of Torlon® and MFI will be discussed before developing the procedures for producing mixed matrix films of the two materials. Lastly, attempts to create successful mixed matrix materials with silane coupling agents and previously developed procedures will be discussed. This chapter will conclude summarizing the applicability of previously used materials and methods and establish requirements for further development.

5.1 Introduction to the MFI/Torlon® Composite

The first and foremost task in evaluating MFI as a mixed matrix candidate is in evaluating the sieve's performance for separating p-xylene from the other xylene isomers, and obtaining a reliable estimate of sieve permeability for comparison with the bulk polymer phase. Fortunately, MFI is a most widely studied molecular sieve, and literature provides a wealth of knowledge to estimate these parameters. This section will evaluate these properties in three sections: MFI transport properties, permeability matching with polymer, and lastly mesoporosity within MFI crystals.

5.1.1 MFI Transport Properties

Producing high quality zeolite films has been extremely difficult, and provide little data that is capable of being attributed to transport through large, single, defect free crystals.

Table 5.1 Diffustion of Xylene Isomers in MFI Type Crystals

Sorbate	Sorbent	Method	D cm2/s	Ref.
p -xylene	ZSM-5	ZLC	6.8 E -9	[1]
	silicalite	ZLC	4.3 E -8	[1]
	silicalite	Monte Carlo	1 E -11	[2]
	MgZSM-5	Monte Carlo	1 E -13	[2]
	silicalite	***Gravimetric***	***3 E -8***	[3]
m -xylene	silicalite	Monte Carlo	1 E -19	[2]
	MgZSM-5	Monte Carlo	5 E -25	[2]
o -xylene	silicalite	Monte Carlo	1 E -15	[2]
	MgZSM-5	Monte Carlo	1 E -22	[2]
	silicalite	***Gravimetric***	***3 E -9***	[3]
ethylbenzene	***silicalite***	***Gravimetric***	***1.5 E -8***	[3]

However, in the absence of traditional membrane permeability data, diffusion and sorption data of the appropriate penetrants can be used to estimated permeability based on equation 2.4. In order to complete this estimate, literature on xylene diffusion and sorption in MFI, type crystals have been collected. Table 5.1 shows various diffusion data for xylene isomers in the MFI crystal system. In addition, Figure 5.1 shows sorption isotherms for xylene isomers in MFI crystals at various relative pressures as compiled by Tsapatsis [4].

In order to estimate the permeability of p-xylene in MFI, we will use the gravimetric diffusion data in silicalite [3], as this is the crystal type to be used in this work. In addition to the p-xylene diffusion at 200°C, the reference also provides diffusion results over the temperature range of ~50°C to 200°C. The diffusion data will be used along with the sorption isotherms developed by Tsapatsis to approximate xylene permeability over the temperature range of 70°C to 200°C. These data, when applied to equation 2.4, yield the results shown in Figure 5.2, and predicts a p-xylene permeability of ~6 Barrers at 200°C. Other references by Tsapatsis et. al., suggest separation factors of *~300 p/o* at this same temperature, when perpendicular to the "b" axis as discussed in Chapter 3.

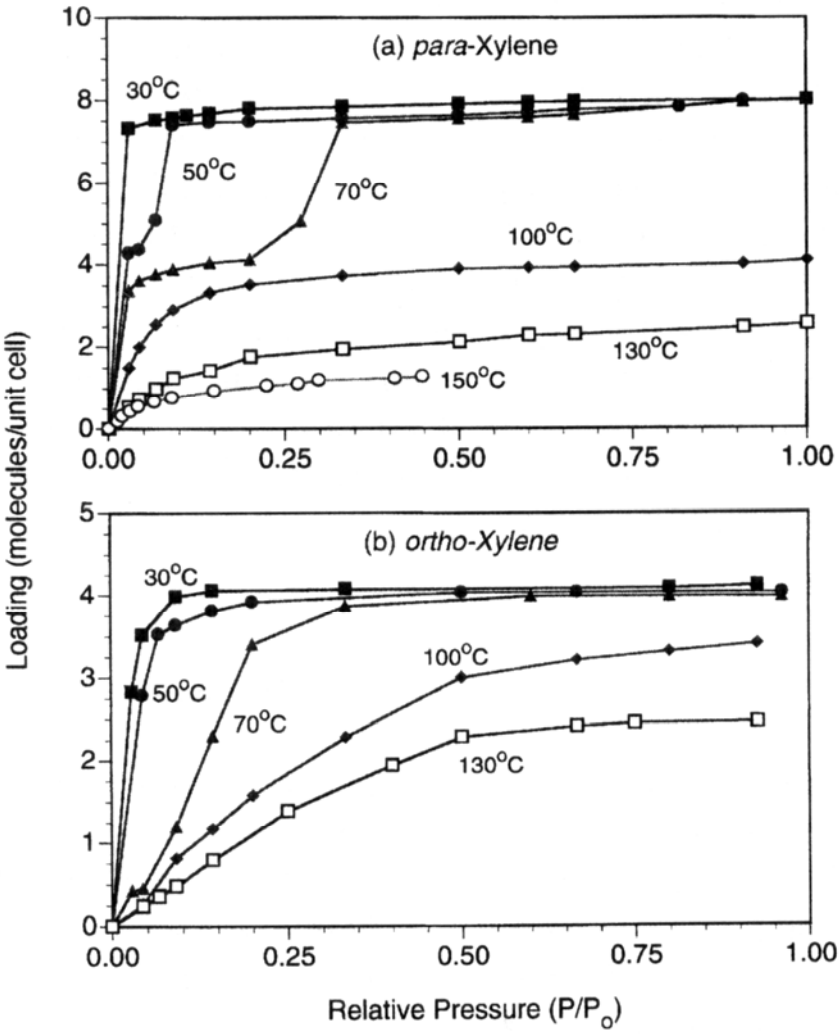

Figure 5.1. Sorption Isotherms for p-xylene and o-xylene single component systems as described by Tsapatsis et. al. [4].

Given that MFI is not a 3-D symmetrical structure, and actually only has transport in 2 directions, we must consider that this permeability is for an oriented structure, through one of the permeable directions. In our system, we will most likely experience ~2/3 of this permeability, by assuming a random distribution of crystals, and approximating that 1/3 of the crystals are oriented such that an impermeable face is orthogonal to the direction of transport. Therefore, from this data, it can be estimated that the permeability

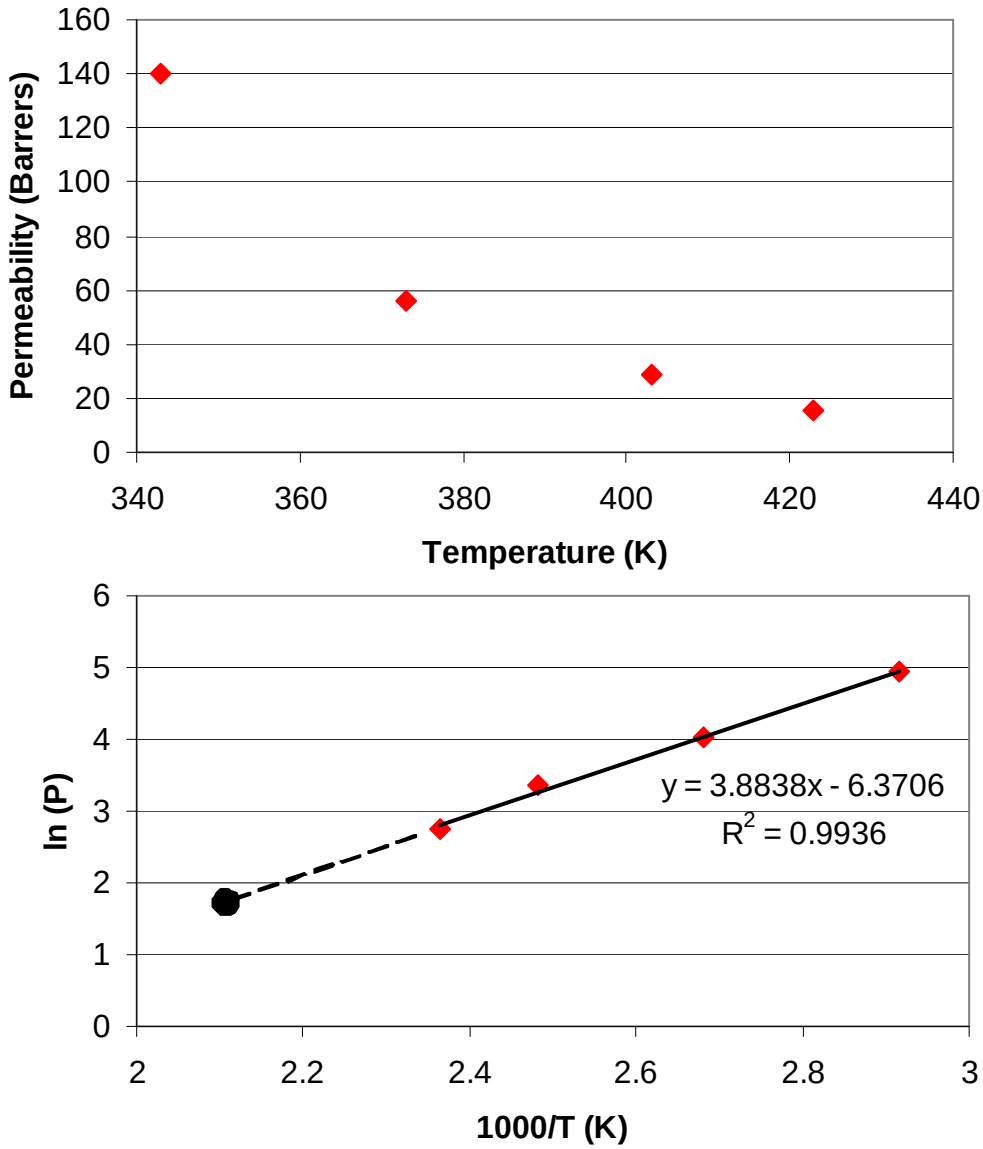

Figure 5.2. Applying literature diffusion and sorption data to equation 2.4, and predicting the permeability of p-xylene in silicalite over the temperature range for 70°C to 200°C. Note: The data point at 200°C (Large Black Dot on bottom graph) is extrapolated from the linear fit of the Arrhenius plot.

of p-xylene in silicalite crystals, randomly distributed about their internal pore structure is

~ ***4 Barrers.***

It should be noted at this point, that the estimation of para-xylene permeability must be corrected in a subsequent chapter, to account for the competing sorption of the other xylene isomers within the zeolite. This result may actually suggest that MFI is not the

optimum zeolite for separation under these operating conditions. However, identification of the "fast-gas" penetrant, and matching the polymer properties to this value, has been an established methodology in previous gas separation applications of mixed matrix materials. This chapter seeks to evaluate such procedures, and therefore this assumption will be implemented in this chapter only. Further information can be found in Chapter 6.

5.1.2 *Permeability Matching*

As previously mentioned in Chapter 2, once the properties of both materials have been investigated, the permeabilities of the materials can be investigated to qualify the potential of the composite. By using the Maxwell Model (Equation 2.17) we can predict the composite transport properties. The results of this comparison can be seen in Figure 5.3. The base Torlon® properties of 0.25 Barrer, and para/ortho selectivity of 3 are used, along with Silicalite properties of 4 Barrers and a para/ortho selectivity of 300, to calculate composite properties. In Figure 5.3, the loading to the molecular sieving phase is changed from 0 wt% to 40wt%, in increments of 5% (each red point) to illustrate the different levels of enhancement possible for ideally engineered composites. The upper bound is the Freeman based approximate upper-bound from Chapter 2 [5]. From the figure it can be seen that the materials appear to be well matched for *para*-xylene, achieving nearly a doubling of selectivity for a loading of 20%.

5.1.2 Mesoporosity in High Silica MFI Crystals

Recently, work has been completed that suggests mesoporosity in zeolite crystals can lead to non-ideal effects in mixed matrix membranes [6]. Mesopores, or large, non-molecular sieving, "holes" in the zeolite would provide a possible pathway for penetrants

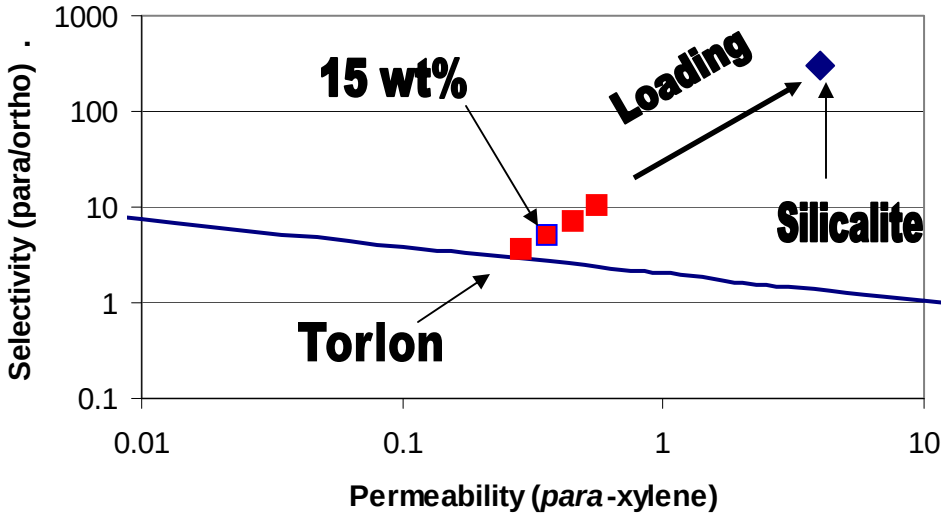

Figure 5.3. Maxwell model predictions of xylene isomer separation for Torlon®/Silicalite mixed matrix membranes at various loadings of dispersed silicalite (0wt% - 35wt%) in 5% increments. Torlon® is assumed to lie on the upper bound. The outlined data point represents 15% loading, while the dark blue represents the pure sieve properties.

to transport non-selectively through the membrane. In addition, diffusion coefficients should be orders of magnitude greater in these "holes" than the zeolite pore, and if a percolation pathway exists, the use of zeolites in the material would be completely negated by the less discriminating, lower resistance, mesopores. In order to determine if any such mesopores exist in the materials to be used for xylene isomer purification, zeolite samples were tested by nitrogen adsorption in a Micromeritics ASAP 2020 pore analyzer. The results of BP large silicalite and small silicalite crystals (introduced in Chapter 3) are shown in Figure 5.4. Generally, nitrogen adsorption isotherms for zeolite samples can be well understood by Langmuir models, and we can use this approach to discuss the isotherms in Figure 5.4. In the extremely low relative pressures, the nitrogen condenses in the micropores of the samples. In a normal Langmuir isotherm, micropore filling stops at the onset of pore saturation, and further increase in relative pressure causes no additional uptake by the material. However in Figure 5.4 there is a secondary

uptake, after micropore filling, in the relative pressure range of ~0.1-0.3 p/p_o . This uptake would generally be associated with another pore size, larger than that of a micropore, and would suggest a mesoporous nature in the zeolite samples in the range of ~25 Å. However, literature has reported a special phenomena in high-silica zeolite (MFI-specific) samples that causes the liquid nitrogen in the pores to alter the preferred type of molecular packing, and thus moves from a liquid like packing state to a solid like packing state [7,8,9]. If this idea is true for the BP silicalite samples, then the nitrogen sorption data erroneously represent the pore structure of the material. In order to represent the true nature of the pore structure, a similar gas adsorption experiment was completed with argon, instead of nitrogen, at the advisement of Micromeritics®, the pore analyzer manufacturer. The results of argon adsorption on the same two samples are shown as dashed lines in Figure 5.4, and show a definite limit in micropore filling (Langmuir type isotherm), and no secondary transition in the linear plot. In the logarithmic plot, it can be seen that argon exhibits a similar transition in much lower pressure ranges, and much less pronounced than the nitrogen transition. If there was indeed a secondary pore size, the isotherm would be identical, regardless of the gas penetrant selected. However, if the phenomena were a characteristic of the gas penetrant itself, a change in the manner of the secondary transition would be expected. In this case, argon goes through a similar transition, although at a much lower pressure, and with a much less pronounced uptake effect due to its spherical nature. The argon adsorption data is sufficient to conclude that mesoporosity is not a significant factor in BP silicalite samples, and should not hinder this research in any way.

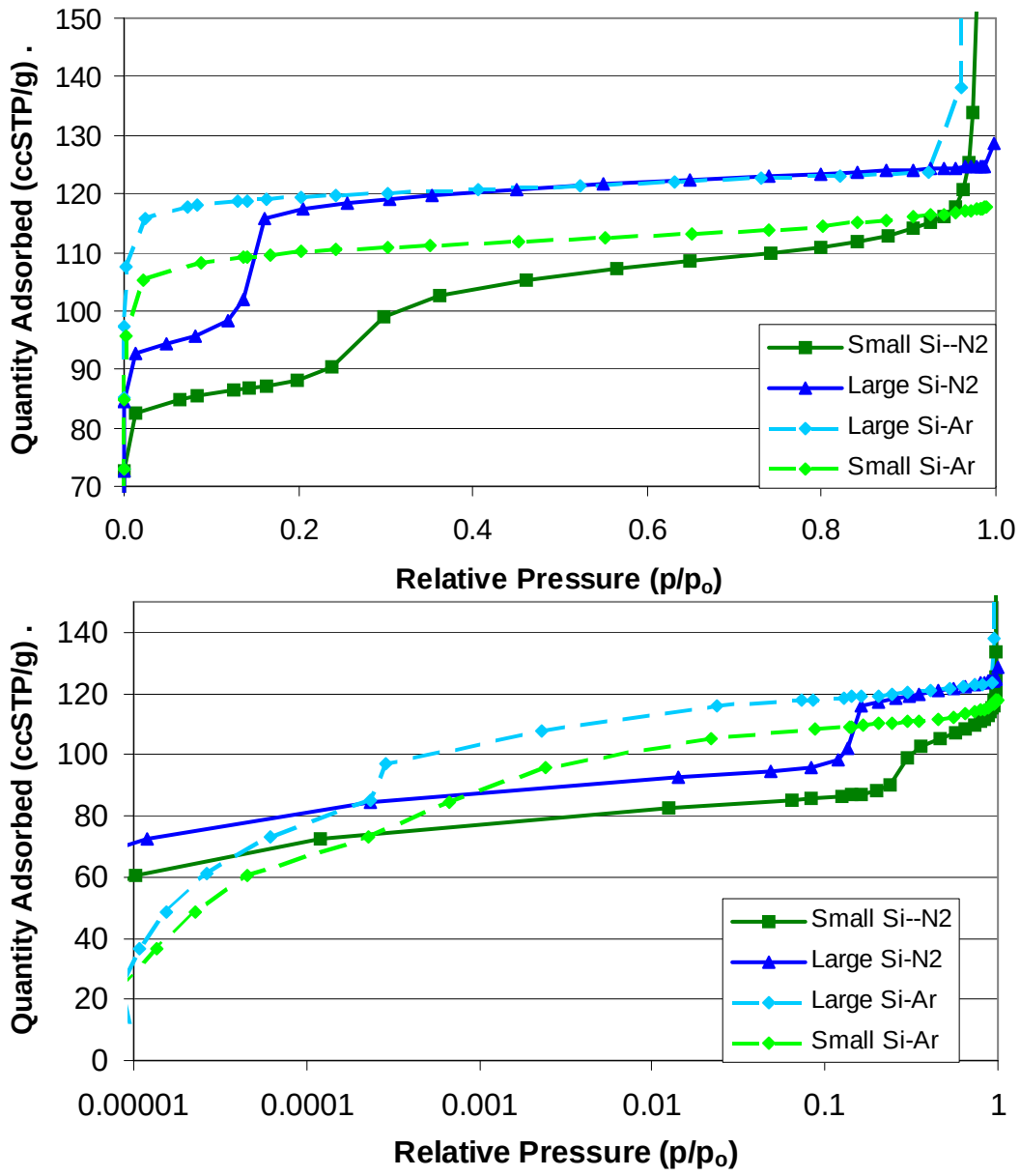

Figure 5.4. Nitrogen and argon adsorption isotherms for large and small silicalite crystals provided by BP. Top (A) plot represents the linear plot of the adsorption isotherms for each gas, while the bottom plot (B) represents the logarithmic plot. The linear plot shows the nitrogen packing transition at ~0.2 p/p_o, while the logarithmic plot shows the argon packing transition at ~0.0005 p/p_o.

Further consideration should also be given to the differences in the adsorption isotherms for the small and large crystals. The large crystal isotherms exhibit a sharp, knee-like transition, where as the small crystal isotherm transition is more rounded. It is unclear at

this time as to why there are differences, other than the obvious fact of the difference in crystal size, and synthesis procedures, of which were not available for this work. In addition the large crystal sample is much more mono-disperse and regular in shape than the smaller crystals, and this randomness in the smaller crystal size may indeed affect the sharpness of the secondary transition in nitrogen. In actuality the details of the postulated "packing-transition" for nitrogen adsorption in high silica materials are not very well understood in the literature. However, the un-questionable results of argon adsorption, compared against the nitrogen isomers, confirm a process that does not appear to be intrinsic to the pore structure. Further investigation into this phenomenon is not in the scope of this work, however future work could possibly investigate the nature and causes for such phenomena. For the remainder of this work, nitrogen isotherms will be used to characterize materials with the understanding that transitions in this range are not likely to represent mesopore presence.

5.2 Mixed Matrix Membranes via Silane Coupling Agents

As previously stated in Chapter's 2 and 3, mixed matrix materials with high glass transition polymers typically do not adhere well to inorganic zeolite surfaces and some form of surface modification must be implemented. This section will discuss the most commonly used surface modification, silane coupling agents, and how they affect the xylene isomer separation.

5.2.1 Selection of Silane Coupling Agents

Previous work on mixed matrix materials for gas separations within the Koros research group at Georgia Institute of Technology has primarily focused on surface modification with the silane coupling agent (SCA) 3-aminopropyldimethylethoxysilane (APDMES). This SCA can be seen in Figure 5.5 which shows all the SCAs investigated for this modification. For this particular application, contrary to previous gas techniques, the commonly used APDMES is small enough to theoretically adsorb into the silicalite pore. This could be a significant problem if APDMES could react internally and clog the pore structure, restricting transport of the xylene molecules during mixed matrix application. The high silica to alumina ratio of the silicalite should render the interior of the sieve organophilic and willing to adsorb organics. Although the high ratio should also have an

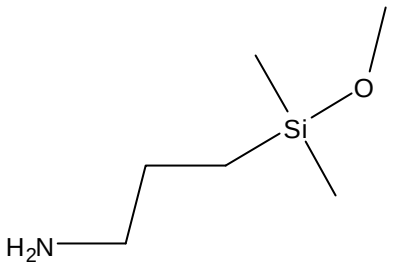

SCA #1.
3-AMINOPROPYLDIMETHYLETHOXYSILANE

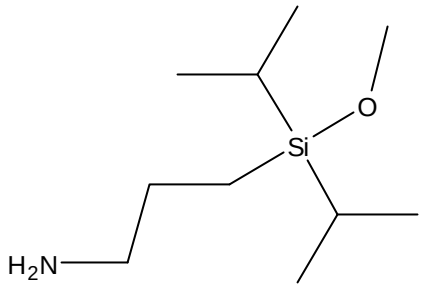

SCA #2.
3-AMINOPROPYLDIISOPROPYLETHOXYSILANE

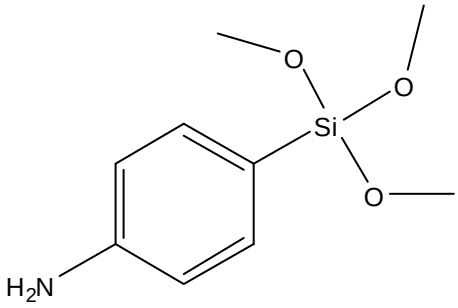

SCA #3.
p-AMINOPHENYLTRIMETHOXYSILANE

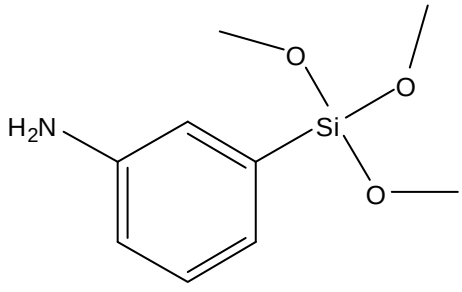

SCA #4.
m-AMINOPHENYLTRIMETHOXYSILANE

Figure 5.5. Silane Coupling Agents (SCA) used to determine proper coupling agents for large pore zeolite (silicalite).

internal structure “essentially” free of hydroxyls, imperfections in the crystals (“hydroxyl nests”) or any other hydroxyl sites could react with SCAs. Therefore, a small SCA will most likely diffuse into the pore structure, but whether or not actual clogging would occur is difficult to determine simply from the silica to alumina ratio. To answer this question, the large BP silicalite crystals were treated with all 4 silane coupling agents as described in Chapter 3, and subsequently all samples were analyzed with nitrogen adsorption. The results are shown in Figure 5.6. It can be seen that each treatment of silane coupling agent causes approximately a 5% reduction in the total pore volume as compared to the clean sample with nitrogen as an adsorbent. It seems that under these conditions, *regardless of SCA size*, the silanated samples adsorb the nitrogen penetrant in a similar manner, with slight differences in the secondary transition previously associated with packing transition of the nitrogen molecules and the isotherm shape in the higher relative pressures. It is hypothesized that these slight changes in isotherm shape are due to surface energy changes due to new silane coupling molecules possibly on the surface of the sieve, which affects the condensed nitrogen maintaining intimate contact with the surface. It is further hypothesized that although a smaller SCA may be able to enter into the pore structure (like APDMES), the molecule does not react to the extent that causes serious depression of the available pore volume. This may solely be due to the mild reaction conditions implemented by this research, based on previous silanation reactions with gas separation membranes. Literature that was not apparent at the time of these initial tests has been reviewed that indeed shows effective silanation of large silicalite crystals, although at more aggressive reaction conditions [13]. In the literature example the silanation reaction was completed at 70°C overnight, instead of 0°C with sonication

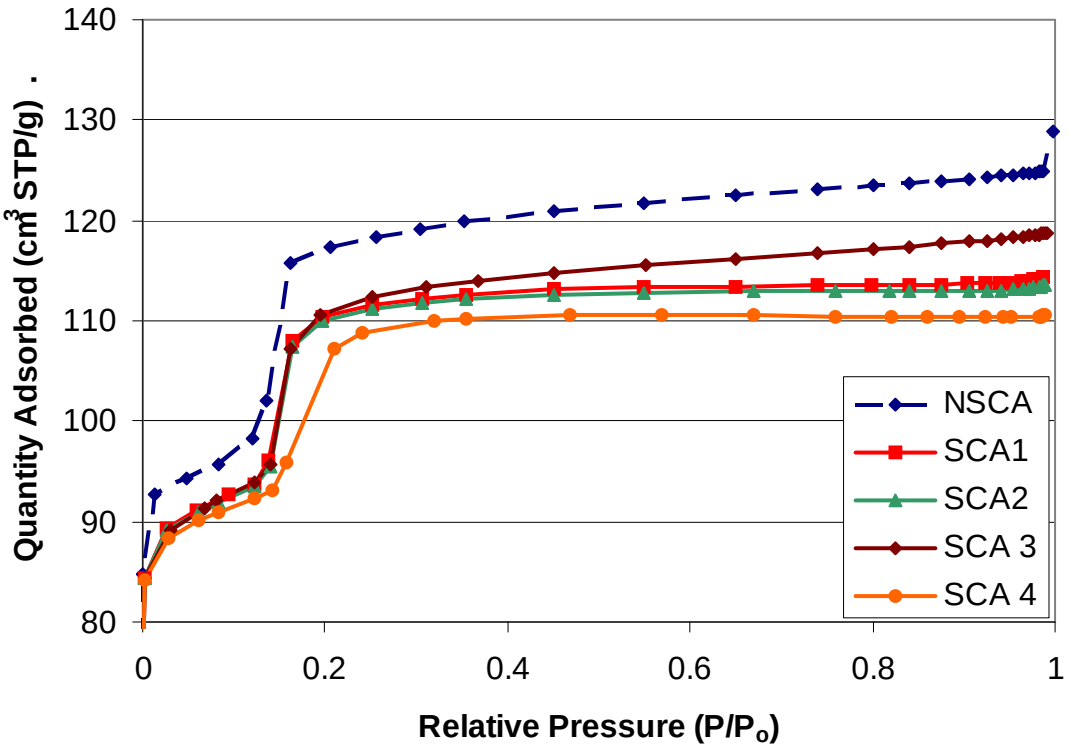

Figure 5.6. Nitrogen adsorption results for large silicalite crystals after silane coupling treatment with various sized silane coupling agents.

over 30mins. Therefore it is possible that the depression observed in Figure 5.6 is due to low reactivity, and the depression would be increased given more reactive silanation conditions.

An attempt was made to prove that silane coupling agent did in fact react with surface hydroxyls with both NMR and IR, however due to the large size of the crystals, and the corresponding low surface area to mass ratio, not enough of the silane coupling type bonds are present to show any definite difference from a clean sample. In fact, it is nearly impossible to see all but the traces of the hydroxyls stretches in the IR spectra on BP large silicalite particles. This result is also indicative of very low extent of reaction of silane coupling agents with the surface hydroxyls. As a result, the color change of the

modified zeolite, before and after drying, is the only evidence of a surface reaction. However, given the fact that the majority of the silanated silicalite porosity is retained after the treatment, and the goal of this chapter is to evaluate previously developed mixed matrix material procedures, these treated sieves were used to develop mixed matrix materials for xylene separation. In addition, due to no significant differences betweens coupling agents, it was determined that there was no need to deviate from the traditional SCA of APDMES for use in mixed matrix membranes for xylene separation.

5.2.2 Membrane Formation and Initial Properties

Two groups of mixed matrix membranes were formed with both the BP large and small silicalite samples as discussed in Chapter 3. Digital photographs of these films in Figure 5.7 show that as the zeolites are dispersed within the polymer the films change from a "yellow-clear", to a "yellow-translucent" color. As shown in Figure 5.7(B), it can be seen that the small size BP crystals form aggregates that are difficult to disperse even

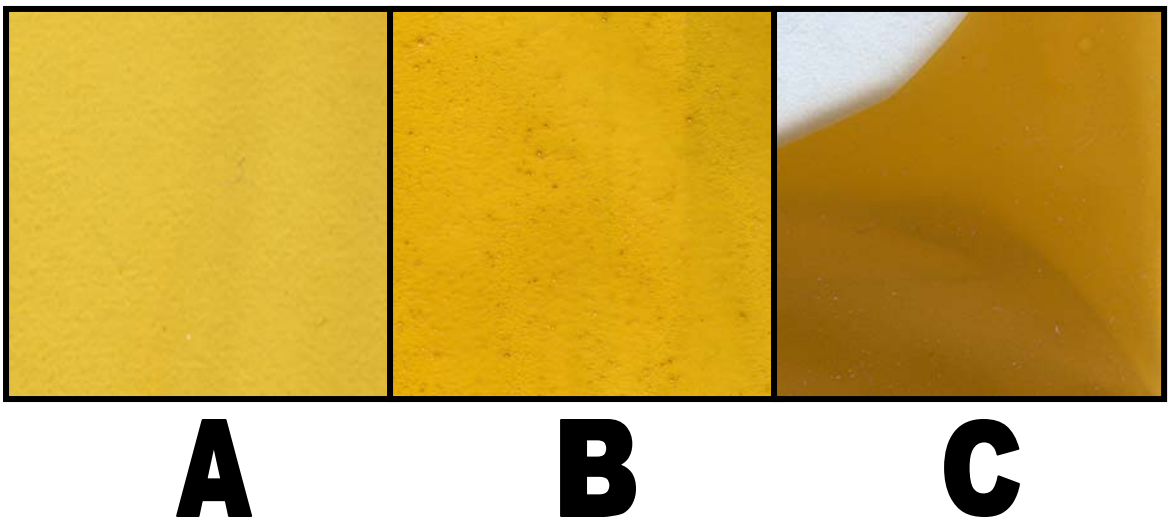

Figure 5.7. Showing the differences in Torlon mixed matrix films with silicalite particles. Picture A is of a neat Torlon 4000T ® film. Picture B is of a Torlon®/small silicalite film showing large particle aggregates. Picture C is of a Torlon®/large silicalite film showing good particle dispersion, and thus the translucent nature. Figure to scale.

with repeated sonication. Initial vacuum tests with films formed from small silicalite samples exhibited a "B" type morphology and were unable to hold adequate vacuum, and thus useless for pervaporation testing. Figure 5.7 (C) shows a well dispersed large silicalite sample, and the translucent nature of a well dispersed mixed matrix film, with no visible aggregates. Initial vacuum tests hold vacuum well, and will be discussed in the next section with respect to pervaporation results. Figure 5.8 and Figure 5.9 follow with SEM's of the cross-section of both large and small BP silicalite samples. Given this close-up view of the interface, it can be seen that even with the SCA treatment, good polymer-zeolite adhesion does not appear to have been achieved with BP large silicalite samples. It appears that better adhesion may be possible with the BP small samples, however large aggregates can be seen that form distinct regions within the mixed matrix film. These aggregates can break through the surface and lead to initial the initial vacuum failure discussed above.

5.2.3 Pervaporation Testing of Torlon®-Silicalite Mixed Matrix Membranes

Torlon®-Silicalite mixed matrix membranes were tested by pervaporation of xylene isomers. The methods were identical to those used to previously characterize Torlon® in Section 4.3 and the results are shown in Figure 5.10. Immediately it can be seen that these films exhibit the same decrease in permeability that the neat polymer membranes exemplified. However, although they maintain very similar selectivities, it is apparent that the silicalite mixed matrix films reach a higher permeability, at 0.32 Barrer, instead of the neat polymer value of 0.25 Barrer. The selectivity results for the material show

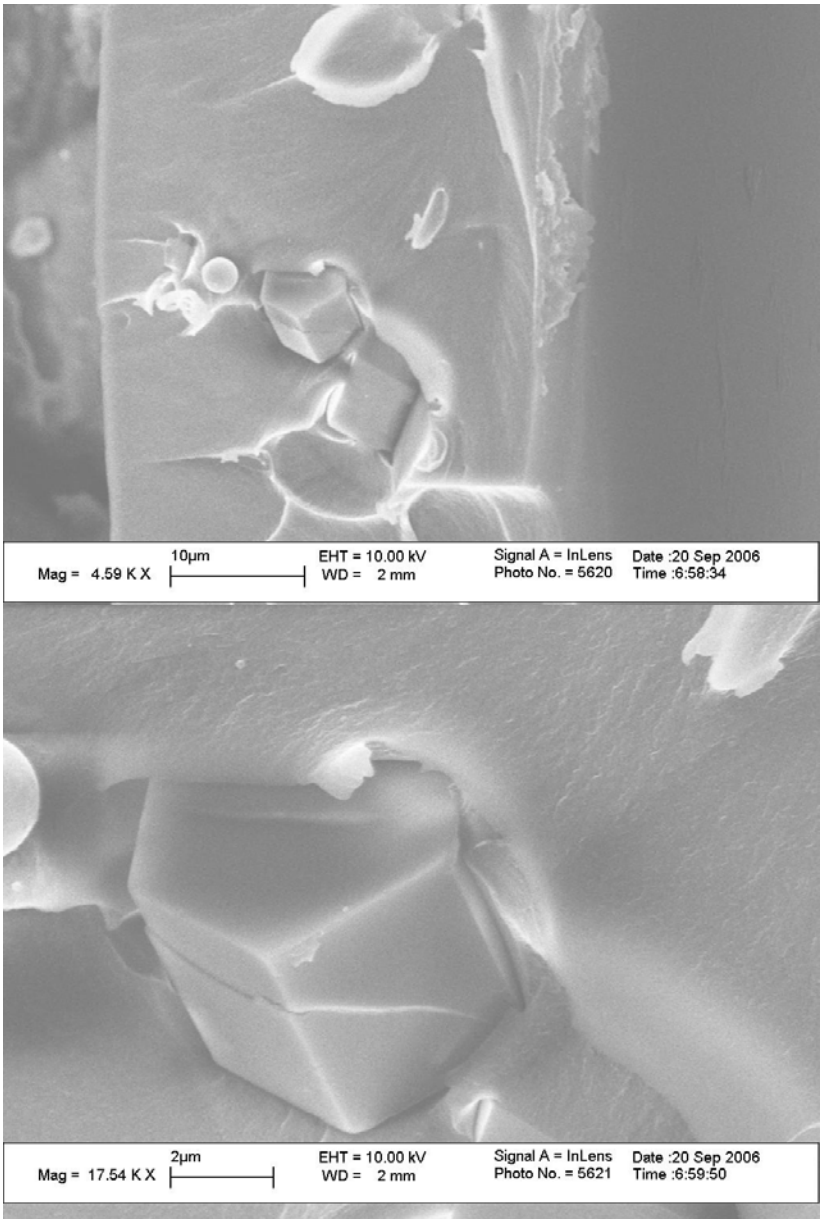

Figure 5.8. SEM of large silicalite crystal embedded in Torlon 4000T mixed matrix membrane. Top image shows two crystals pertruding from the polymer, while the higher magnification bottom image clearly shows the gap at the sieve/polymer interface.

some slight improvement, however this should be completely within the experimental error of the selectivity measurement. Given the very similar selectivity results compared to the neat polymer, it is very reasonable to conclude that the increase in permeability is due to "sieve-in-a-cage" type morphology as discussed in Chapter 2. The SEM's pictures

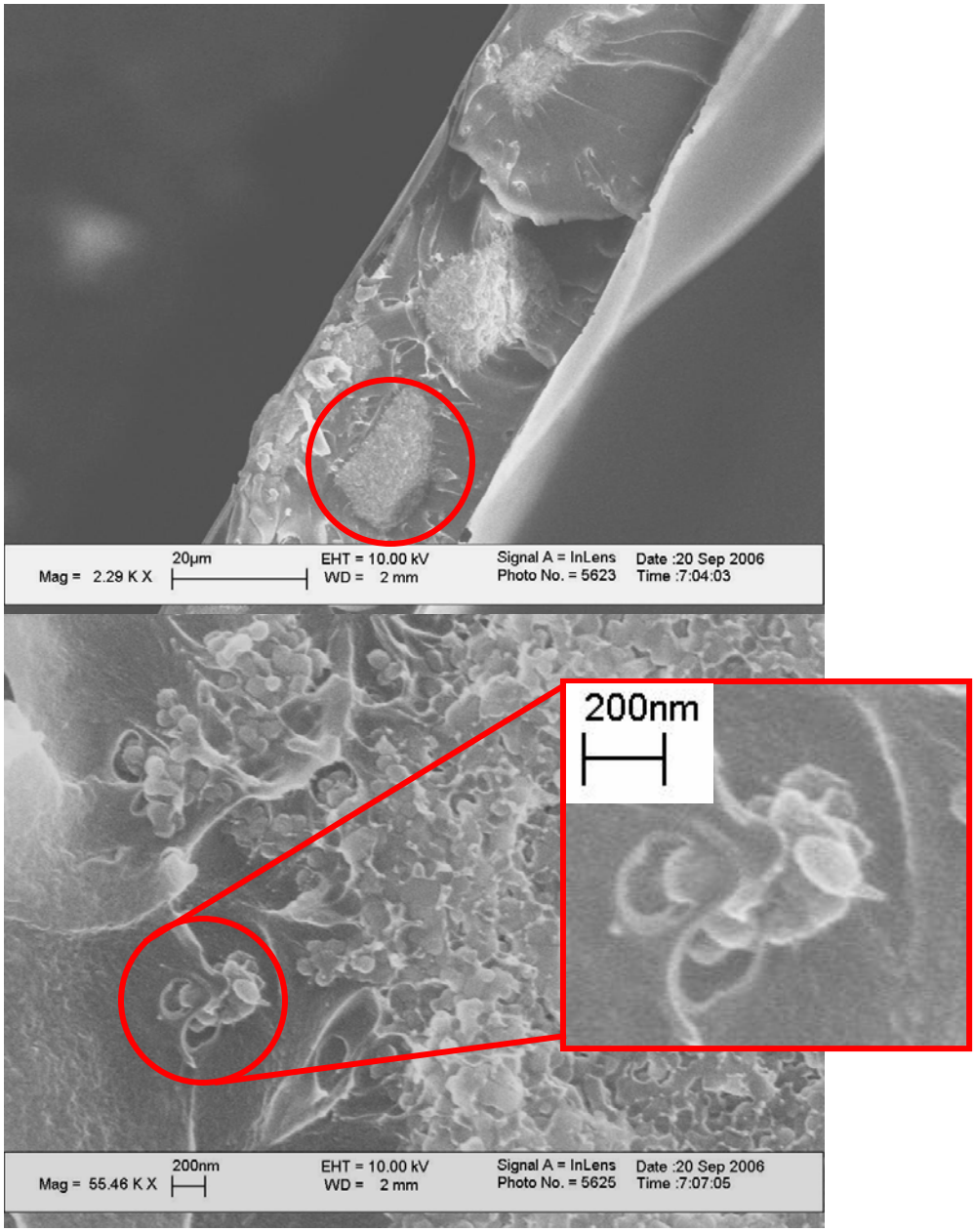

Figure 5.9. Small silane treated silicalite crystals dispersed in Torlon 4000T® mixed matrix film. Top image clearly shows large aggregate particle that form separate regions within the membrane. Bottom, high magnification image, shows questionable adhesion on the surface of the agglomerated particle.

in 5.2.2 also suggest this phenomenon. In addition, FTIR spectra were obtained for both neat polymer samples as well as mixed matrix samples and can be seen in Figure 5.11. No differences in imide ring bonding, amide bonding, or any bonding differences at all can be ascertained from the IR spectra. These spectra and the evidence for "sieve-in-a-

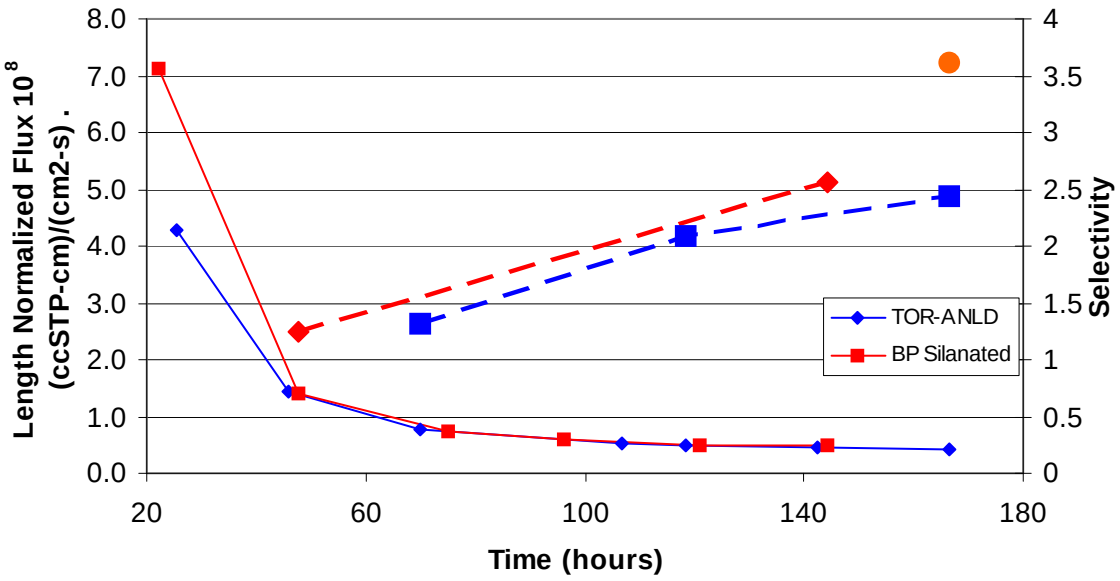

Figure 5.10. Pervaporation properties of two mixed matrix membranes formed with large silicalite crystals. Poor interfacial adhesion leads to "sieve-in-a-cage" morphology with higher composite membrane permeability than the neat polymer. Solid lines represent flux; dashed lines represent selectivity. The Maxwell prediction of a silanated film @ 10% loading is shown as the orange dot—3.6 p/o.

cage" morphology suggest that the SCA modification was insufficient in binding the polymer to the zeolite surface. The only apparent difference in this modification and previous SCA modification with rigid polymers is the use of the polyamide-imide, and the use of higher silica to alumina ratio zeolites. Although the presence of the amide group changes the reactivity of the polymer backbone, it should not drastically alter the reactivity of the imide group itself, and should add some degree of mobility to the polymer chain. Therefore, it is reasonable to conclude that the absence of the more acidic alumina tetrahedra in the zeolite structure cause inherent problems in tethering the zeolite surface to the bulk polymer. Although the zeolite surface is more organophilic in the absence of the acidic alumina hydroxyls, it is also much less susceptible to attack from silane coupling agents. Therefore it is hypothesized that the high silica to alumina ratio

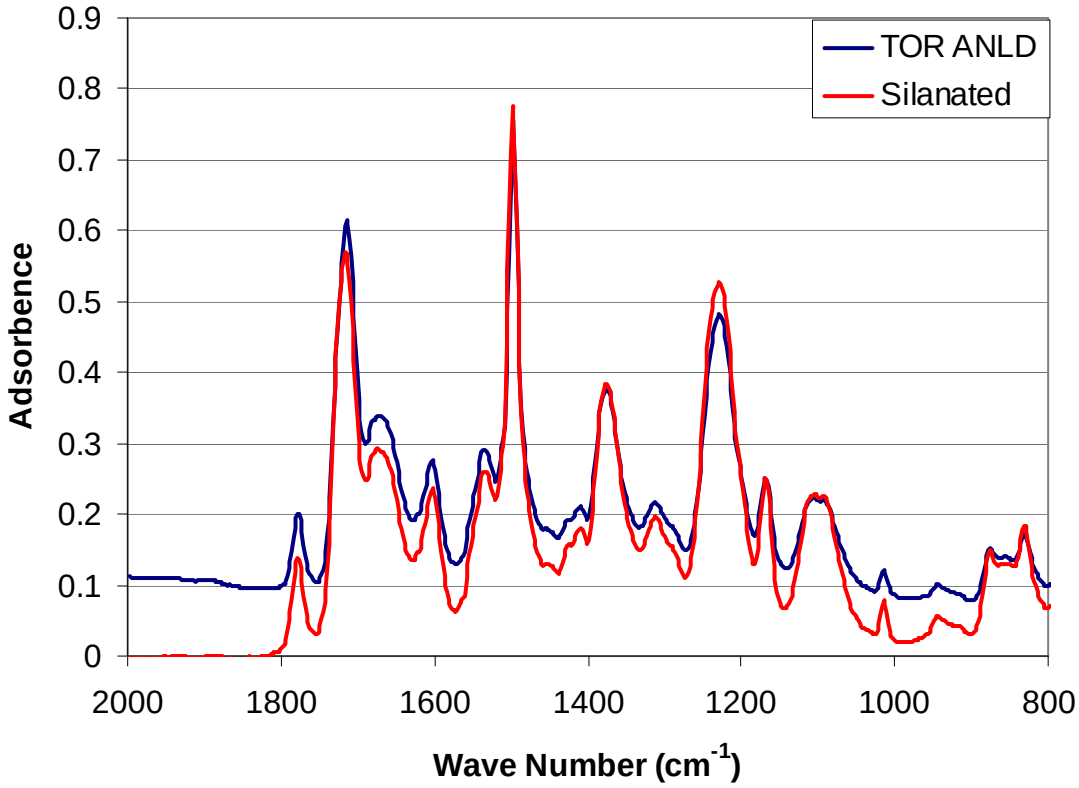

Figure 5.11. ATR spectra of Torlon® neat polymer and silanated films. These spectra show little if any difference, suggesting no bonding changes in the silnated state.

prohibited effective treatment of silane coupling agents onto the zeolite surface under the preparation conditions suggested by Gelest Inc. Unfortunately this is a difficult hypothesis to prove for two main reasons. First, replacing silicalite with a lower silica-alumina ratio zeolite (a ZSM-5 variety) will change the transport properties in a manner less favorable for xylene isomers due to the increase in hydrophillicity caused by the increase alumina hydroxyls, and the low quality (amorphous nature) of such materials. Therefore the advantageous transport properties of silicalite would undoubtedly change, and most likely to a much less favorable state. Secondly, there is not an effective method available to probe the fractional conversion of surface hydroxyls on zeolites with few alumina tetrahedra. Several authors have shown methods to elucidate the fractional conversion of alumina hydroxyls on zeolitic surfaces, and often refer to the silica

hydroxyls as catalytically inert [10,11,12]. Given these difficulties, and the emergence of a new method (Chapter 6) for improving zeolite-polymer binding, the SCA method will be not be pursued any further for mixed matrix membrane with high silica zeolites. It would be of interest for future researchers to investigate the extent of surface reaction of silane coupling agents, however in light of a more attractive method (discussed in Chapter 6), this issue will receive no further consideration in this work.

5.3 Initial Mixed Matrix Summary

After attempting to apply previous mixed matrix procedures to the silicalite/Torlon® system it is clear there are several distinct results. First, the para-xylene permeability in silicalite matches well to Torlon® system for an ideal, uni-molecular case. (further discussed in Chapter 6). Second, it appears that previous silane coupling agent procedures are not adequate to graft SCAs to the silicalite surface and maintain an effective interface. Conditions may exist that increase the reactivity, however increased reactivity may lead to a clogged pore structure, as low reactivity reduced pore volume by ~5%. And lastly, it is difficult to determine silane coupling loading with large crystals, and it would be useful to perform TGA and IR analysis on mono-disperse small crystal samples to attempt to quantify surface reactivity. These challenges are ideal for future work, however a new surface modification technique offers promise for this application, and therefore further development of silane coupling procedures will no longer be investigated in favor of this new technique, which will be discussed in Chapter 6.

5.4 References

1. Han, Minghan; Yin, Xiuyan; Jin, Yong. Ind. Eng. Chem. Res. 1999, 38. p. 3172.

2. Takaba, Hiromitsu; Suzuki, Takato; Nakao, Shin-ichi. Fluid Phase Equilibria. 2004, 219. p. 11.

3. Karger, Jorg; Ruthven, Douglas. Diffusion in Zeolites. John Wiley & Sons. New York. P467-508.

4. Tspatsis, M. et.al. Microporous and Mesoporous Materials. 2000, 38. p. 61.

5. Freeman, B.D.; et. al. Macromolecules. 1999, 32. p. 375.

6. Hillock, A. Crosslinkable Polyimide Mixed Matrix Membranes for Natural Gas Purifications. PhD dissertation, Georgia Institute of Technology, 2005. Atlanta, Georgia.

7. Voogd, P.; Scholten, J. Colloids and Surfaces. 1991, 55. p. 163.

8. Muller, U.; Unger, K.K.. Studies in Surface Science and Catalysis. 1988, 39. p. 101.

9. Carrot, P.; Sing, K.. Chemical Industry. 1986, p. 405.

10. Choudhary, V.R.; Srinivasan, K.R.; Singh, A.P. Zeolites. 1990, 10. p. 16.

11. Handreck, G.; Smith, T. Zeolites. 1990, 10. 745.

12. Hedlund, Jonas; et.al. Microporous and Mesoporous Materials. 2005, 78. p. 1.

13. Duval, Jean-Marc. Adsorbent Filled Polymeric Membranes. PhD dissertation, University of Twente, 1993. Enschede, Netherlands.

CHAPTER 6

GRIGNARD TREATED MATERIALS

FOR P-XYLENE PURIFICATION

Recent work in gas mixed matrix membranes has developed successful mixed matrix composites via a pseudo-Grignard reaction that appears to not only solve interfacial delamination issues, but also has lead to successful Maxwell model performance for mixed matrix composites. This chapter will first introduce the technique by reviewing the work by Husain and Shu [1-3], and then develop what modifications must be addressed in the Torlon-Silicalite system in order to implement the procedure. Finally, this chapter will discuss characterization of Grignard treated particles and membranes for use in p-xylene purification.

6.1 Grignard Treatments for Mixed Matrix Materials

6.1.1 Grignard Treatment Motivation

The Grignard techniques were discovered by Shabbir Husain, Shu Shu, and Alexis Hillock in the Koros Research Group at Georgia Institute of Technology while attempting to replace acidic zeolite surface hydroxyls with organophilic methyl groups [1,2,3]. Over the course of this section this work will be reviewed. The initial concept was that by reducing the hydrophillicity of the zeolitic surface, the solvent (NMP)/zeolite interaction and thus the polymer/zeolite interaction would become more favorable. Previous literature has reported methods to attach methyl groups directly to silica surfaces via a silicon-carbon bond [4-6]. The procedure reacts the surface with a chlorinating agent

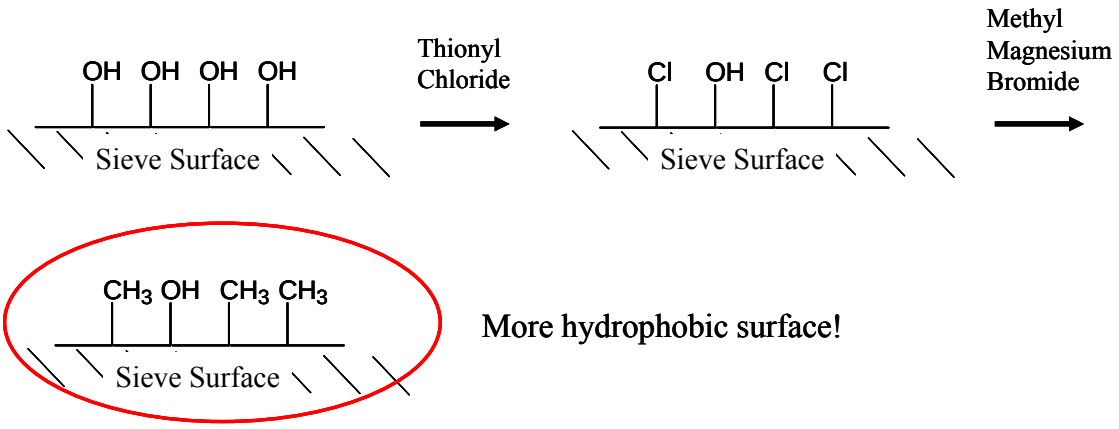

Figure 6.1. Schematic of envisioned hydrophobizing reaction on the zeolite surface. Adapted from [1].

(thionyl chloride for example) followed by reaction with a Grignard agent such as methyl-magnesium bromide. The following surface chemistry was initially proposed [4]:

$$\langle Si\rangle - OH + SOCl_2 \rightarrow \langle Si\rangle - Cl + SO_2 + HCl \tag{6.1}$$

The chlorinated surface is reacted with a Grignard reagent to form the silicon-carbon bond as follows:

$$\langle Si\rangle - Cl + RM \rightarrow \langle Si\rangle - R + MCl \tag{6.2}$$

The silicon-carbon bond is resistant to hydrolysis, and due to the methyl group the surface is rendered more hydrophobic after the treatment. These same steps were envisioned by Husain to occur on a surface by Figure 6.1. From these steps, the basic procedure, as discussed in Chapter 3, and shown here in Figure 6.2, was developed. It was later shown that the above *chemistry is not entirely accurate for this situation*, and de-alumination of the zeolite may be occurring [1]. This hypothesized chemistry will be discussed later in this section.

6.1.2 Grignard Treatment Procedure

The following procedures were developed by Husain [1]. These procedures were

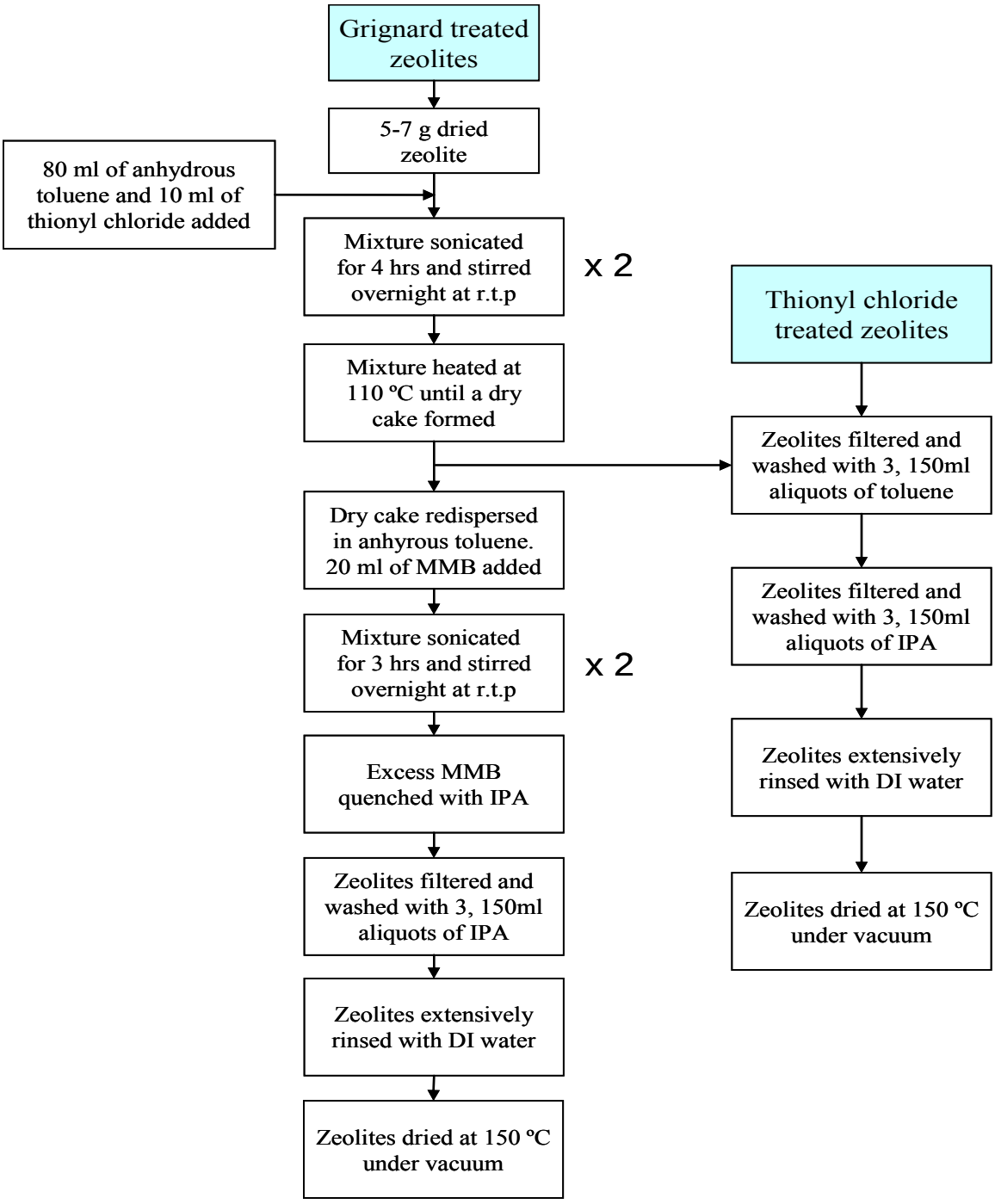

Figure 6.2: Reaction procedure for Grignard and thionyl chloride treated zeolites. Adapted from Husain [1].

utilized to develop gas separation membranes in his work, and will be followed carefully to Grignard treat zeolites for xylene isomer purification. Since the work by Hussian is the basis for Grignard treatments, the procedure text will be repeated exactly.

6.1.2.1 Reaction with Thionyl Chloride—Adapted from Husain [1]

Zeolites to be Grignard treated are dried at 150°C for 24 hours to remove any water. Under anhydrous conditions in a sealed flask, ~4-8 grams of the sieves were sonicated at low intensity in 80 ml of anhydrous toluene and 10 ml of thionyl chloride ($SOCl_2$) for 4 hours in a sonication bath. For each dispersion step, the lowest sonication energy sufficient to disperse the sieve particles was used. The dispersion was allowed to stir overnight with a dry nitrogen sweep at room temperature and then sonicated in a sonication bath for 4 hours. This step was followed by heating at temperatures varying between 90-110°C with stirring until the sieves formed a dry cake. A vacuum was applied on the sieves to remove remaining solvent/reactant.

6.1.2.2 Grignard Reaction—Adapted from Husain [1].

The sieves from the above step were re-dispersed in anhydrous toluene using a 130W sonication horn for a total of 8 minutes.

To the above sieve dispersion, 20 ml of MMB was gradually added with stirring under anhydrous conditions. Thereafter the dispersion was sonicated in the sonication bath for 3 hours. A thin bore needle was used as a vent to prevent pressure build-up within the flask. After sonication, the flask was stirred overnight at room temperature. Sonication in the bath was repeated for 3 hrs. The excess MMB was quenched by slowly adding isopropanol (IPA) while cooling in an ice bath. The sieves were collected using a high pressure filtration setup with 0.2 micron polytetrafluoroethylene (PTFE) or polyvinylidene fluoride (PVDF) filters. The sieves were washed with three aliquots of

150 ml of IPA followed by 200 ml aliquots of DI water until the conductivity of the filtrate reached 40 microSiemens. The sieves were then dried at 150 °C for 24 hours.

To test the effect of thionyl chloride on the de-alumination tendencies, thionyl chloride only treated zeolites were obtained by omitting the Grignard treatment step*. The zeolites were rinsed with anhydrous toluene followed by washing with anhydrous IPA. The zeolites were then dispersed in DI water using sonication and the rinses continued until a low conductivity of the rinse water was obtained. This step was included to remove any aluminum chloride that is believed to be generated during the de-alumination step. This mechanism is discussed in more detail in later in this Chapter. A final exchange with IPA was done with the sieves dispersed by a wrist-shaker and the zeolites were dried in the vacuum over at 150 ºC for 12-24 hours. Figure 6.2 outlines the processing steps carried out during the Grignard treatment.

6.1.3 Grignard Treatment Results for Gas Separation Application

Husain applied the Grignard treatment to two different gas separations, and two different polymer-zeolite systems [1]. Oxygen/Nitrogen separation as well as Carbon Dioxide/Methane separation are common gas separations for evaluating membrane gas separation performance and have important industrial applications [1]. The results show a marked improvement in separation performance in the composite membrane over the neat polymer membrane for each given separation and can be predicted by the Maxwell model discussed in Chapter 2 [1]. It is postulated that the increase in separation performance is due to a change in the particle morphology of the zeolite crystals. Figure

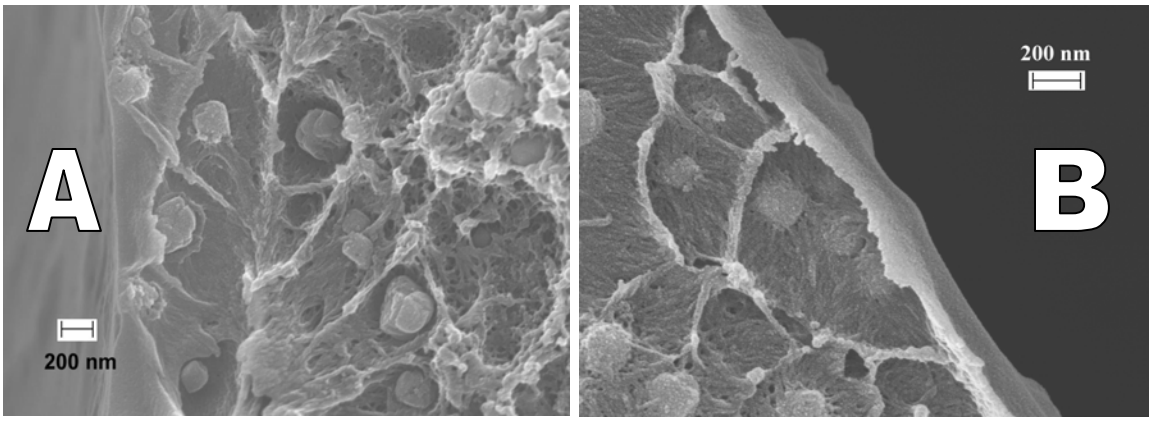

Figure 6.3. Mixed matrix hollow fibers made with non-Grignard treated zeolites (A), and Grignard treated zeolites (B). Composite system is a proprietary sieve (PS) dispersed in Ultem®. Adapted from Husain [1].

6.3 shows SEM's of zeolites embedded in hollow fiber films both before and after Grignard treatments. For the specific crystals used for Husain hollow fiber work, there are distinct differences in permeation properties and in the silicon to alumina ratio. For reasons of confidentiality, the permeation differences will not be discussed here, however it is hypothesized that the silica to alumina ratio can affect the bonding properties of the materials when exposed to the Grignard reagents. In light of achieving Maxwell model results, the next section will attempt to summarize why such an increase could occur.

6.1.3.1 Hypothesized Grignard Particle Treatment Theory

As the previous section defined an improvement caused by Grignard treatment, this section will review current reasoning on why such an effect takes place. The initial motivation for the Grignard process was to hydrophobize the surface via replacing the surface hydroxyls with methyl groups. However, subsequent XPS testing and IR testing revealed no conclusive evidence that methylation had occurred [1-3]. Instead, it was

discovered that after treatment with thionyl chloride some de-alumination takes place [1]. Where aluminum is present in the structure, dealumination with thionyl chloride can occur via a mechanism initially proposed by Fejes [7] for carbonyl chloride (similar in reactivity):

$$\{AlO_2^-\}H^+ + COCl_2 \rightarrow \{AlO_2^-\}C^+Cl_2OH \xrightarrow{-HCL} \{AlO_2^-\}C^+OCl \qquad (6.4)$$

Based on Fejes' postulated reaction pathway, it can be conjectured that thionyl chloride primarily acts to remove aluminum from the zeolite framework leaving behind hydroxyl nests. Next the Grignard reagent is added to the reaction, and deposits magnesium hydroxide onto the surface of the zeolites. The zeolites now have the roughened morphology shown in Figure 6.4, and upon addition to a mixed matrix membrane form successful composites. In addition, Shu has shown that magnesium hydroxide on the surface alone is not sufficient to obtain quality composites, and the roughened surface is required to give quality composites [2-3].

Husain has suggested that the reasons for successful composites are two-fold based on the previous proposed pathway [1]. First, addition of magnesium hydroxide to the zeolite surface increased the solution stability of the particle, and allows for well dispersed mixed matrix dope solutions to be created [1]. This high quality dispersion leads to non-agglomerated zeolites in mixed matrix films, which was identified as a problem in silicalite-Torlon® materials in Chapter 5. Moreover, the surface roughening and presence of the magnesium hydroxide appears to increase the potential of a favorable

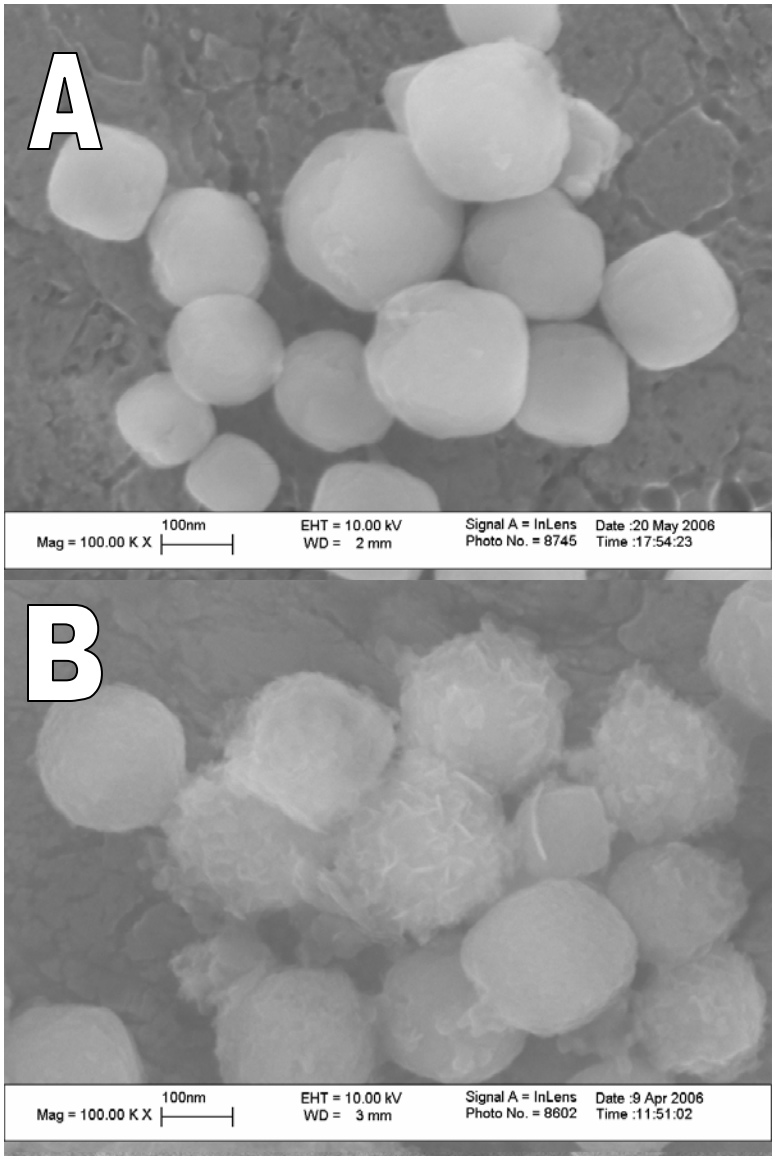

Figure 6.4. SEM's of zeolite 4A after thionyl chloride treatment (A), and after subsequent Grignard treatment (B). Adapted from Husain [1].

interaction between the polymer and the inorganic zeolite by removing the number of acid sites on the zeolite surface [1].

6.2 Optimization of MFI for Grignard Treatment

In the previous section Husain's Grignard treatment was reviewed as a possible solution to interfacial adhesion and solution dispersion problems in mixed matrix membranes. In this section, MFI will be optimized to take advantage of this treatment.

6.2.1 MFI-Grignard Applicability

From previous discussions of MFI's use for p-xylene separations there are two issues that immediately stand out when contemplating Husain's Grignard treatment. The predominant MFI chemistry chosen for p-xylene separation is silicalite due to its organophilicity (and corresponding transport properties), and its' availability in quantity and information. The first Grignard treatment issue that arises from this choice is the lack of any aluminum, other than trace amounts, in the crystal structure. When applied to the Grignard reaction conditions, the proposed pathway, would most likely not occur due to lack of de-alumination, which in turn leads to problems in solution stability and would most likely results in agglomerated crystals as in Figure 5.9. The second issue that arises as a result of lack of aluminum is that a MFI crystal with aluminum in the framework (ZSM-5) is more hydrophilic, and leads to less favorable xylene transport properties. However, this work will seek to solve these issues and provide a method to treat silicalite crystals with Husain's Grignard process by synthesizing a zoned silicalite particle.

6.2.2 Synthesis of Zoned Silicalite Molecular Sieves

In response to the issues above, it is hypothesized that a silicalite particle with only a thin layer of aluminum containing crystalline material on the surface could still perform well as a molecular sieve, while also providing a surface for de-alumination as required by the

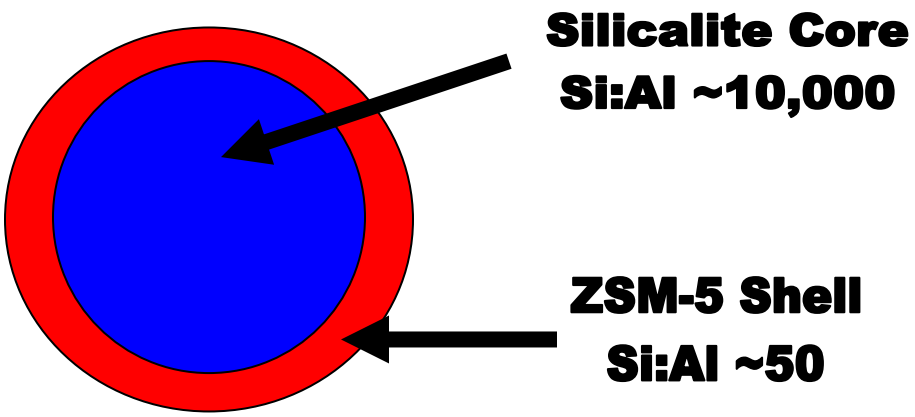

Figure 6.6. A cartoon representation of desired core/shell MFI particle.

Grignard treatment [1]. It is assumed that as long as the porosity of the sample remains un-clogged, and the coating layer is thin, the transport properties will be relatively unchanged. Several authors have synthesized zoned particles, however all located literature has synthesized silicalite regions over ZSM-5 crystals [8-13]. This work seeks to perform the opposite, and synthesize ZSM-5 regions over silicalite crystals. A cartoon of what is desired is shown in Figure 6.6. It is hypothesized that since ZSM-5 and silicalite are both part of the same parent zeolite structure, MFI, that the interface between the two would be seamless. Previous silicalite used in this work has contained only trace amounts of aluminum, with a Si:Al ~10,000. This work will seek to synthesize shells with a Si:Al of 50. This value was chosen based on previous successful Grignard treatments with proprietary materials in Husain's thesis.

6.2.2.1 Modification of BP Provided Crystals.

The simplest path to obtaining an applicable zoned zeolite is to modify the large and small silicalite crystals provide by BP. In order to develop a synthesis procedure several references were examined that involved the reverse synthesis of a ZSM-5 shell on a

silicalite core [8-10]. Synthesis reactants and reactant concentration were determined based on successful core/shell formation, ZSM-5 seed preparation information, and availability of reactants. The silica source was chosen as sodium metasilicate nonahydrate (98% Aldrich), and the aluminum source was selected to be aluminum sulfate octadecahydrate (Aldrich). The molar ratio for the synthesis mixture was set to be 30 Na_2O : 1 Al_2O_3 : 100 SiO_2 : 4000 H_2O. A one gram sample of the small BP silicalite and the large BP silicalite were placed in separate Teflon lined hydrothermal reactors, and approximately 600ml of the reaction mixture was added. The seeded mixture was hydrothermally reacted at 180°C for 16 hours. SEM's of the resulting particles from large particles are shown in Figure 6.7. SEM's of the resulting particles from small particles are shown in Figure 6.8. It can be seen that the particles are very irregular, and of no uniform shape or size. Close examination of the high magnification images in Figure 6.7 shows what appears to be crystal growth directly off the silicalite crystal which results in aggregated and inter-grown structures. It is not clear whether crystal growth is nucleated off the crystal surface only, or if crystal growth can be nucleated either at the seed crystal or in free solution away from the crystal. Regardless, both Figure 6.7 and 6.8 suggest that the new growth completely dominates the material, instead of being a thin layer on existing crystals. This is clearly undesirable. Elemental analysis was performed by Galbraith Laboratories (Knoxville, Tennessee), and is shown in Table 6.1 along with XPS results for the same samples. XRD and Nitrogen adsorption data are available in Appendix E, and show the new composite samples to be MFI crystalline and microporous, with no visible amorphous regions. In retrospect, this method may indeed provide layered silicalite crystals, however it appears that the

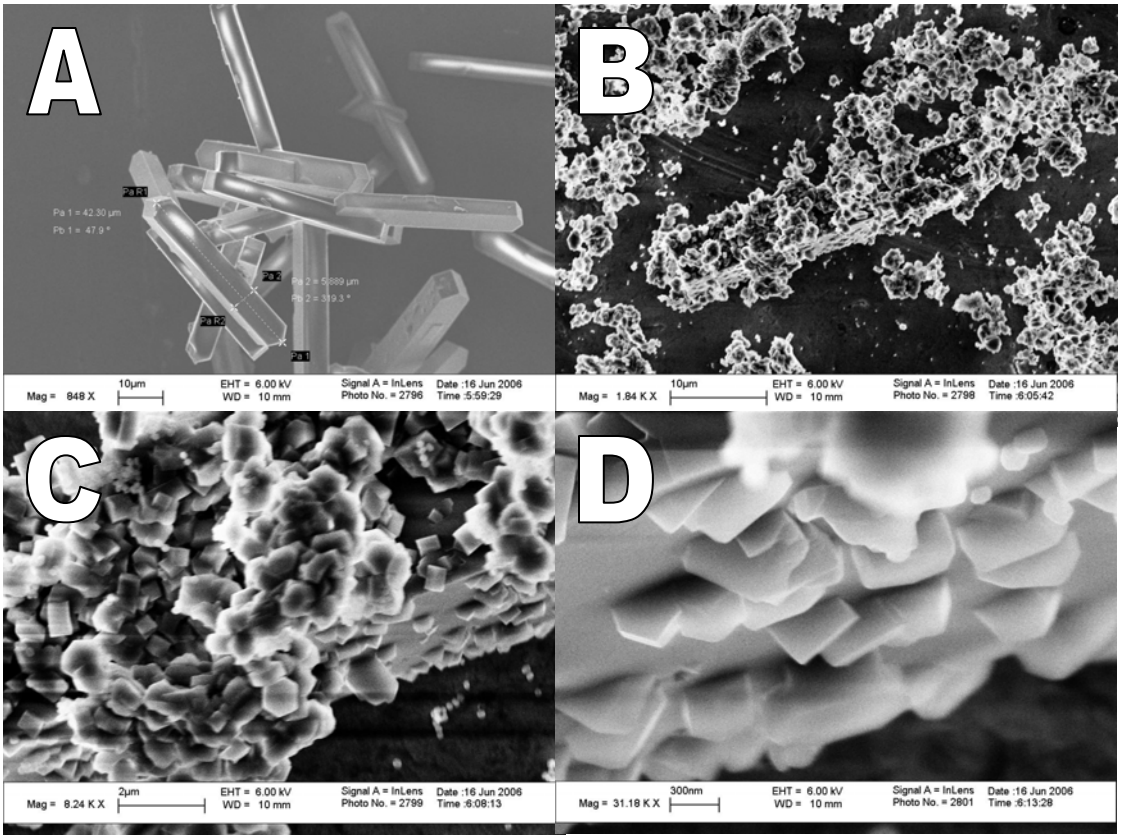

Figure 6.7. SEM's of core/shell modification of large BP silicalite crystals. (A) Large silicalite crystals before modification. (B) Large crystal after modification 1.84KX. (C) 8.24KX. (D) 31.18 KX. It can be seen in higher magnifications that crystals are in intimate contact with the silicalite surface.

reaction temperature was in too high and allowed crystal growth to proceed rapidly. Also, due to the unclear nucleation issue, new crystals may be formed by this method which is undesirable for this application. In conclusion, it may be more feasible to synthesize a core/shell zeolite without the use of seed crystals.

6.2.2.2 Synthesis of Core/Shell Particles Without Seed Crystals

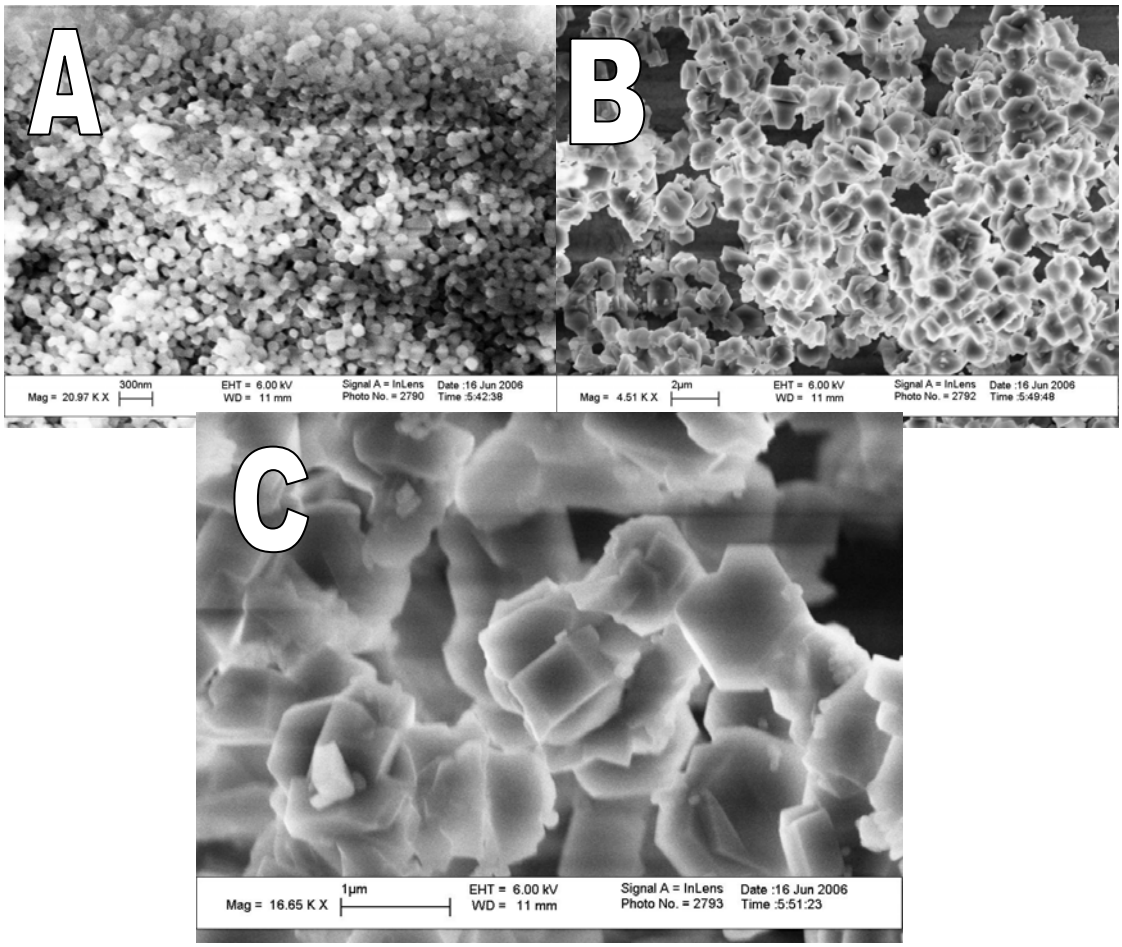

Figure 6.8. SEM's of core/shell modification of small BP silicalite crystals. (A) Small silicalite crystals with no modification. (B) 4.51 KX image of modified crystals. (C) 16.55 KX of modified small crystals.

The second method to synthesize a core/shell particle was to synthesize the particle completely, with no seeding. No literature references could be found that completed this core/shell process in this order. Therefore the first attempt was to reverse a zoned crystal synthesis illustrated by Hedlund [8]. For this synthesis the silica source was TEOS (98% Aldrich), the aluminum source was Aluminum Isopropylate (Aldrich), the Sodium source was Sodium Hydroxide, and the structure directing agent was TPAOH (Aldrich). Initially the reactant molar concentration was adjusted to 5 TPAOH : 25 SiO_2 : 480 H_2O :

Table 6.1. XPS and ICP Results for BP Silicalite Core/Shell Synthesis.

Sample	ICP			XPS		
	Si wt%	Al wt%	Si:Al	Si mol %	Al mol %	Si:Al
Large BP Silicalite	45%	0%	1396	24%	0.0%	>1000
Large BP Zoned Silicalite	39%	3%	15	23%	1.2%	19
Small BP Silicalite	44%	0%	1131	24%	0.0%	>1000
Small BP Zoned Silicalite	39%	3%	14	22%	1.3%	17

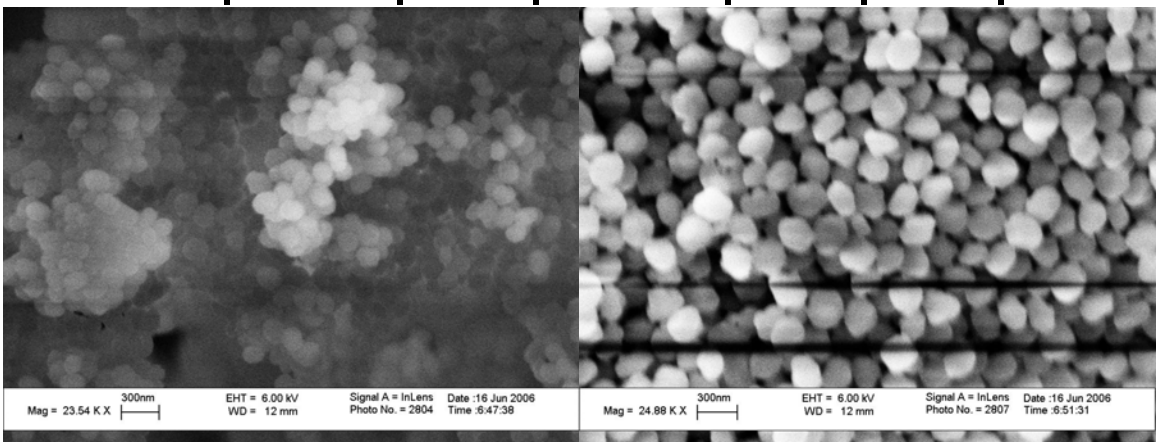

Figure 6.9. Synthesis of RWC004 core/shell zeolites. (A) Synthesis results after 24 hours, 100°C. (B) Synthesis results after addition 16 hours, 100°C, and addition of aluminum reagents. Note: Magnification is slightly different in each micrograph, and size comparison should be done with the provided scale.

100 EtOH . Approximately 600ml of the solution was hydrothermally reacted in a Teflon lined vessel at 100°C for 24 hours to form the silicalite cores. Next, the vessel is allowed to cool, and the aluminum and sodium sources are added such that the final molar composition of the reaction mixture is 5 TPAOH : 0.25 AL_2O_3 : 25 SiO_2 : 480 H_2O : 100 EtOH : 0.1 Na_2O. The solution is re-heated to 100°C and hydrothermally reacted for an addition 16 hours to continue crystal growth with aluminum in the framework. Samples were calcined in air at 500°C to remove the structure directing agent. *This synthesis*

Table 6.2. XPS and ICP Results for RWC004 Synthesis

Sample	ICP			XPS		
	Si wt%	Al wt%	Si:Al	Si mol %	Al mol %	Si:Al
RWC004 24hr No Al	43%	0%	1327	26%	0.0%	>1000
RWC004 24hr +16 hr, Al	43%	1%	83	24%	0.7%	34

was coined sample RWC004. Figure 6.9 shows the synthesis results after the first 24 hours, and after the final 16 hours. It appears that there is a slight change in particle size, growing from ~200nm to ~250 nm. It appears that initially the samples are agglomerated, and after the second synthesis the samples appear to be more dispersed. Table 6.2 shows XPS and elemental analysis data for the new synthesis, and it is clear that there is no aluminum in the crystals after the first 24hours, but there is aluminum in the framework after the final hydrothermal step. An important observation is that of the silicon to aluminum ratio of the particle verses that of the surface only. The elemental analysis shown in Table 6.2 (ICP) yields the silicon to aluminum ratio for the entire particle: silicalite core and the aluminum containing shell. The XPS data only describes the outer surface of the particle (Top 10-20 Angstroms), and yields no information about the particle core. Therefore, it is expected that this particle silicon to aluminum ratio should be higher than the surface in a zoned material, and that is the case shown in Table 6.2. In fact, if the suggested size difference of 50 nm in diameter is used to approximate the change in particle size in the final 16 hours of synthesis is used in conjunction with the total particle silicon to aluminum ratio, a simple volumetric balance can predict a silicon to aluminum ration of ~40, which is very close to the XPS surface silicon to aluminum ratio of 34.

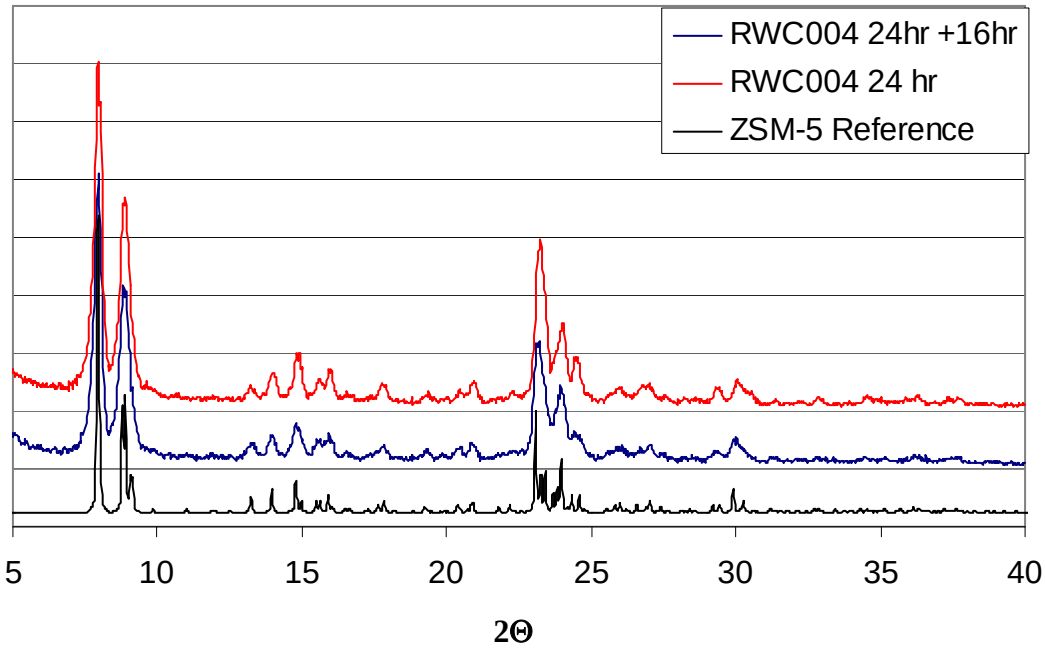

Figure 6.10. XRD patterns for RWC004 during each synthesis step. ZSM-5 reference pattern is given for comparison [14].

In addition to the chemical composition, the crystallinity and porosity of the RWC004 sample were analyzed. Figure 6.10 shows the XRD for the RWC004 sample at 24 hours, and after the additional 16 hours with aluminum reagents (both samples are calcined). Figure 6.11 shows the nitrogen isotherm for the RWC004 sample, which has a BET surface area of ~300 m^2/g, which is very similar to BP silicalites of similar size. .Given the porosity, crystallinity, and chemical makeup of the RWC004 synthesis, it appears that a core/shell particle with a silicalite core and a ZSM-5 type shell has been synthesized. This particle now meets the surface chemistry requirements for Grignard treatment, and should still maintain transport properties for p-xylene transport.

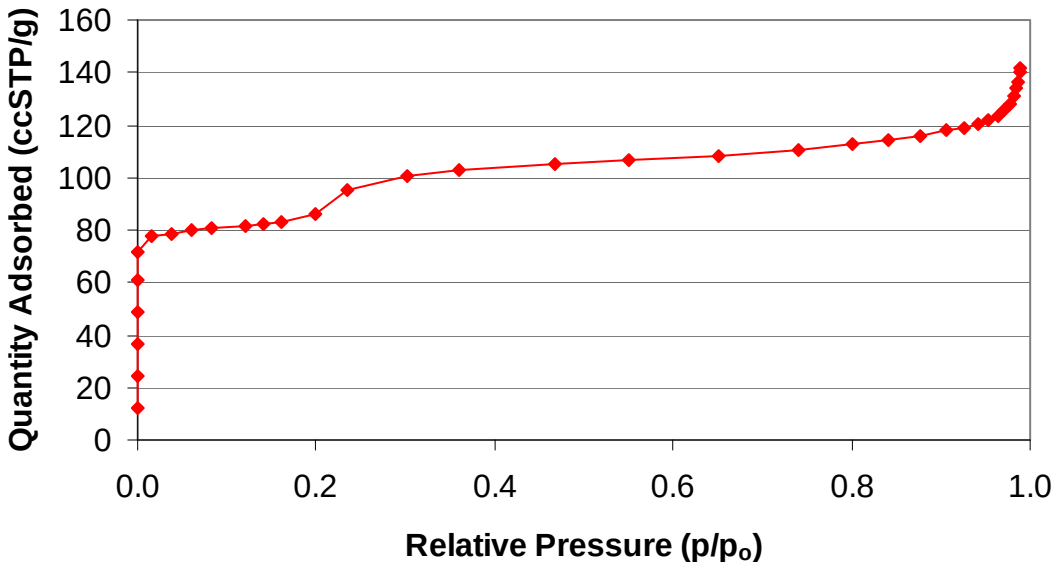

Figure 6.11. Nitrogen adsorption isotherm for RWC004.

6.3 Grignard Treatment of RWC004 for Mixed Matrix Membranes

6.3.1 *Grignard Treatment of RWC004*

RWC004 particles were treated via the Grignard procedures reviewed in Section 6.1. The resulting particles can be seen in Figure 6.12, compared with the original untreated RWC004 particles. The treated samples exhibits an increase in surface roughness similar to that shown by Husain and Shu [1-3], although it appears that it may not be to the same degree as in Figure 6.4. Husain and Shu did show differences in the amount of surface roughening which could have been attributed to either the silicon to aluminum or the amount of available surface area, both pertaining to the hypothesis that de-alumination is connected to surface roughing.. It is unclear at this time as to exactly why these differences occur; nevertheless the effect does seem to be expressed in the RWC004 with a similar morphology. This is further indicative of aluminum present on the structure,

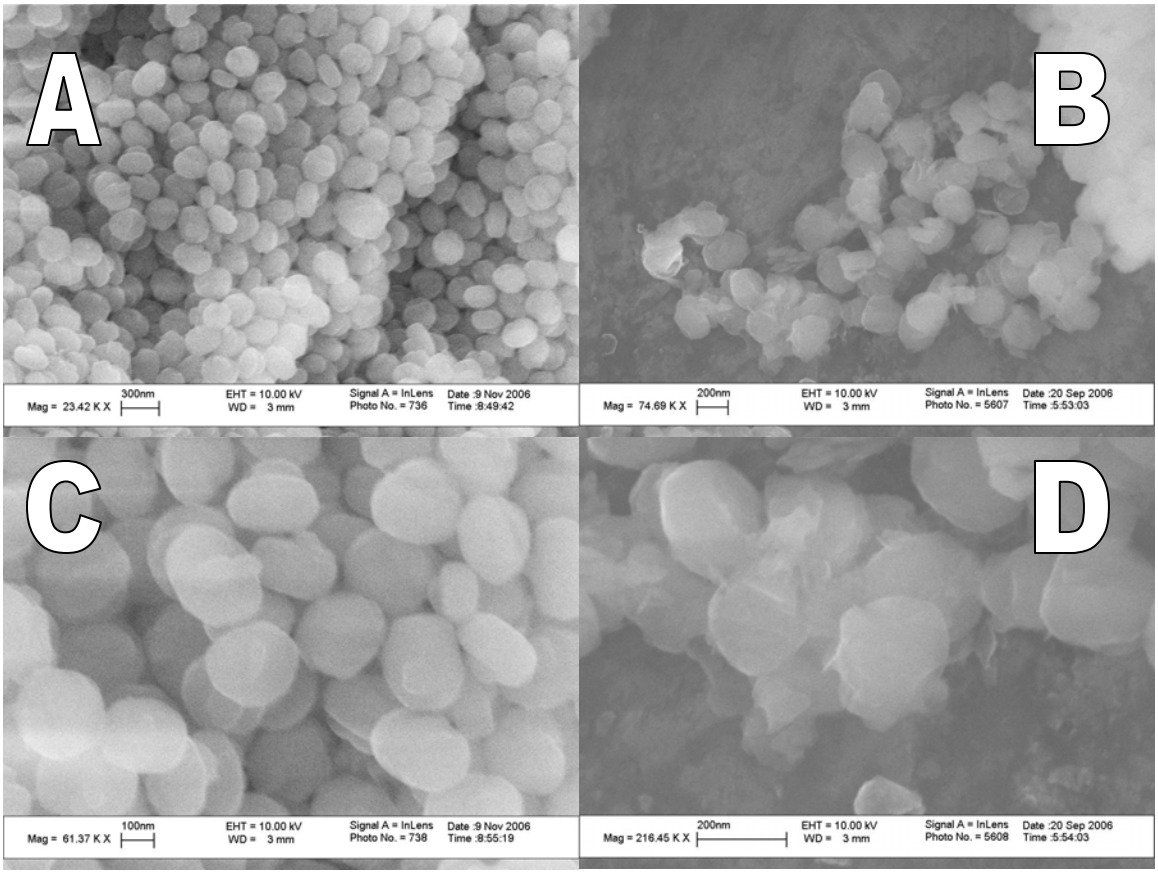

Figure 6.12. Comparison of RWC004 particles before and after Grignard treatment. (A) Untreated RWC004 particles—low magnification. (B) Grignard treated RWC004—low magnification. (C) Untreated RWC004 particles—high magnification. (D) Grignard treated RWC004—high magnification.

due to the current hypothesize that deposition of magnesium hydroxide is linked to the de-alumination and subsequent formation of hydroxyl nests [1].

In addition to SEM's nitrogen adsorption was also used to analyze particles both before and after the Grignard treatment. The results are shown in Figure 6.13, and compared to that of a non-treated sample of the RWC004 sieve. Unlike Husain's results, there is virtually no change in the porosity of the material. The BET surface area for the Grignard treated and untreated RWC004 samples are both ~304 m^2/g. However, there are slight differences in the shape of the nitrogen adsorption isotherm, particularly in the

regions just beyond micropore filling, and the onset of multilayer condensation. It is reasonable to suggest based on Husain's results, and SEM results in Figure 6.12 that the surface of the treated sieves is no doubt changed. This change in surface composition (most likely magnesium hydroxide) will affect how multilayer condensation will begin [15], and could very easily account for the slight differences seen in Figure 6.13. Another difference could be that if the particles maintain a true shell and core fashion, de-alumination can only take place in the outer levels of the particle, maintaining the internal porosity. This is unlike the case presented by Husain in that de-alumination can take place throughout the particle, and is only limited by access to thionyl chloride. In other words, only a finite amount of de-alumination can take place in a shell-core particle, and only in the shell layer. Moreover, depending on how the aluminum atoms are distributed through the shell layer will affect how that process may occur. High concentrations of aluminum at the surface could "expose" aluminum within the framework to addition de-alumination agent. But in contrast, low concentration at the surface could limit de-alumination to only those areas. Future work could attempt to elucidate how aluminum is distributed through the shell layer by breaking the reaction into steps and analyzing each step sequentially via XPS for surface composition.

6.3.2 Mixed Matrix Membrane with Grignard Treated Core/Shell RWC004

The above Grignard treated particles were used to form mixed matrix membranes via procedures developed in Chapter's 3 and 4. The resulting films were of a translucent nature nearly identical to those in Figure 5.7C. Figure 6.14 shows SEM's of membrane cross-section. The micrographs show two distinct improvements over the silanated cases

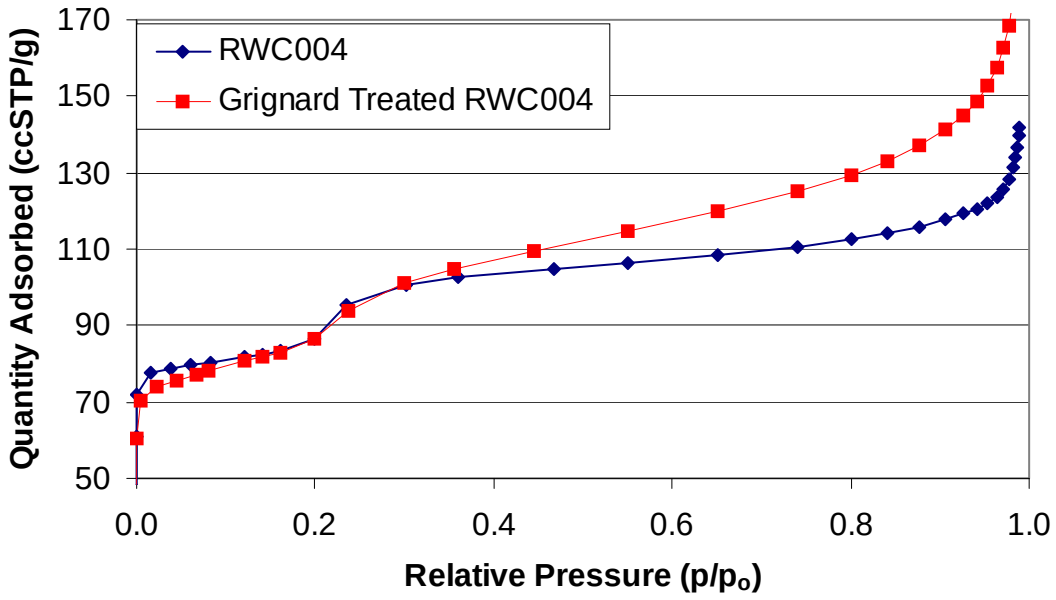

Figure 6.13. Nitrogen adsorption analysis of Grignard treated RWC004. BET surface area of both samples ~304 m^2/g.

in Chapter 5. First, it seems the large particle agglomerates no longer exist, and that particles are more evenly spread in either single crystals or two and three crystal clumps. Secondly, it seems that the polymer has much more intimate contact with the sieve surface. Both of these characteristics we observed by Grignard treated films and the respective reasons for such improvement were discussed in Section 6.1 The first reason for improvement suggested was the deposition of magnesium hydroxide that eventually leads to particles of even dispersion throughout the polymer [1-3]. It appears that based on the SEM evidence of morphology change in Figure 6.12, and the excellent random dispersion in Figure 6.14 that this conclusion can be applied to this system as well. The second reason for improvement attributed the enhanced surface adhesion by roughing the surface and reducing the hydrophillicity of the surface by de-alumination and hence removal of the more acidic and hydrophilic acid sites. It is unclear if this step in of itself would have substantially benefited the silicalite/Torlon® system due to the pre-existing

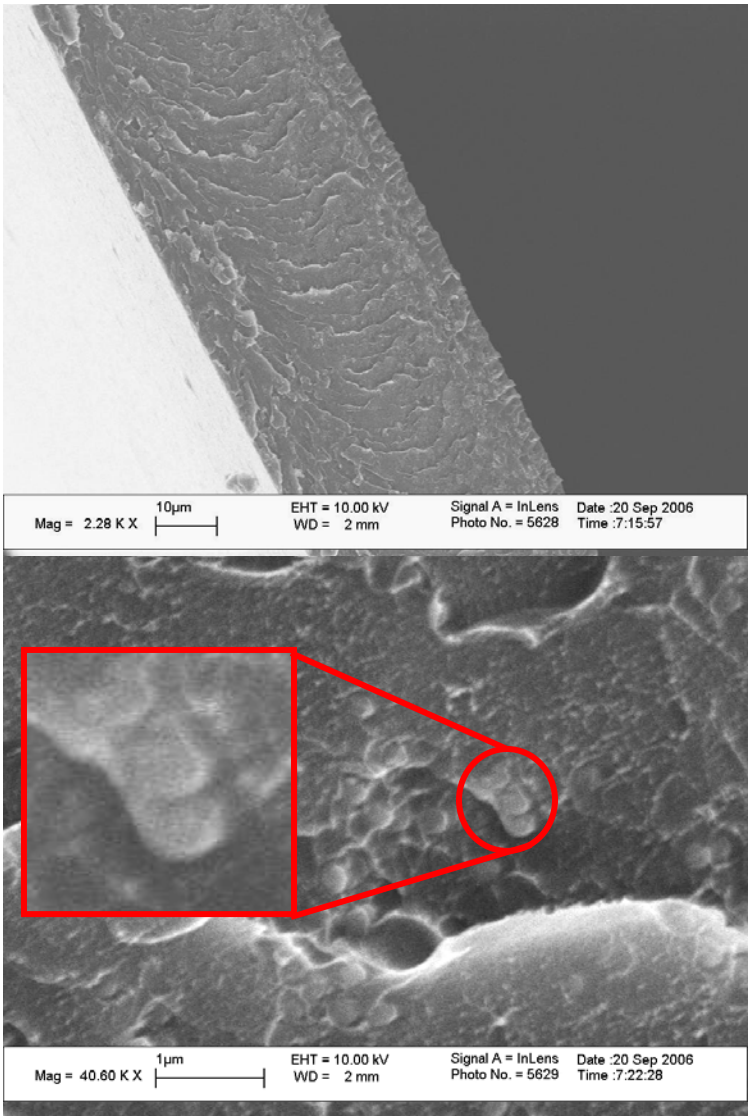

Figure 6.14. SEM's of Torlon® Grignard treated mixed matrix films. There are no large aggregate regions as in silanated samples, and samples seem to be dispersed in single crystals with decent polymer adhesion.

hydrophobic nature of the silicalite surface. It is difficult to argue against the dispersion advantages, given the grossly agglomerated aggregates in Figure 5.9, and of which are not apparent in Figure 6.14. It would be interesting for future work to develop Grignard treated particles of two distinctly different sizes, and compare the morphological and pervaporative mixed matrix results.

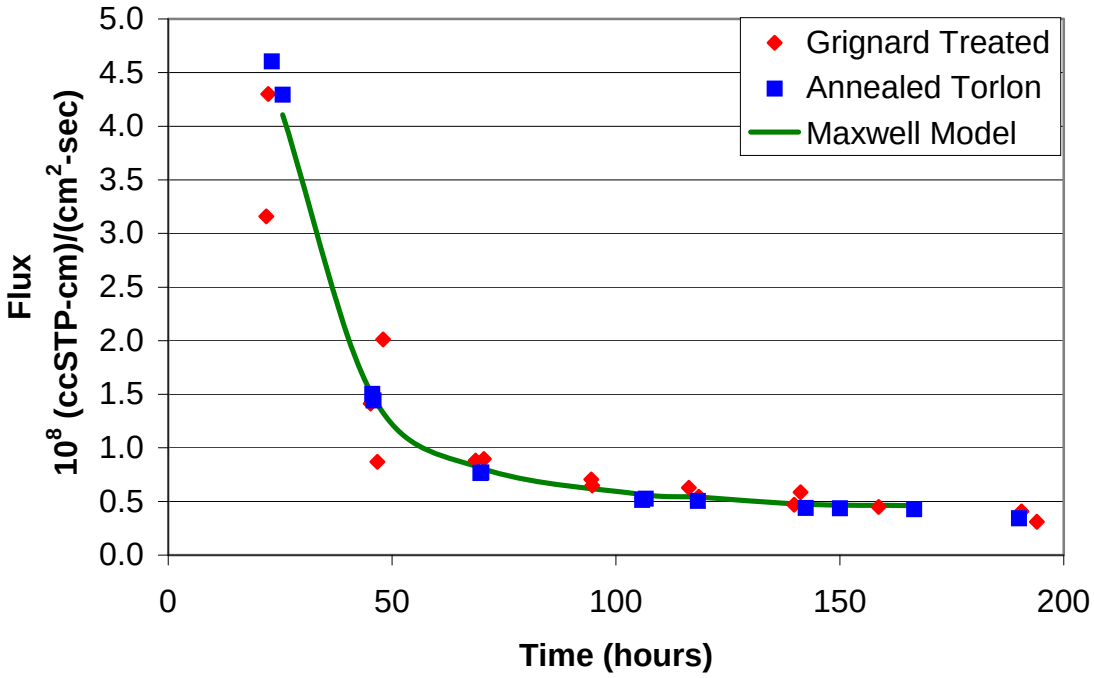

Figure 6.15. Total flux results for Grignard treated Torlon ® mixed matrix membranes at 10% loading. Grignard treated membranes (Red data points), are compared to annealed Torlon films (Blue data points) and the predicted Maxwell results (Green line).

The Grignard treated mixed matrix films were also tested for xylene isomer purification via methods established in Chapter's 3 and 5. The results are shown in Figure 6.15 and compared to the neat polymer films of Chapter 4. It can been seen that the Grignard treated films behave in a similar manner to annealed neat Torlon® films with respect to total membrane flux. However, it is difficult to ascertain any differences in the two materials, as the variance in the data seems to overlap. In addition, it appears that a Maxwell model prediction for total flux of a successful mixed matrix composite also falls within the variance when using total flux as the metric. However, if the final permeabilities (after 180 hours) of the individual para-xylene *isomers* are compared against annealed samples it is obvious there is definitely a change in the system. Figure 6.16 shows the permeability and selectivity of both neat and Grignard treated Torlon®

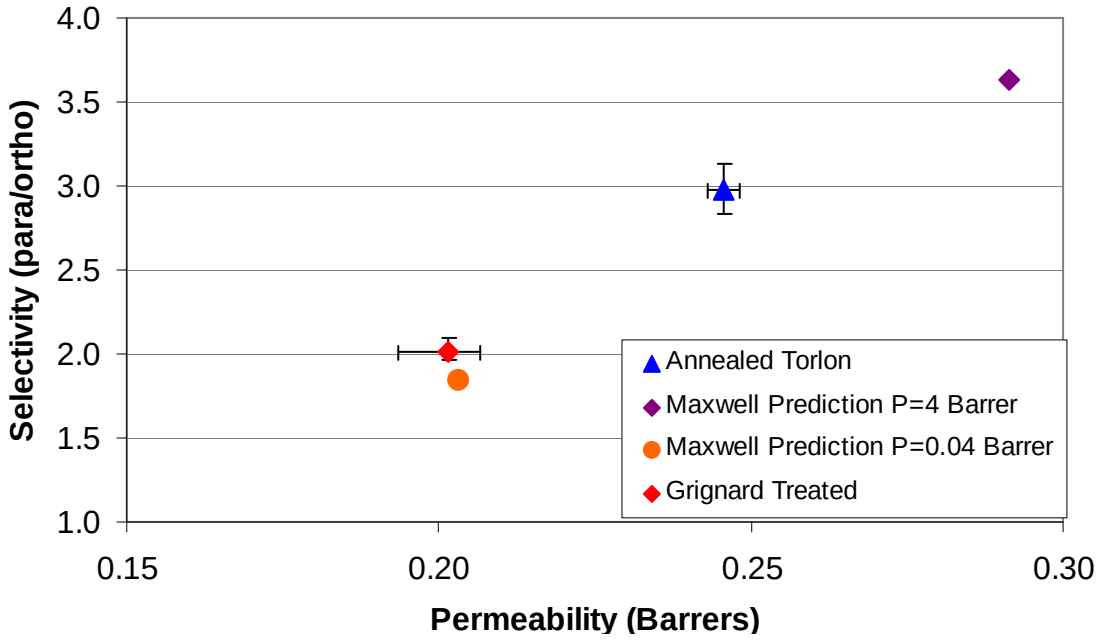

Figure 6.16. A comparison of the permeability and selectivity of annealed Torlon and Grignard treated mixed matrix membranes (Blue and Red data points, respectively). Maxwell model predictions for nominal para-xylene transport, and single file diffusion limited by ortho-xylene are shown as purple and orange data points, respectively. Operating temperature of 200°C.

films. It can be seen that the permeability of the para isomers has decreased by 20%, instead of increasing toward the Maxwell prediction. This is a unique result, in that most defects in mixed matrix composites result in delamination and a corresponding increase in permeability. Reductions in permeability are usually associated with plugged sieves and unimproved selectivities; however this case is accompanied by a reduction in selectivity. Selectivity reductions are usually associated with poor surface adhesion and increased permeability, but this cannot be the case with Grignard treated samples due to the permeability decrease. Therefore, these results suggest good adhesion consistent with the permeability decrease, but they also demand an answer to why the selectivity decreases. Nitrogen adsorption data (Figure 6.13) suggest that there is no apparent blockage in the pore structure after the Grignard treatment, and there is no immediately

Table 6.3. Permeation and Selectivity Values for Grignard Treated Mixed Matrix Membranes (MMX).

Membrane	Membrane Results		Zeolite Modeling Properties	
	P_{px} (Barrer)	$\alpha_{p/o}$	P_{px} (Barrer)	$\alpha_{p/o}$
Annealed Torlon	0.25	2.98		
Grignard Treated MMX	0.20	2.01		
Initial Maxwell Model Prediction	0.29	3.64	4	400
Corrected Maxwell Model Prediction	0.20	2.15	0.01	0.1

obvious reason to clog the zeolite pore in mixed matrix formation. This leads to the conclusion that the material may suffer a clogging issue that is inherent to the xylene isomer system.

Several authors have reported that the MFI structure in a binary system can "flex" due to the presence of the para-xylene isomer and will allow the less compact ortho-xylene molecules to enter the channels at a larger rate than in a pure ortho-xylene system. Although this may contribute somewhat to the negative result, it is believed that this effect is more pronounced with the para-xylene molecules adsorbed into the straight channels of the zeolite, which occurs at more moderate temperatures (< 100°C) [16]. However, due to the pore structure in the MFI structure, there is some concern about "single-file-diffusion" within the crystals. Such a process could ultimately lead to the permeation within the crystals being slowed by the bulkier ortho isomer. Literature has shown that above ~100°C the channels become unfavorable adsorption sites and therefore only the intersections of the straight and sinusoidal channels will be occupied [16]. The isotherms of this effect have been shown in Figure 5.1, and an illustration can be seen in Figure 6.17. Further examination of the isotherms reveals that ortho-xylene actually achieves a higher loading at 130°C. At these high temperatures, it appears that

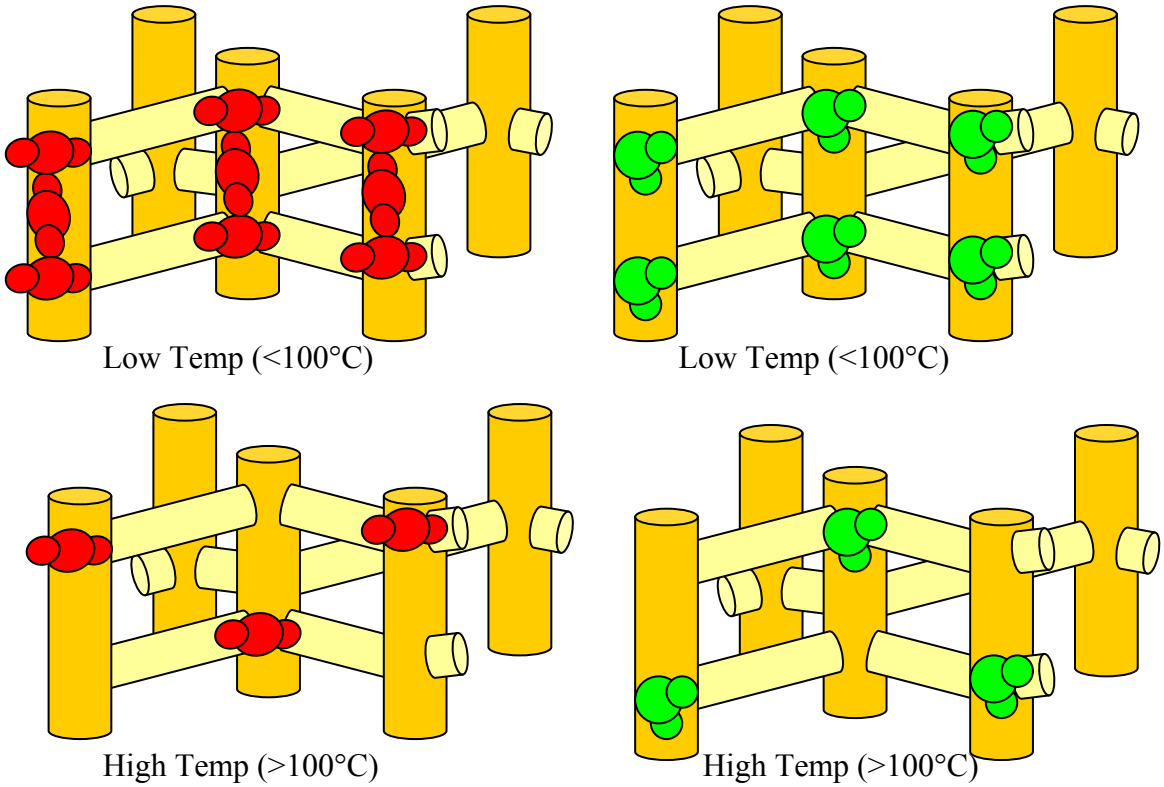

Figure 6.17. Illustration of para and ortho isomer sorption in silicalite pore structure. At low temperatures (<100°C) para xylene (red) has access to the straight channels of the MFI network (Saturation ~8 molecules/cell) while ortho (green) can only adsorb into the straight and sinusoidal channel intersection (Saturation ~4molecules per cell). At higher temperatures, (>100°C) para xylene no longer has access to the straight channels, and is now forced to adsorb only into the channel intersection. Ortho xylene is also only able to adsorb into the channel intersection at high temperatures. As the temperature is increased, the molecules have more motion, and sorption favors the more compact ortho isomer. Illustration conceived from Figure 5.1 and discussion by Tsapatsis [16].

ortho xylene becomes the favored molecule for adsorption, possibly due to its shorter, "stubbier," nature, which could lead to more forgiving entropic effects once inside the channel intersection. Given the fact that ortho-xylene permeates through this system at least two orders of magnitude slower than para-xylene, and that at higher temperatures ortho-xylene may be the favored adsorbate, it is conceivable that at a certain loading of ortho-xylene the crystals could become unfavorable for para-xylene separation, and slightly selective for the ortho-xylene isomer. It is difficult to predict how the transport

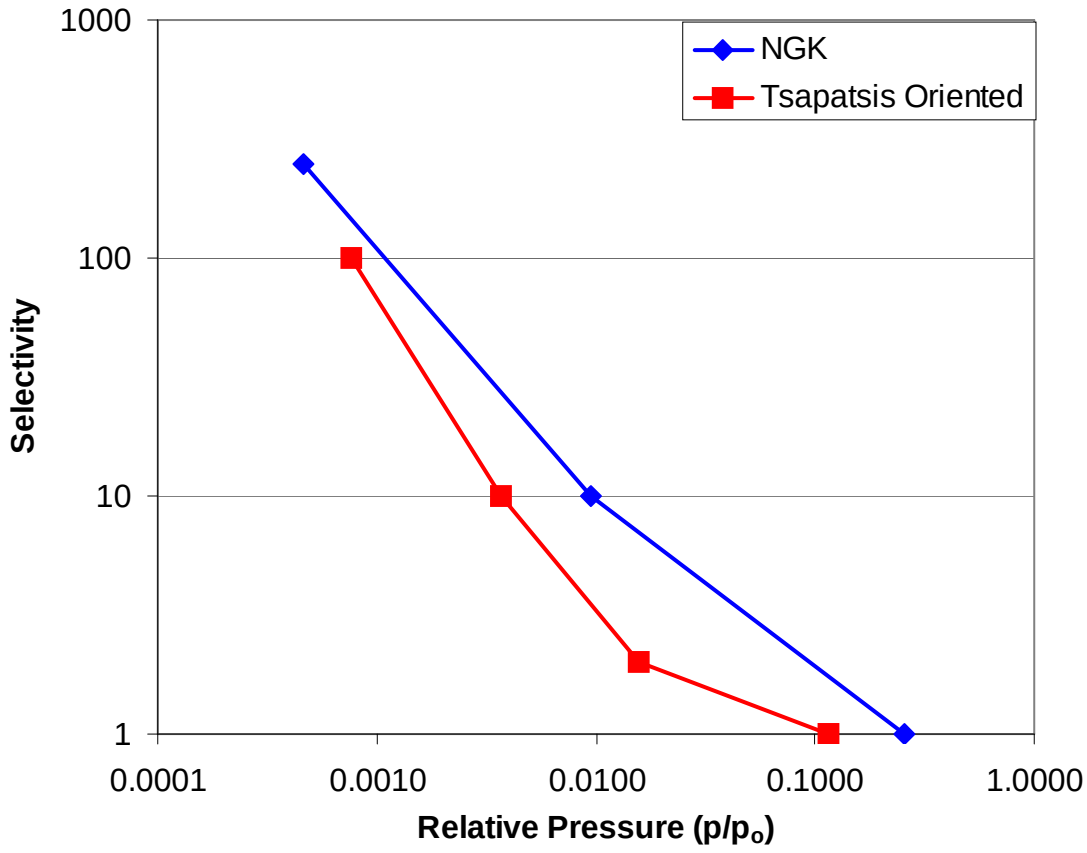

Figure 6.18. Selectivity results for NGK [17], and Tsapatsis [18] zeolite membranes. Attractive selectivities are achieved for para-xylene over the ortho isomer, however these results occur at very low relative pressure. $p_{px} \approx p_{ox}$ in all experiments.

properties of material will behave given the lack of multi-component sorption and diffusivity data. However, from using the sorption data in Figure 5.1, the diffusivity of the slower ortho-xylene molecule, and the same Arrhenius calculations used in Section 5.1.1, a permeability preference for the ortho-xylene molecule on the order of 14:1 can be predicted at 200°C (See Appendix G for Calculation). Using this result and the limiting diffusivity of the ortho-xylene molecule, a Maxwell prediction of a composite membrane can be estimated, and this result is shown in Figure 6.16 as the orange data point. These

results seem to agree with the observed permeability and selectivity of the Grignard treated materials.

If popular xylene-silicalite literature is further reviewed in light of the preceding argument, an even more interesting conclusion can be made. In Figure 6.18 results from NGK Insulators [17], and Tsapatsis [18], are shown, along with their operating relative pressures, and selectivities. In both papers, the feed partial pressure of each isomer was fixed, and the temperature changed, thus changing the relative pressure. It can be seen from all sources, that any operation of these zeolite membrane over ~0.1 p/p_o results in a selectivity of 1 for the para-ortho isomers. In fact, all of the extremely attractive para-xylene separation data at 200°C is obtained at relative pressures of ~0.0005 p/p_o. This result is very disturbing in that it implies that in order to take advantage of this particular zeolite separation, and operate at high temperature, the system needs to operate at very low partial pressures. At the higher relative pressure, and higher operating temperatures, ortho-xylene preferentially adsorbs and restricts para-xylene from taking advantage of diffusion selectivity. NGK has completed work with binary xylene transport above 200°C, and in the same extremely low relative pressure ranges, and a definite maximum is seen in the flux of both para-xylene permeance and separation factor at ~200°C [17]. This is only possible if the sorption of ortho-xylene in the zeolite overcomes the advantages of the diffusion of the smaller para-xylene molecule at the higher temperatures.

In light of these results, it is the opinion of this author that the MFI system is not well suited to perform under these conditions. It would be interesting to lower the operating temperature of the membrane, to approach the MFI "flex" point, or rather when the MFI channels begin to become favorable for adsorption, and re-examine the mixed matrix system as a function of partial pressure, and determine if there is indeed a point at which selectivity falls off. However this is a difficult experiment to conceive due to the low flux of xylene at 200°C, and undoubtedly lower flux at lower temperatures. This creates sampling problems, and reliability in selectivity and permeability measurements. Therefore to progress with mixed matrix separation of xylene isomers, it is suggested that other possible sieves be investigated such as FAU (Zeolite X and Y; 7.4Å), MEL (ZSM-11; 5.4 Å) or LTA (5A, 5 Å). All of these structures can be seen in Figure 6.19. FAU has a pore size that should not discriminate between the isomers at temperatures, but could increased the permeability in a mixed matrix film and maintain polymer selectivity values. MEL could be a discriminating structure, as well as the 5A Chabazite. The MEL structure could suffer from similar sorption effects as MFI, but the 5A structure has open cages that could alleviate sorption problems. Unfortunately the 5A pore window is slightly smaller than the accepted critical diameter of para-xylene, and therefore diffusion into the zeolite will be very slow and limit application. It could possibly be worthwhile to investigate the creation of a new zeolite, with a more chabazite like structure, with an open cage region, controlled by pore windows of ~6 Å.

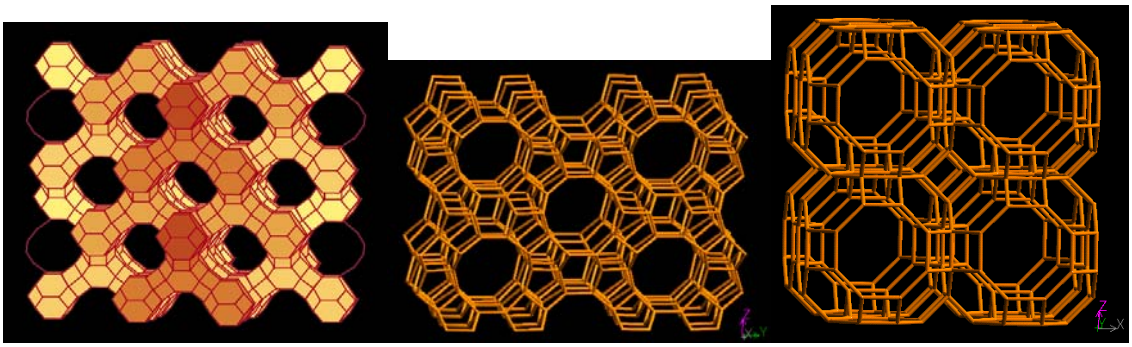

Figure 6.19. Representative structures of FAU, MEL, and LTA from Left to Right. [19].

6.4 References

1. Hussain, S. Mixed Matrix Dual Layer Hollow Fiber Membranes for Natural Gas Separation. PhD dissertation, Georgia Institute of Technology, 2006. Atlanta, Georgia.

2. Husain, S; Shu, S; Koros, W.J. Journal of Physical Chemistry, In Press.

3. Husain, S; Shu, S; Koros, W.J. Industrial and Engineering Chemical Resources. In press.

4. Tao, T. and Maciel, G.E. Journal of the American Chemical Society, 2000. 122, 13. p. 3118-3126.

5. Bansai, A.; Li, X.; Lauermann, I.; Lewis, N.S.; Yi, S.I., and Weinberg, W.H. Journal of the American Chemical Society. 1996, 118, 30. p. 7225-7226.

6. Bansai, A.; Li, X.; Lewis, N.S.; Yi, S.I., and Weinberg. Journal of Physical Chemistry B, 2001, 105, 42. p. 10266-10277.

7. Fejes, P.; Kiriesi, I.; Hannus, I.; Kiss, A.; and Schobel, G. Reaction Kinetics and Catalysis Letters, 1980, 14,4. p. 481-488.

8. Qinghua, Li; Wang, Z;, Hedlund, J; Creaser, D.; Zhang, H. Zou, X., and Bons, A. Microporous and Mesoporous Materials, 2005, 78. p. 1-10.

9. Miyamoto, M.; Kamei, T.; Nishiyama, N., Egashira, Y. and Ueyama, K. Advanced Materials, 2005, 17. p. 1985-1988.

10. Weber, R.W.; Fletcher, J.C.Q; Moller, K.P.; O'Conner, C.T. Microporous Mateirals, 1996, 7. p. 15-25.

11. Van Vu, D.; Miyamoto, M.; Nishiyama, N.; Egashira, Y.; Ueyama, K. Journal of Catalysis, 2006, 243. p 389-394.

12. Naderi, N.; Sharifi-Sanjani, N.; Khayyat-Naderi, B.; and Faridi-Majidi, R. Journal of Applied Polymer Science, 2006, 99. p. 2943-2950.

13. Lee, C.S.; Park, T.J.; Lee, W.Y. Applied Catalysis A. 1993, 96. p. 151-161.

14. van Koningsveld, H., Jansen, J.C. and van Bekkum, H. Zeolites, 1990, 10. p. 235-242. Via the *Database of Zeolite Structures*. http://www.iza-structure.org/databases/.

15. Brunauer, S.; Emmett, P.H.; and Teller, E., J. Am. Chem. Soc. 1938, 309. p. 60.

16. Xomeritakis, G.; Nair, S.; Tsapatsis, M. Microporous and Mesoporous Materials, 2000, 38. p. 61-73.

17. Sakai, H.; Tomita, T.; Takahashi, T. Separation and Purification Technology, 2005, 25. p. 297-306.

18. Lai, Z.; Tsapatsis, M.; Nicolich, J. Advanced Functional Materials, 2004, 14. p. 716.

19. *Database of Zeolite Structures*. http://www.iza-structure.org/databases/.

CHAPTER 7

CONCLUSIONS AND RECOMMENDATIONS

7.1 Summary and Conclusions

This work represents one of the earliest attempts to apply mixed matrix technology to pervaporation of xylene isomers. All of the objectives outlined in Chapter 1 were addressed and the following conclusions can be made.

7.1.1 Polymer Characterization

Torlon® polyamide-imide has unique properties that are useful as a pervaporation membrane for para-xylene purification at high temperatures. As a result of this work, the following conclusions about Torlon® 4000T can be made.

- The resulting permeability and selectivity over the ortho and meta isomers for a Torlon® 4000T dense film are 0.25 Barrer, ~3.0, and ~2.0, respectively.
- During formation of Torlon® membranes, an annealing step to 300°C was introduced that removes essentially all of the remaining NMP solvent from the dense film. This step may not be required for a hollow fiber application as solvent exchange and low temperature heating over several days may achieve a similar result. This is key, as maintenance of asymmetric morphology will be compromised by excessive time above T_g (280°C).
- Pervaporation of an a representative industrial feed (30% para, 30% meta, 30% ortho, 10% ethyl benzene) at 200°C has revealed a "permeability crash" that appears to be an accelerated conditioning of the free volume distribution in the

Torlon® membrane. This conditioning effect is not observed with heat alone, and could possibly be due to enhanced mobility of the Torlon® chains in the presence of the interacting aromatic penetrants.

7.1.2 Zeolite Characterization

A MFI zeolite was selected for this mixed matrix application based on the wealth of knowledge about MFI and the well established application of MFI with xylene isomers. The high silica form of MFI, silicalite, was investigated and the following conclusions can be made.

- The silicalite surface, although free of the more acidic alumina hydroxyls, is not hydrophobic enough to achieve a quality interface without surface modification.
- When considering the para-isomer alone, silicalite appears to have attractive transport permeabilities at 200° (4 Barrers).
- Literature values at high temperature and low relative pressure suggest para to ortho selectivities at approximately two orders of magnitude.
- Gas adsorption at 77K has shown that zeolites used in this work are free of mesopores and should behave as normal molecular sieves in mixed matrix applications.

7.1.3 Polymer/Sieve Engineering

Torlon® 4000T and various silicalite samples were prepared by previously developed procedures [1] to form mixed matrix composites. Based on mixed matrix testing, the following conclusions can be made.

- Treating silicalite with silane coupling agents under previously developed [1] mild reaction conditions does not clog the internal silicalite pore structure, but also does not adequately tether the surface to Torlon® for use as a successful membrane composite. More aggressive reaction conditions may be needed, but may clog the internal pore structure.
- Grignard techniques developed by Husain and Shu [2, 3, 4] show promise for mixed matrix materials but require aluminum in the zeolite framework.
- A "zoned" zeolite particle was synthesized that appears to be a silicalite core with a thin ZSM-5 type shell with a Si:Al ratio of ~35. This particle is hypothesized to maintain its preferential para-xylene properties with a hydrophobic core, but apply to the Grignard procedures with its more acidic surface.
- Grignard techniques applied to the above zoned particle appear to provide improved particle dispersion within the polymer as compared to the silanated samples, as well as improved interfacial properties.
- Grignard prepared mixed matrix membranes exhibit a reduction in permeability and selectivity that is postulated to be due to an inherent transport phenomena in the dispersed zeolite phase.
- When a mixture of the para and ortho xylene isomers is considered for transport in the dispersed silicalite phase at high temperatures and high relative pressures, it appears that much of the selectivity enhancement due to molecular sieving is lost due to preferential ortho-xylene sorption and single file diffusion. This severely questions the use of MFI under these operating conditions.

7.2 Recommendations for Future Work

In light of the conclusions of this work, several key questions have been raised that remain unanswered. This section will seek to provide some of these questions, as well as possible strategies to answer these issues in a scientific manner.

7.2.1 Polymer Characterization

The permeability decrease described in Chapter 4 is an unusual phenomenon that is thought to occur due to the highly interacting penetrant, and the temperature proximity to the glass transition temperature of the polymer. The proposed free volume hypothesis at the end of Chapter 4 makes practical sense given the data; however more concrete proof of the free volume distribution movement would be an excellent addition to this work. Positron Annihilation Lifetime Spectroscopy (PALS) has been employed to determine the free-volume hole size, fraction, and distribution in a variety of polymers [5-7], and has been shown to correlate with gas permeability [7]. Access to this technique is limited, but applying PALS to the Torlon® system before, after, and during pervaporation conditions could directly support the idea of a free-volume shift and thus a more favorable transport mechanism for the para isomer. This research group is currently developing ties with Dr. Jean at the University of Missouri, for exactly such PALS applications, and there may indeed be a future opportunity for this experiment.

In addition to the PALS investigation, it would equally interesting to probe the Torlon®/xylene system with different penetrant pairs in order to further understand the type of transition that may be occurring in the free volume distribution. For example, pervaporation of xylene isomers, saturated with a gas such as CO2 or N2, could show

interesting effects as the xylene conditions the polymer. According to the hypothesized sketch in Figure 4.7, the amount of free volume accessible to xylene would decrease with such a free volume shift, but the amount of free volume accessible to a smaller penetrant would change as well. It would be interesting to probe this system with several different gas sizes, in the presence of xylene to help further define the free volume relaxation.

Finally, Torlon® 4000T is the first tested out of several variants in the Torlon® family of polyamide-imides. It would be worthwhile to at test Torlon® AI-10, as it does exhibit a slightly different backbone structure that may indeed increase the permeability of the matrix, and alleviate the large membrane area requirements for such low flux polymers. In addition, Solvay® has expressed interest in increasing the applicability of Torlorn® membranes, and has many non-commerical experimental samples that may be useful for organic liquid separation. If a certain backbone chemistry adjustment can be suggested that may have more optimum properties, it is entirely possible that Solvay® may be able to provide such a material on an experimental basis.

7.2.2 Zeolite Characterization

At the conclusion of this work there are two main questions yet to be resolved concerning silicalite and its application to mixed matrix materials and xylene separation. First, it would be beneficial to further explore the use of silane coupling agents for this application, albeit briefly. This technique was primarily halted in this work due to the availability of the more promising Grignard treatment and its corresponding success in other applications. It would be worthwhile to obtain a new sub-micron, mono-disperse, silicalite sample and treat it with both the small APDMES SCA as well as one of the

bulkier SCAs established in Chapter 5. Treating this sample under much more aggressive conditions (most likely 70°C overnight) could attempt to approach a maximum conversion of the silicalite silanols. The use of a sub-micron, mono-disperse, sample should allow for more readily characterized surface chemistry due to is higher surface area to mass ratio, and more conclusive results about the coverage of the zeolite surface could be obtained. If a non-clogged zeolite, with a well-silanated surface could be obtained, it should be possible to disperse in a polyamide-imide, and possible corroborate the results of the Grignard treated materials at high temperature.

Second, it would be extremely beneficial to obtain sorption data for the zeolite isomers at high temperatures (150°C-250°C), and further corroborate the postulated behavior. However due to increasingly low sorption values, the flammability of the xylene isomers at this temperature range, and the pressures required to maintain high relative pressures, this experiment is extremely difficult and most likely not possible.

7.2.3 Polymer/Sieve Engineering

As described in the previous section it would be interesting to see if the results of the Grignard treated mixed matrix membranes tests can be duplicated by similarly sized, silanated particles. In addition, it would be equally interesting to continue experimentation on the Grignard treated polymers by lowering the operating temperature. Lowering the temperature from 200°C will have the effect of enhancing the para-xylene sorption in the zeolite, although it will slow down diffusion of both isomers considerable, as well as diffusion through the polymer. The challenge in this experiment is in obtaining reliable permeability and selectivity results, as flux through the material will be slow.

Current "permeability-crash" experiments in Torlon® last approximately 180-200 hours, and selectivity measurements require sample collection over two days. This collection time will no doubt be increased, and collecting a sample for an accurate GC measurement will be difficult. None-the-less if a mixed matrix composite could be probed through both states of para-xylene sorption (in both the channels and intersections) it could provide interesting academic results.

Finally, in order to optimize the system as a tool for purification of para-xylene, it appears that it may be advantageous to explore new zeolites for this application. Given the high temperature requirement of this work, it may be beneficial to try ZSM-11 (which is a ZSM-5 with two dimensions of straight channels), a larger pore zeolite with a caged structure similar to 4A (maybe 5A), or possible a new structure. An optimum structure would be a caged structure that is controlled by pore windows in the 5.5-6Å range. This structure could take advantage of the size difference between the xylene isomers, but sorption effects would possibly not be as serious as the MFI case due to open cages instead of channel intersections. This author is not aware of any such structure that exists at this time. It would be interesting to simply test a larger pore zeolite that is available on the market like zeolite X, or Y. These materials would most likely not be very selective at low temperatures due to high sorption amounts, and large pore windows, but they may be useful at high temperatures when molecules have more energy, and lower sorption values.

7.3 References

1. Moore, T. Effects of Materials, Processing Conditions, and Usage Conditions on the Morphology and Gas Transport Properties of Mixed Matrix Membranes. PhD dissertation, The University of Texas at Austin, 2004. Austin, Texas.

2. Hussain, S. Mixed Matrix Dual Layer Hollow Fiber Membranes for Natural Gas Separation. PhD dissertation, Georgia Institute of Technology, 2006. Atlanta, Georgia.

3. Husain, S; Shu, S; Koros, W.J. Journal of Physical Chemistry, In Press.

4. Husain, S; Shu, S; Koros, W.J. Industrial and Engineering Chemical Resources. In press.

5. Jean, Y.C.; Hong, X. Macromolecules. 1996, 29 7859-7864.

6. Jean, Y.C.; et al. In *Positron Spectroscopy of Solids*, Dapasquir, A,; Mills, A. Ohmsha, 1995, p. 563.

7. Jean, Y.C. et. al. Journal of Polymer Science, B. 1995, 33, 2365.

APPENDIX A

TORLON® VARIANTS

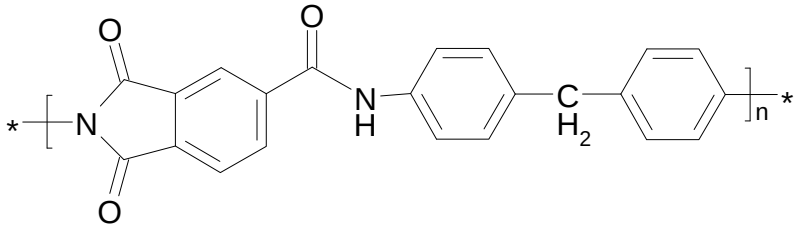

Torlon ® AI-10
Distributed as 95% imidized and 50% imidized (AI-30)

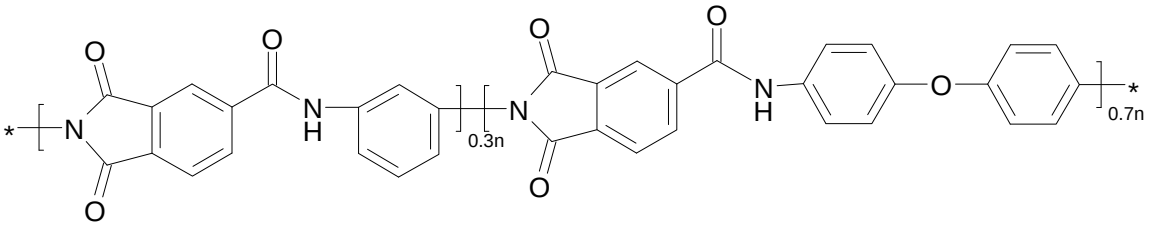

Torlon ® 4000T
Distributed as 99% imidized and ~50% imidized (AI-50)

APPENDIX B

AUTOCAD DRAWINGS OF PERVAPORATION CELL

AutoCad® drawings of the pervaporation apparatus used for this work are shown on the following page. This drawing is not to scale, and some text may be unreadable due to scaling. A complete and detailed electronic copy of the AutoCad® file can be found on the DVD associated with this thesis, or on the retired group drives of the Koros Research Group.

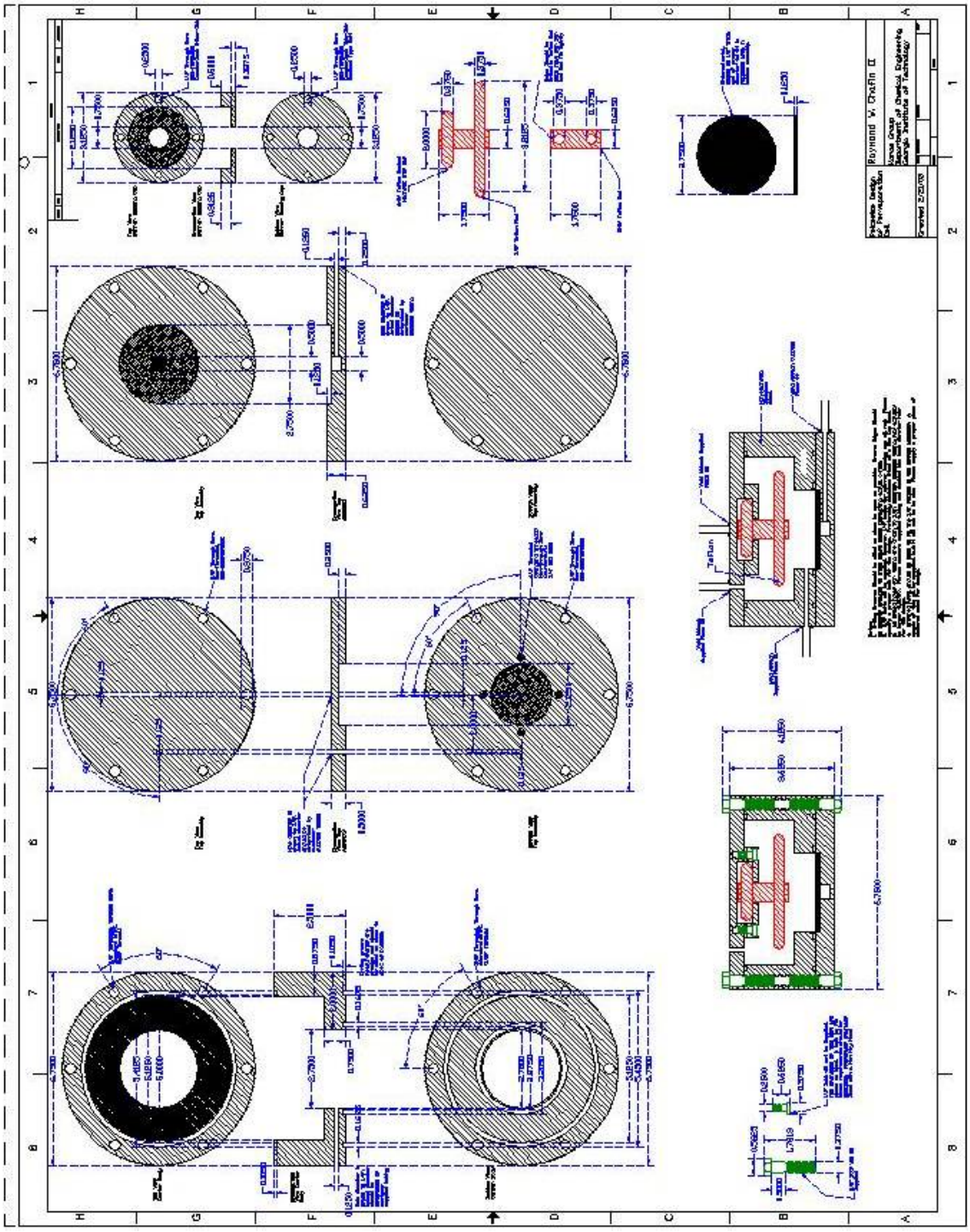

APPENDIX C

ADVANCED POLYMER STRUCTURES

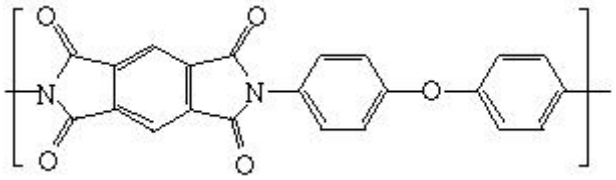

KAPTION®

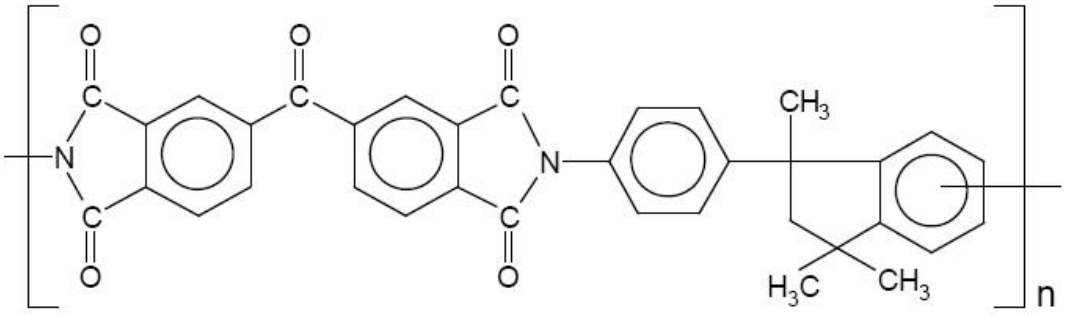

MATRIMID®

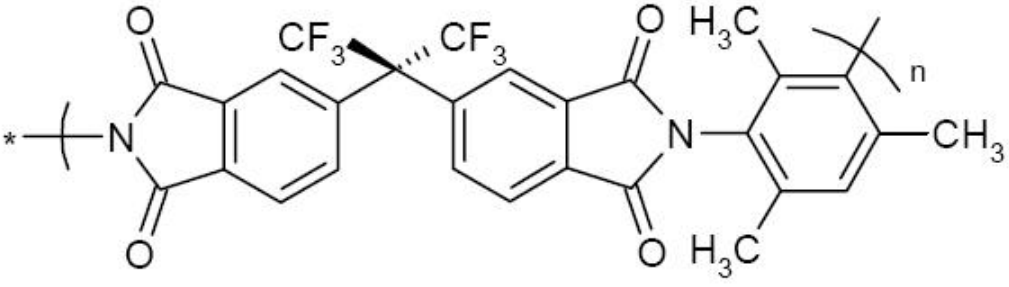

6FDA-DAM

APPENDIX D

MEMBRANE AREA CALCULATIONS

The following calculation will estimate the area required for a hollow fiber membrane unit that enriches 25% of a 500 KMTA feed to a para-xylene recovery process. The assumed conditions will be as follows:

- Feed condition of 30% para-xylene, 30% meta-xylene, 30% ortho-xylene, and 10% ethylbenzene.
- Operating temperature of 200°C
- Hollow fiber skin thickness of 0.1 μm.

Torlon® has been shown to have para-xylene permeabilities of 0.25 Barrers, and this number will be used here.

$$500KMTA = 500{,}000{,}000\frac{kg}{yr}$$

$$0.25Barrer = 0.25\times10^{-10}\frac{cc(STP)\cdot cm}{cm^2\cdot \sec\cdot cmHg}$$

Converting….

$$0.25\times10^{-10}\frac{cc(STP)\cdot cm}{cm^2\cdot \sec\cdot cmHg}\times\frac{1mol}{22400cc(STP)}\times\frac{106g}{1mol}\times\frac{1kg}{1000g}\times\frac{3600\sec}{1hr}$$

$$\times\frac{24hr}{1day}\times\frac{365day}{1yr}\times\frac{100^2cm^2}{m^2}\frac{1}{0.1\mu m}\times\frac{10{,}000\mu m}{1cm}\times88cmHg = 328\frac{kg}{m^2\cdot yr}$$

$$0.25\times500{,}000{,}000\frac{kg}{yr}\times\left(\frac{m^{2\cdot}yr}{328kg}\right) = 381{,}000m^2 \approx 400{,}000m^2$$ **area needed., to handle a 25% cut of the feed.**

APPENDIX E

XRD AND NITROGEN ADSORPTION DATA FOR ZONED BP SILICALITES

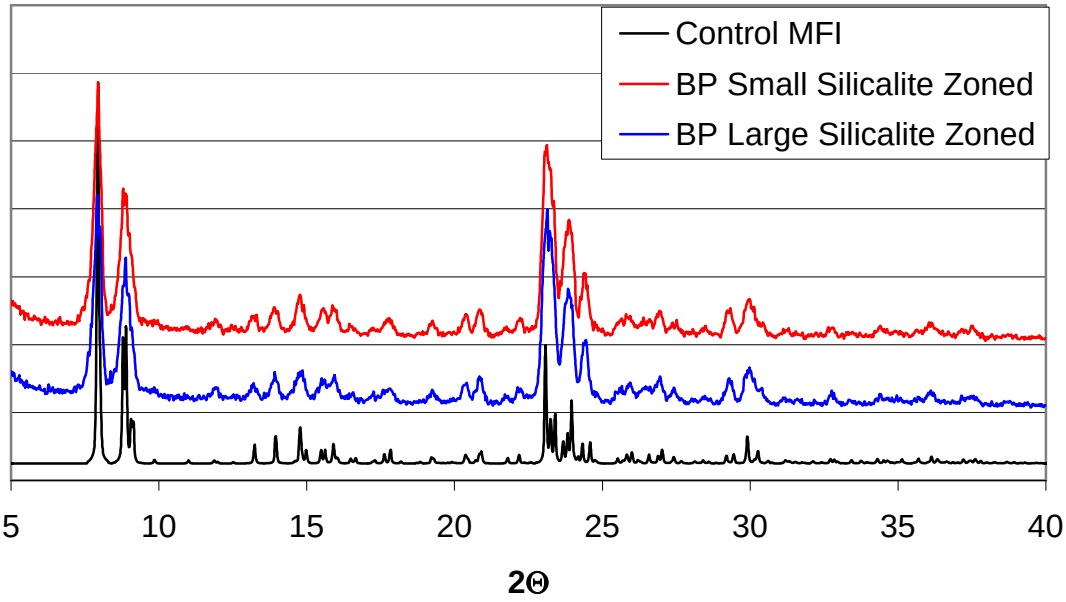

Figure E-1. XRD Spectra of zoned BP large and small silicalites.

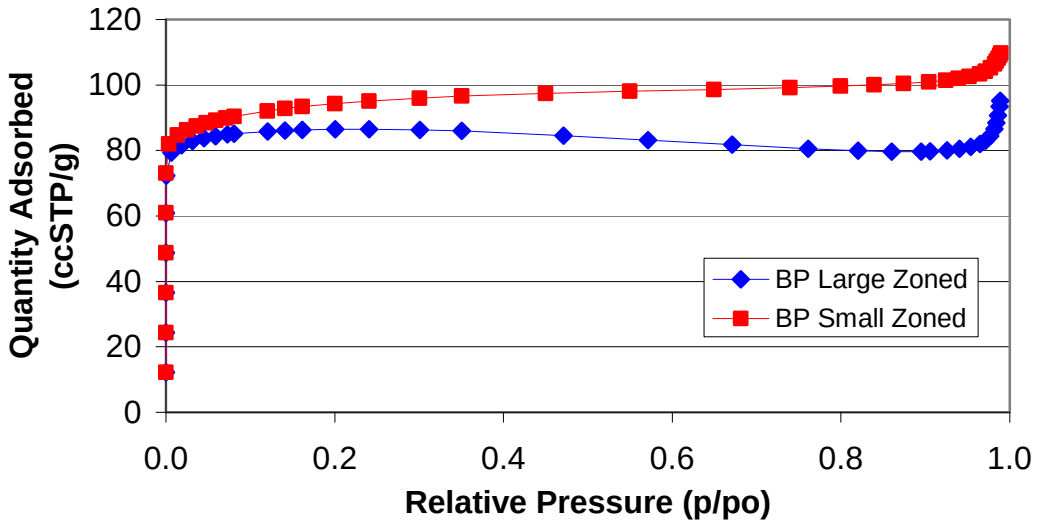

Figure E-2. Nitrogen adsorption data for both large and small BP zoned particles. There is a slight free space error in the large zoned sample causing the slight dip at relative pressures. This experiment could easily be repeated, but will not due to the lack of applicability of this zeolite.

APPENDIX F

ESTIMATING THE PERMEABILITY AND SELECTIVITY OF A BINARY MIXTURE OF PARA XYLENE AND ORTHO XYLENE IN SILICALITE AT 200°C

The following reasoning explains the choices for the *corrected* permeability and selectivity used in Maxwell calculations in Figure 6.16 and Table 6.13. The basic assumptions for the following calculations are:

1. Diffusion through the zeolite can only be as fast as the slowest penetrant, i.e. "single-file-diffusion."
2. The sorption isotherms in Figure 5.1 are used to extrapolate a sorption coefficient for both isomers at 200°C and a relative pressure of 1. For the para isomer, only the curves for 100°C, 130°C, and 150°C used due to the channel sorption sites available below 100°C.

Based on these two assumptions, permeability for para and ortho xylene was calculated by the following. First, diffusion coefficients can be estimated at 200°C by extrapolating diffusion data given in Table 5.1, and the corresponding reference temperature dependant diffusion data based on gravimetric methods. This linearized Arrhenius extrapolation can be seen in Figure A-1, as well as the predicted points at 200°C. The resulting values are shown in Table A-1. Next, sorption values from Figure 5.1 are extrapolated in a similar manner, and are shown in Figure A-2. The resulting sorption values are shown in Table A-1. Based on assumption #1, both isomers are assumed to diffusion at the same rate, which is the slower ortho isomer diffusivity. Permeabilities are calculated by simple multiplication of the ortho diffusivity, and each of the respective sorption coefficients,

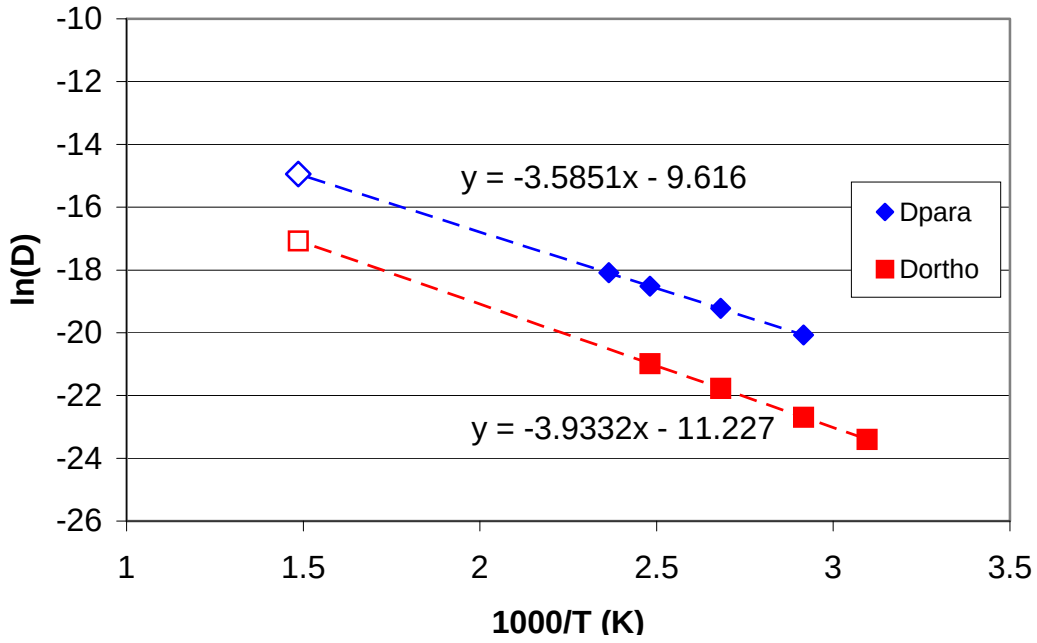

Figure A-1. Extrapolation of diffusion data to determine individual isomer values at 200°C

and are shown in Table A-1. Based on this method, 200°C, and saturated liquid, the silicalite is selective for ortho xylene at nearly 15:1. Therefore for a para xylene based Maxwell model, a permeability of 0.04 Barrer and a para/ortho selectivity of 0.07 are utilized, as shown in Table 6.3.

Table A-1. Estimated Permeability of para and ortho Xylene in Silicalite at 200°C, and relative pressure of 1.

Isomer	Diffusivity (cm^2/s)	Sorption ($ccSTP/(cm^3\text{-}cmHG)$)	Permeability (Barrer)
para	3.24E-07	9.87E-05	0.04
ortho	***3.86E-08***	1.39E-03	0.54
Ideal Selectivity		14	

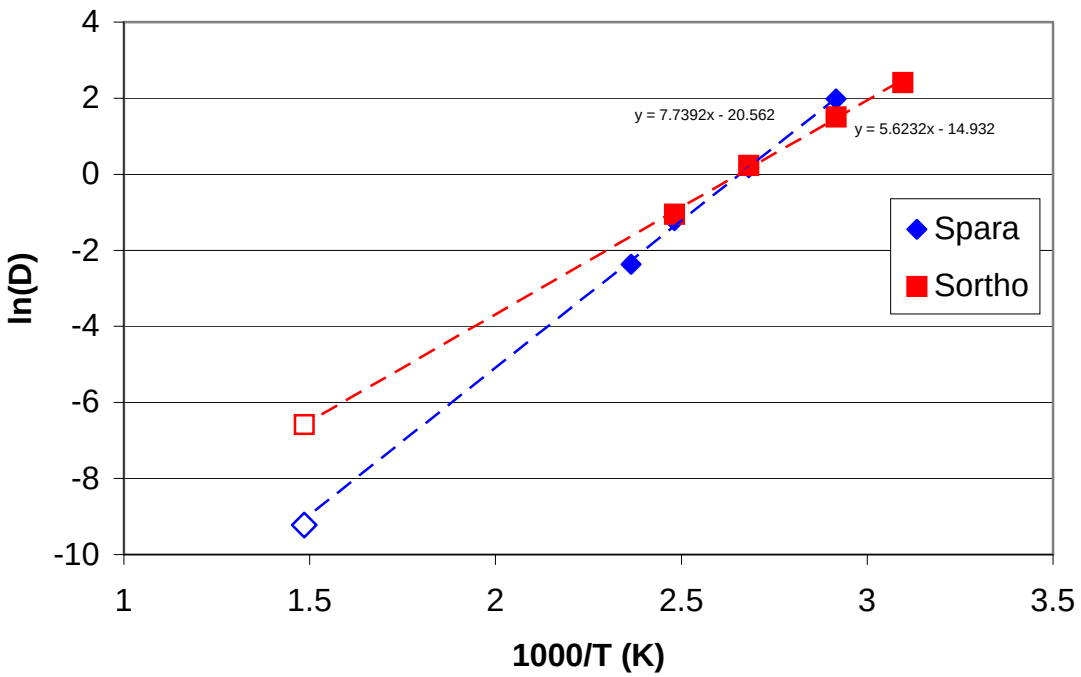

Figure A-2. Extrapolation of Sorption values given in Figure 5.1 at relative pressure of 1.